CHALMERS
UNIVERSITY OF TECHNOLOGY

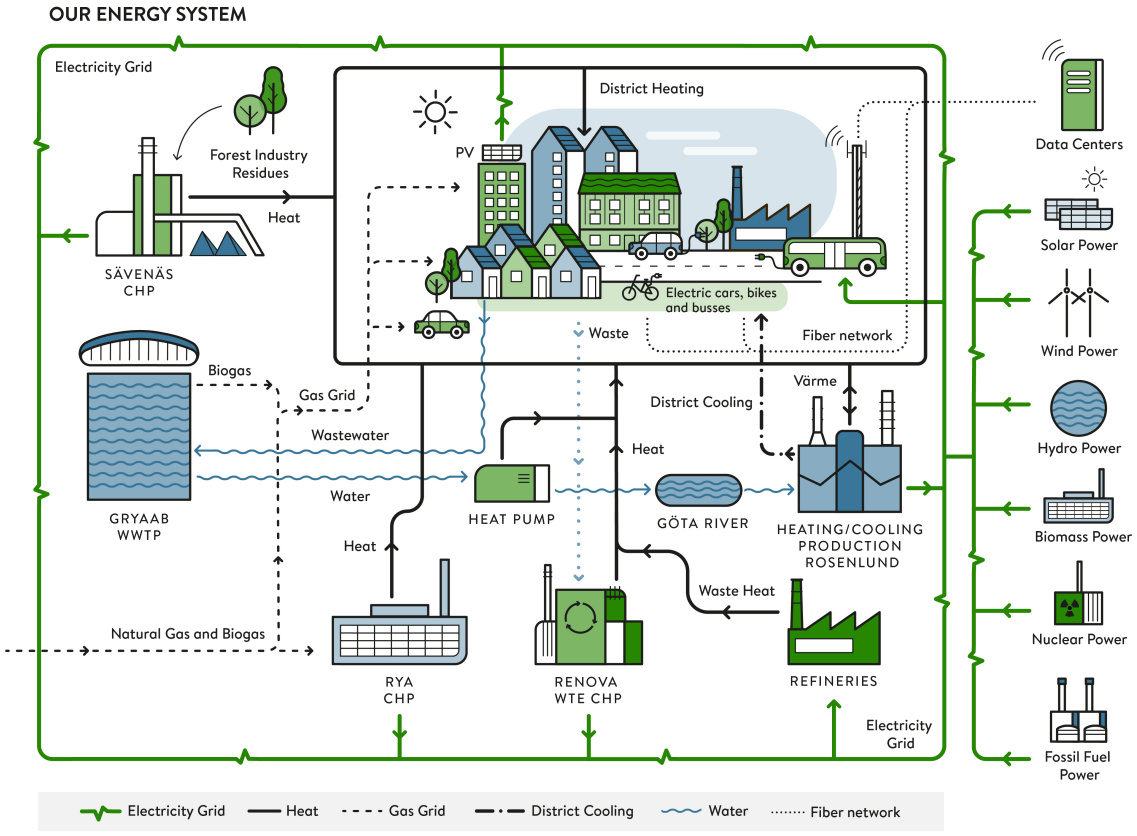

The Role of Large-Scale Heat Pumps in the Future Energy System

A Case Study of Gothenburg's Energy System

Master's thesis in Sustainable Energy Systems

ADAM GUNNARSSON
MALTE ARFVIDSSON NILSSON

DEPARTMENT OF ENVIRONMENTAL AND ENERGY SCIENCES
CHALMERS UNIVERSITY OF TECHNOLOGY
Gothenburg, Sweden 2026
www.chalmers.se

Master's thesis 2026

The Role of Large-Scale Heat Pumps in the Future Energy System

A Case Study of Gothenburg's Energy System

ADAM GUNNARSSON

MALTE ARFVIDSSON NILSSON

CHALMERS
UNIVERSITY OF TECHNOLOGY

Department of Environmental and Energy Sciences
Division of Energy Technology
Chalmers University of Technology
Gothenburg, Sweden 2026

The Role of Large-Scale Heat Pumps in the Future Energy System
A Case Study of Gothenburg's Energy System

ADAM GUNNARSSON
MALTE ARFVIDSSON NILSSON

Supervisor: Joel Bertilsson, Department of Environmental and Energy Sciences
Supervisor: Mariliis Lehtveer, Division of Strategy and Innovation, Göteborg Energi
Supervisor: Lars Holmquist, Division of Strategy and Innovation, Göteborg Energi
Examiner: Lisa Göransson, Department of Environmental and Energy Sciences

Master's Thesis 2026
Department of Environmental and Energy Sciences
Division of Energy Technology
Chalmers University of Technology
SE-412 96 Gothenburg
Telephone +46 31 772 1000

Cover: Visualization of the energy system of Gothenburg. Illustration: Göteborg Energi.

Typeset in LaTeX
Printed by Chalmers Reproservice
Gothenburg, Sweden 2026

The Role of Large-Scale Heat Pumps in the Future Energy System
A Case Study of Gothenburg's Energy System
ADAM GUNNARSSON
MALTE ARFVIDSSON NILSSON
Department of Environmental and Energy Sciences
Chalmers University of Technology

Abstract

With recent trends toward renewable, intermittent energy sources, such as solar- and wind power, there has been a higher penetration of variable low cost electricity. Power-to-heat technologies, such as large-scale heat pumps and electric boilers have become more and more cost-effective for district heating due to their flexibility. This could be one important cornerstone in reducing emissions from district heating and to increase the competitiveness of renewable sources. Previous studies on the district heating system of Gothenburg have indicated future cost-effective solutions with large-scale heat pumps as the main energy provider in the system. However, these earlier studies have had simplified representations of heat pump availability and coefficient of performance. The purpose of this study was to refine the representation of heat pumps with new constraints and operating conditions specific to Gothenburg and evaluate the potential for different heat pump types. The new constraints were then implemented into an already existing linear programming model of the Gothenburg district heating- and electricity system for future investments and dispatch. The model works as one node and includes heating- and electricity demand, weather conditions and electricity prices from weather year 2019. The model optimizes dispatch and investments until year 2080. Four main scenarios were constructed to account for different future potentials in medium-grade waste heat and varying hydrogen demand. Sensitivity analyses were conducted to test different future outcomes. Most scenarios indicated system configurations with large investments in heat pumps, together with thermal energy storages and peaking units of electric- and heat-only boilers. The future role of heat pumps is highly dependent on cheap available electricity, and limitations due to transmission constraints in the electricity grid and district heating network. Existing units in the district heating system were shown to have a large impact on the optimal solution until decommissioned. Few scenarios studied showed new investments in combined heat and power plants, indicating a lower system cost if heat pumps can be utilized.

Keywords: large-scale heat pump, district heating, power-to-heat, waste heat, linear programming, energy systems modeling, coefficient of performance, electricity.

Acknowledgments

From Chalmers, we'd firstly like to thank our supervisor, Joel Bertilsson, for your constant availability and good answers to our many questions we've had under this project. Thank you Sofia Rosén for guiding us through model difficulties and acting as our bonus supervisor. A big thank you to our examiner Lisa Göransson for your continuous support and encouragement, and for helping us think about problems from new perspectives. Also, thank you everyone at the Division of Energy Technology for your including atmosphere and for the continuous laughs that we've shared during this period, it's been great working at your division.

From Göteborg Energi, thank you our supervisors, Lars Holmquist and Mariliis Lehtveer, for the constant feedback, your explorative thinking and wise criticism that has brought forth new ideas for the project. Thank you Jennie Rodin, for being available with data we've needed for many parts of the project, we could not have done it without you. Also, thank you Fredrik Lindblom, for showing us the heat pump facilities in Gothenburg. A big thank you to the people at Göteborg Energi for welcoming us into your workspace.

Thank you all organizations in addition to Chalmers and Göteborg Energi, for answering questions in your areas of expertise.

Adam Gunnarsson & Malte Arfvidsson Nilsson, Gothenburg, May 2026

List of Acronyms

Below is the list of acronyms that have been used throughout this thesis listed in alphabetical order:

BF	Battery Factory
BP	Back Pressure
BTES	Borehole Thermal Energy Storage
CCGT	Combined Cycle Gas Turbine
CCS	Carbon Capture and Storage
CHP	Combined Heat and Power
COP	Coefficient Of Performance
CTES	Cavern Thermal Energy Storage
DC	District Cooling
DEA	Danish Energy Agency
DH	District Heating
DHn	District Heating Network
DHPC	Dry Hydrated Potassium Carbonate
DSO	Distribution System Operator
EB	Electric Boiler
ELLI	ELectricity Long-term Investment
EV	Electric Vehicle
FLH	Full-Load Hour
GW	Giga Watt
GWh	Giga Watt-hour
HOB	Heat-Only Boiler
HP	Heat Pump
HPC	Hot Potassium Carbonate
H2	Hydrogen
LP	Linear Programming
MEA	Monoethanolamine
MSW	Municipal Solid Waste
SMHI	Sweden's Meteorological and Hydrological Institution
SOC	State Of Charge
PEM	Proton-Exchange Membrane
PV	Photovoltaic
P2H	Power-To-Heat

RT	Roots and Tops
tCO2	tonnes of Carbon Dioxide
TES	Thermal Energy Storage
TTES	Tank Thermal Energy Storage
V2G	Vehicle-to-grid
WG	Biogas

Nomenclature

Below is the nomenclature of indices, sets, parameters, and variables that have been used throughout this thesis.

Indices

y	Index for year
p	Index for plant
t	Index for time step
e	Index for electric vehicle type

Sets

τ	Set of time steps
τ_{winter}	Subset to τ for all time steps in winter
Y	Set of years
E	Set of electric vehicles
P	Set of technologies
P_{El}	Subset to P for all electricity generating technologies (incl. CHP)
P_{St}	Subset to P for all storage technologies
P_{ElSt}	Subset to P for all electricity storage technologies
P_{H2St}	Subset to P for all hydrogen storage technologies
P_{HSt}	Subset to P for all heat storage technologies
P_{HStHP}	Subset to P for all heat storage technologies with heat pump
P_{H}	Subset to P for all heat producing technologies (incl. heat pumps)
P_{HP}	Subset to P for all heat pump technologies
P_{CHP}	Subset to P for all combined heat-and-power technologies
P_{P2H}	Subset to P for all power-to-heat technologies

Parameters

γ_t	Availability profile at time t [-]
α_p	Power-to-heat ratio for technology p [-]
η^{WH}	Efficiency for converting electricity to heat in electrolyzer [-]
η_p	Efficiency for technology p [-]
$\eta^{ch}_{y,p}$	Charging efficiency for storage type p in year y [-]
$\eta^{dch}_{y,p}$	Discharging efficiency for storage type p in year y [-]
ϕ_t	Normalized Heat Demand Profile at time t [-]
$L_{y,p}$	Constant loss term for storage type p in year y [-]
$C^{inv}_{y,p}$	Annualized CAPEX for technology p in year y [MEUR/GW/yr]
$C^{O\&M_{fix}}_{p}$	Fixed O&M costs for technology p [MEUR/GW/yr]
C^{run}_{p}	Variable running costs for technology p [MEUR/GWh]
$C^{el}_{y,t}$	Hourly cost of importing electricity or price of selling electricity to the regional grid at time t in year y [MEUR/GW]
C^{fuel}_{p}	Fuel cost for technology p [MEUR/GWh]
$COP_{p,t}$	Coefficient Of Performance (or η for EBs) for technology p at time t [-]
w_{is}	Isentropic work
$D^{el}_{y,t}$	Electricity demand at time t in year y [GWh_{el}/h]
$D^{heat}_{y,t}$	Heat demand at time t in year y [GWh_{th}/h]
F_Q	Heat loss ratio [-]
F_{corr}	Correction factor [-]
K	Electricity demand for compressing H_2 [GWh_{el}/GWh_{H_2}]
$\dot{Q}_t$	Heat flow at time t [GWh_{th}/h]
T_t	Temperature at time t [°C]
$\bar{T}$	Logarithmic mean temperature difference [K]
ΔT	Temperature difference [°C]
$\Delta\bar{T}_{pp}$	Logarithmic pinch point temperature difference [K]
$\Delta\bar{T}_{r}$	Entropic mean temperature difference [K]
$X_{y,t}$	Heat from refineries and Renova at time t in year y [GWh_{th}/h]
Y_{start}	Starting year to which the costs are discontinued [yr]

Variables

$b^{ch}_{y,p,t}$	Charging to storage type p at time t in year y [GWh/h]
$b^{dch}_{y,p,t}$	Discharging from storage type p at time t in year y [GWh/h]
c_{tot}	Total system costs [MEUR]
$c^{start}_{y,p,t}$	Start-up costs for technology p at time t in year y [MEUR/h]
$c^{partload}_{y,p,t}$	Part-load costs for technology p at time t in year y [MEUR/h]
$c_{N,y}$	Normalized cost of producing heat in year y [MEUR/GWh]
$ev^{ch}_{y,e,t}$	Charging of electric vehicle type e at time t in year y [GWh/h]
$ev^{dch}_{y,e,t}$	Discharging from electric vehicle type e (V2G) at time t in year y [GWh/h]
$g_{y,p,t}$	Generation by technology p at time t in year y [GWh/h]
$i_{y,p}$	Invested capacity in technology p in year y [GW]
$soc_{y,p,t}$	Storage level in storage type p at time t in year y [GWh]
$w_{y,t}$	Import/export of electricity at time t in year y [GWh/h]

Contents

List of Figures

List of Tables

1
Introduction

Sweden has adopted a legally binding target of reaching net-zero greenhouse gas emissions by 2045, with negative net emissions thereafter [1], [2]. Reaching this goal partly includes increasing the deployment of intermittent sources, mainly wind and solar [3]. Due to the flexibility of heat pumps (HPs) and electric boilers (EBs), incentives for investing in wind- and solar power are increased as these power-to-heat (P2H) technologies can make use of the variability in power production. Thereby increasing the competitiveness of renewable sources. The coupling between the heating sector and the electricity sector would lead to a more efficient utilization of the resources, which could pave the way for a low-carbon energy system [4].

Out of a variety of technologies that can be used for coupling the electricity- and heating systems [5], this study will mainly focus on large-scale HPs, EBs and thermal energy storages (TES), using the Gothenburg energy system as a case study, to analyze their role in a cost-minimized system from a techno-economic perspective. HPs uses ambient sources such as seawater, air, geothermal and industrial waste heat as heat sources and transfers the heat to a heat sink by using electricity, leading to a temperature lift [6]. The advantage of using HPs is their ability to deliver more useful heat compared to the electricity input [7], and thus utilize otherwise lost heat.

To make HPs competitive with other heat generating technologies, it is important to increase the number of full-load hours (FLHs) due to a higher initial investment cost [8] compared to for instance EBs. This includes operating the HPs during a variety of electricity prices, while avoiding peak prices indicating a shortage of intermittent resources. As the city of Gothenburg aims at being carbon-neutral by 2030 [9], centralized HPs will mainly compete with bio-based plants for heating. However, due to the competitiveness of bio materials with other sectors [10] it has been shown in previous studies that a constraint on the availability of biomass supply might create a window of opportunity for P2H technologies to be introduced in the future energy system [11].

There have been multiple studies in which the sector coupling between the electricity and heating sectors have been analyzed. Bertilsson et al. [12] investigated how city-specific characteristics impact the cost-optimal configuration of the cities energy systems. Using a linear programming (LP) model it was concluded that P2H technologies are favored, provided sufficient import capacity and therefore access to cheap electricity. Similar results were found in the studies by Rosén et al. [13] and García et al. [14]. Common for the before mentioned studies were a simplified

representation of HPs with a constant coefficient of performance (COP) and a single type of HP.

In highlight of the uncertainties regarding the future of the energy system, there is a need for research regarding the role of large-scale HPs in the future energy mix. This thesis builds upon previous research by applying a more comprehensive analysis of HP characteristics in an energy systems cost-minimization model while also considering specific city-characteristics such as electricity demand for transportation, demand for hydrogen (H2), heat source availability and demand for heating.

1.1 Aim and Research Questions

The aim of this thesis is to deepen the understanding of large-scale HPs, their future role, and evaluate under which conditions investments in such facilities are motivated in Gothenburg.

In order to reach the aim of the study, a set of research questions were formulated, listed as:

- *RQ1*: How do existing heat production units, transmission limits in the district heating network and electricity generation units in Gothenburg impact the optimal investments and dispatch of different units from a total system cost-minimization perspective?
- *RQ2*: Electric boilers vs. heat pumps: under what price- and operating conditions is one more preferable than the other?
- *RQ3*: How does the electrification of the refineries in Gothenburg impact the role of heat pumps in the district heating system?
- *RQ4*: How do different expenses such as taxes and fees impact the cost of producing heat?
- *RQ5*: Is it cost optimal to invest in TES and what TES size is the most optimal?

This study is conducted in a cooperation between Chalmers University of Technology and Göteborg Energi AB.

1.2 Limitations

There are certain limitations in this study that needs to be taken into account when interpreting the results. One such limitation is the fact that the applied model is a LP optimization model, meaning that all constraints and functions have to be linear [15]. The largest reason for this is that non-linear models can have local optima, meaning if the solution is non-convex, there is a possibility that the global optima is not reached. A part of it is also to reduce computational time and that the computers used have limited computational memory.

The model used in this work only represents Gothenburg as a single node, meaning that it does not take into account the physical placement of different units within the city or the network layout. Instead, it uses additional constraints to account for these factors and aggregates the production units into fleets consisting of the total capacities of different types of plants and technologies. Furthermore, the model does not explicitly consider the required pipeline infrastructure that needs to be built or the costs associated with these. As a result, the optimization model optimizes the investments and dispatch of units from a broader perspective. It is however important to consider that extra work is needed to evaluate the feasibility of the results ensuring that the implementation of the dispatch units is possible within the current network layout, considering congestion in the district heating network and electricity grids as well as the costs associated with these. In this work, the availability of heat sources and the maximal capacity of different types of HPs have been examined exogenously to capture some of the spatial limitations, with the restrictions modeled as extra constraints.

The model assumes perfect foresight indicating that future events are assumed to be known such that the model can plan for events occurring at any time of the year. In reality however, this is not the case and unplanned events can have large impacts on the energy system as a whole and might mean that some energy transition pathways even become infeasible as new circumstances arises. Evaluating the consequences of assuming perfect foresight can be done through sensitivity analyses, where key parameters are changed to analyze how these affect the structure of the energy system.

Data given to the model exogenously is based on the weather year 2019. Meaning weather conditions, heat demand etc. are all based on this year. One reference year has to be used as correlations across data is often the case. It can be of relevance to look at several weather-years, however this could not be done as electricity prices originates from another model [16], which only had data available for weather year 2019.

The flexibility of thermal plants is analyzed using a two-variable approach as presented by Göransson et al. [17], where flexibility limits are modeled based on aggregated fleets rather than for individual plants. This is mainly due to computational limits, since the modeling of flexibility for the individual thermal units would require binary variables for each plant, which would give too large computational loads.

2
Theory

The following sections will explain the theory needed to understand the thesis. The first sections includes descriptions of district heating, characteristics of HPs, and how varying levels of details of COP affect the results in energy systems modeling. This is then followed up by thermal energy storages and the energy market. Towards the end of the chapter, an overview of the Gothenburg energy system is presented.

2.1 District Heating

The working principle of district heating (DH) is to supply heat in a system, usually a city, with heated water through a network of pipes. The whole system is therefore called a district heating network (DHn). The heating is mainly used for space heating and domestic hot water preparation for housing, combined with some industry demand. Heating load varies in the system, both daily and by season. Load variations can be described either by social- or physical loads [18]. Social load is associated with consumer patterns, where many people have the same habits. For example, showering in the morning or cooking in the evening. Physical load is associated with building insulation, wind variations, solar irradiation and temperature differences. Seasonal differences are more notable for colder countries, as DH load mainly varies with the outside temperature. Colder outside temperatures lead to higher heating demand. Daily- and hourly variations are also dependent on physical load, but are combined with social load. Daily variations in solar irradiation and wind affect the heating demand for the buildings. Demand is the highest during morning and evening, where most people consume heat and electricity. This means that the highest demand during a year is usually during one of the coldest days of the year, often during a morning-, or evening hour.

2.1.1 District Heating Functions

In order to meet the demand in the system, there are currently two ways to change the energy supply. The first way is to increase the temperature, which often implies increasing the temperature difference between the supply and return pipes of the system. A temperature lift is often done during winter. The other way to supply more energy, is to increase the mass flow of water [18].

Thermal energy comes from many different sources in DH systems. Combustion of fuel, solar collectors and EBs, are examples to actively produce heat. However,

thermal energy can also be utilized via waste heat from other sectors. Waste heat is in this project defined as heat that cannot be directly used in its area or sector of origin, due to temperature quality. However, waste heat in one sector can often be utilized for DH, in one way or another. Waste heat can be categorized into different grades depending on temperature; low-grade (< 100 °C), medium-grade (100 - 400 °C) and high-grade (> 400 °C), where waste heat usually is low-grade [19]. Low grade waste heat often needs to be upgraded in order to fit into the existing DH system, often through HPs. The heat can also be upgraded by other technologies, such as combustion or EBs. Sources of waste heat include for example; waste incineration, data centers, supermarkets and sewage streams [19].

Waste heat can be utilized differently, depending on how old a DH system is. There are different generations of DH, named 1st generation (oldest) up to 5th generation (future) [20]. The 1st generation used steam to distribute heat, but was replaced by hot water above 100 °C in the 2nd generation. The 3rd generation decreased supply temperature to 80 °C. The 4th generation aims to reduce the supply temperature to 60 °C, with additional generation coming from renewable intermittent sources. Future 5th generation aims to reduce the supply temperature down below 40 °C, which has many benefits, such as increased energy efficiency, better utilization of waste heat, and higher COP for HPs.

2.2 Heat Pumps

From a system perspective, there are two ways to integrate HPs. Either by small individual installations directly at end-users, for which the production is handled by the individual consumer, or by integrating large-scale HPs in the DH system. There are competitive advantages to use large-scale units [21]. *(1)* There is fuel flexibility in heat supply, as large-scale HPs often are coupled with combined heat- and power (CHP) plants or other units. During occasions of low electricity cost, driven by for example high wind production, heat from CHP plants becomes more expensive. Heat from HPs have a reversed effect, decreasing the price for production during high wind penetration. *(2)* Individual HPs in residential buildings produce after the individual consumer demand, resulting in production at times where electricity prices are high. Large-scale HPs can stop production during high electricity prices. *(3)* Large-scale HPs can be coupled with heat storages, which leads to greater reception. *(4)* Absorption of surplus electricity production (low electricity prices) can be made cheaper due to economy-of-size. *(5)* There is more potential to use advantageous heat sources (such as waste water). Individual HPs in residential buildings do have advantage in rural areas, where DH becomes infeasible. They also benefit from not requiring the same kind of infrastructure that the DHn does.

This means that there is a larger potential to use renewable energy technologies for large-scale HPs, as their production and storage capacity can be adapted to the intermittency of for example wind power production. Individual HPs have a certain degree of flexibility as well but still run the risk of producing heat when electric-

ity production from renewable sources is low. This could then lead to increased electricity prices, and a less efficient utilization of renewable energy sources.

2.2.1 Heat Pump Functions

The HPs analyzed in this project are vapor compression HPs. These types of HPs transfer heat from a heat source to a heat sink [6]. This is done by evaporating a refrigerant in an evaporator at low pressure. The refrigerant is then compressed using electricity, which increases the temperature. Following this, the refrigerant is condensed, transferring heat to the heat sink. The refrigerant is then expanded, decreasing the temperature again, which allows the liquid to once again absorb heat from the heat source. The cycle for a single-stage HP is seen in figure 2.1. The temperature lift over the HP is defined as the temperature difference between the heat source and the heat sink [22].

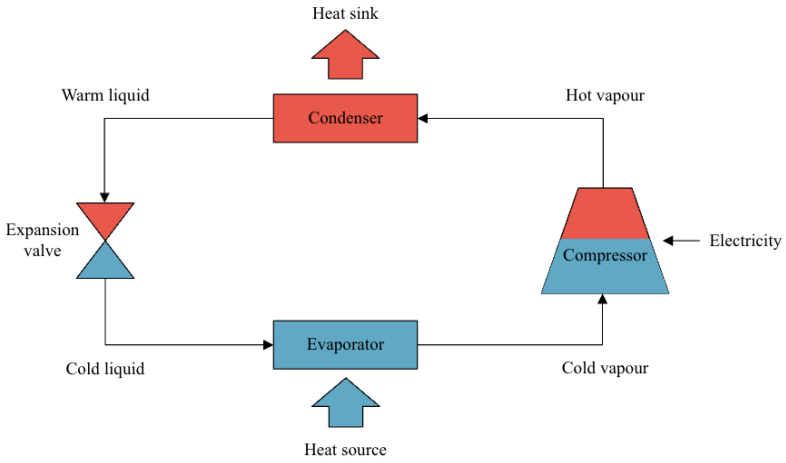

Figure 2.1: Heat pump schematic.

The pressure on the side of the evaporator is dependent on the refrigerant, the evaporator pinch point temperature and the heat source temperature. The pinch point is characterized as the minimum temperature difference (ΔT_{min}) between the hot and cold streams [23]. This is designed to occur at the end of the heat exchanger, to not violate pinch point principals. The minimum temperature difference depends on the area of the heat exchanger. Increased area reduces ΔT_{min}, which in turn increases the heat savings. But increased area increases capital costs. For the evaporator, the refrigerant must have a lower temperature than the heat source. This is reversed for the condenser, where the refrigerant is hotter than the desired heat sink temperature. Pressures are used to control the refrigerant's temperature to boil during the evaporation process. Higher pressures lead to higher evaporation temperatures. When the evaporated steam enters the compressor, the increase in pressure will increase the temperature as well [22]. The maximum temperature lift is thus determined by the pressure increase over the compressor, and ΔT_{min} for both the evaporator and the condenser.

The lower the temperature on the heat source, the larger the pressure difference becomes over the compressor. Increased pressure difference increases the work (electricity) needed, decreasing the COP. The showed cycle in figure 2.1 is the most basic configuration of HPs, with a single-stage compression cycle. However, often multiple compression stages are implemented, to decrease losses and improve both compression efficiency/operation and therefore allows for higher temperature lifts [24].

2.3 Impact of COP on Modeling Results

One important aspect of using HPs compared to other P2H technologies is that they are able to provide a higher heat output compared to the electricity input [7]. The COP depends on the temperature levels of the heat source and heat sink respectively. This means that for heat sources and heat sinks where the temperature levels changes over the year, the COP will also vary. Assuming a constant COP over the year can thus alter the results as there is a risk of overestimating the performance during the winter when the temperature levels generally are lower (especially for some heat sources) and the DH supply temperatures are higher.

There are several studies that have analyzed the effects of using different estimation methods for the COP. Pieper et al. [25] compared the results between four different methods of estimating the COP with a thermodynamic 2-stage HP operating under design conditions, using the case study of Nordhavn as an example. The applied method was a mixed integer optimization model with the objective function of minimizing the total system costs, including four different types of HPs, an EB and TES. The heat sources considered were ambient air, groundwater, seawater and sewage water. Both the heat sources and the heat sink had an hourly resolution of temperature levels. The results show that using a constant COP leads to significant deviations compared to the thermodynamic model, with deviations reaching up to 40% in the summer for ambient air. It is also shown that the different methods for estimating the COP affect the optimal choice of the type of HP to be invested in. Based on the results, it is concluded that using the method proposed by Jensen et al. [26] results in the most similar results compared to the thermodynamic model, showing smaller deviations and also less dependency on assumptions regarding input parameters.

Similar results can be found in the study by Bogdanov et al. [7], where the impacts of using constant COP-values compared to hourly based ones using Finland as a case study were investigated. In the study a linear optimization model called the LUT Energy System Transition model [27] with an hourly time resolution was modified to include hourly COP-values based on a formula presented by Ruhnau et al. [28]. The findings of the study indicated that assuming a constant COP did not have significant effects on the total system costs where it only decreased by 0.26%, but significantly impacted the dispatch of the units. Assuming a constant COP also led to miscalculations regarding energy consumption and an overestimation of the po-

tential for HPs, with higher overestimation for colder regions. Further conclusions were that a constant COP-value led to a primary energy demand that was 5.8% lower compared to the hourly based ones for the heating sector in 2050.

Overall, the literature review can be summarized as: (*1*) Using a constant COP value can give significant deviations from real life performance of HPs, (*2*) when doing energy systems modeling, it is important to be as detailed as possible to enable a fair and realistic comparison of different production units.

2.4 Thermal Energy Storage

One main benefit of using TES coupled with P2H technologies is that the storages can be charged during off-peak hours when the electricity prices are low and later be discharged when the demand, and consequently also the electricity prices, increases. This creates flexibility in the system, which is essential for a system with a high share of renewables due to their intermittency. There are various types of TES, and in this section the ones relevant for this case study will be introduced. Characteristics of the storage types included in the model are seen in table 2.2 under section 2.6.3.

2.4.1 Cavern Energy Storage

Cavern thermal energy storages (CTES) are variants of underground storages. This type of storage floods large spaces with heated water [29]. The storage can either be designed from scratch, or retrofitted from already existing spaces that previously stored other materials (commonly oil reserves). CTES are therefore often closed systems. Retrofitted storages are limited to store water below 100 °C, as they aren't capable of increasing pressures. The storage placement is fixed, so retrofitting might not be reasonable from start. A benefit with retrofitting however, is that investment costs decrease, as excavation stands for large costs.

One key property of CTES is stratification, where hot water is accumulated at the top, while cooler water drops to the bottom of the tank due to density gradients. The boundary layer between the hot- and cold part is called the thermocline [29]. Thermal stratification is important to reduce losses for the storage. Mixing of temperatures induce internal losses and decrease exergy. When attaining stratification, it is possible to extract a higher temperature on the water, as water is extracted from the top and looped back to the bottom.

2.4.2 Borehole Energy Storage

A Borehole thermal energy storage (BTES) is also a type of underground storage, where the properties of the surrounding rock is important for the energy storage capacities [30]. The storage consists of several drilled vertical holes, each with a

collector tube to heat exchange water with the surrounding rock. The number of holes can vary, from a few to hundreds, where the efficiency of the storage increases (to limited extent) with the size. The depth of the holes can vary from 20-300 meters and the diameter of each hole can be up to 15 cm in diameter [31]. Energy is stored by heating the surrounding rock through the holes with warm water. During high periods of demand, this heat can be extracted either through a heat exchanger, or via HPs. One drawback of this storage type is that the charge- and discharge speed is slow relative to the size of the storage.

2.4.3 Tank Energy Storage

Tank thermal energy storages (TTES) are typically made out of stainless steel or reinforced concrete, plus additional insulation against heat losses and leakages [32]. TTES have the advantage of higher discharge- and charge capacities in comparison to the total storage capacity. TTES generally have higher costs compared to a BTES. However, the system might benefit from the higher discharge- and charge capacities. Tank storages store water at the same temperature level as the DH supply water [33].

2.5 Marginal Cost of Generation, the Energy Market and the Spot Market

The marginal cost of electricity is the cost to produce an additional unit of electricity in a certain time step for a certain region [34]. This goes for the same of marginal cost of heat. What the model could do to cover this extra demand could be: produce more from existing capacities, cover production with a storage, thus producing extra in another time step, or to invest in more capacity of a certain technology. If this extra demand occurs during peak production, and all units are generating at full capacity, the only way to cover this extra demand is to either invest in more capacity or to discharge more from a storage (if available capacity is enough to cover).

There are two marginal costs of electricity in the model, called the local- and regional electricity cost. The regional cost is the marginal cost of electricity, defined as the SE3 electricity price. During hours where import is not constrained, the local cost is the same as the regional cost, unless it is cheaper to produce locally and the whole demand can be covered by local production. However, during hours when imports are constrained, the model has to cover the load by producing locally. This will lead to a local marginal cost of electricity. The model makes an artificial marginal electricity cost, as the marginal cost will be set by the units inside the node. This can lead to times when production units in the local node will produce, even though the SE3 electricity price won't cover the running costs. In the energy market, this type of behavior does not exist, as the prices are only set in each price zone (in this case SE3).

How the model creates this artificial local electricity price, can be compared to a

nodal market of electricity prices, where the congestion will force the local electricity price to increase. A nodal pricing would create a more granular energy market, where the zones would be divided into substations or cities. Nodal pricing has been a topic of discussion, with the increasing wind power penetration into the grid, with trends of higher congestion in the electricity grid and limits in how much the grid can expand [35].

As the model can run expensive units, even though electricity prices are low, the individual plants will not cover their running costs. There has been a consideration to implement local flexibility markets for distribution system operators (DSOs) to cover local congestion in the electricity grid [36]. In the model, the theoretical pay above the electricity price the units would get is the difference between the local- and regional electricity price when the regional marginal cost of electricity is lower than the local marginal cost. One such example of a bidding market to support flexibility was conducted in Stockholm [37]. The region around Stockholm and Uppsala has one of the most congested electricity grids in Sweden, therefore a test was made for such a market. A market of this kind can only exist if the costs for expanding the grid are more expensive than implementing the market structure itself. Additionally, this type of flexibility is not the only option, as other methods for flexibility compete for the most cost-effective solution.

2.6 The Energy System of Gothenburg

The energy system of Gothenburg consists of a complex system with multiple sectors coupled with each other [38]. The DHn is coupled with the electricity system through for instance P2H technologies, where electricity is used to heat water for the DHn. Due to this interconnectedness between various parts of Gothenburg, a change in one of the sectors can have significant impacts on other parts and it becomes relevant to consider the energy system as a whole when analyzing an impact in one sector.

2.6.1 The DHn of Gothenburg

The DHn of Gothenburg consists of a distribution network reaching over 1400 km [38]. The main goal of the DHn of Gothenburg is that it should, to the largest possible content, be based on recovered heat as it is more resource efficient, compared to using bio-based fuels as these can be utilized elsewhere [38]. A unique characteristic of the energy system in Gothenburg is the availability of medium-grade waste heat originating from two refineries (Preem, St1) and a waste-incineration plant (Renova) that can supply the heating demand during the summer.

The demand for heat in Gothenburg varies by year and season, mostly dependent on the outside temperature. The total supplied heat in Gothenburg the year 2019 was 3316 GWh [39]. The average heat demand is expected to not increase in Gothenburg due to optimizations in the system, counteracting the overall growth of the heat demand [40].

In Gothenburg, the supply temperature varies over the year from 70 °C to 105 °C [33]. The DHn is therefore defined as a 2nd or 3rd generation DHn, if the definition is only associated with DH supply temperatures. Figure 2.2 shows how the wanted supply temperature of the DHn in Gothenburg varies with the outdoor temperature.

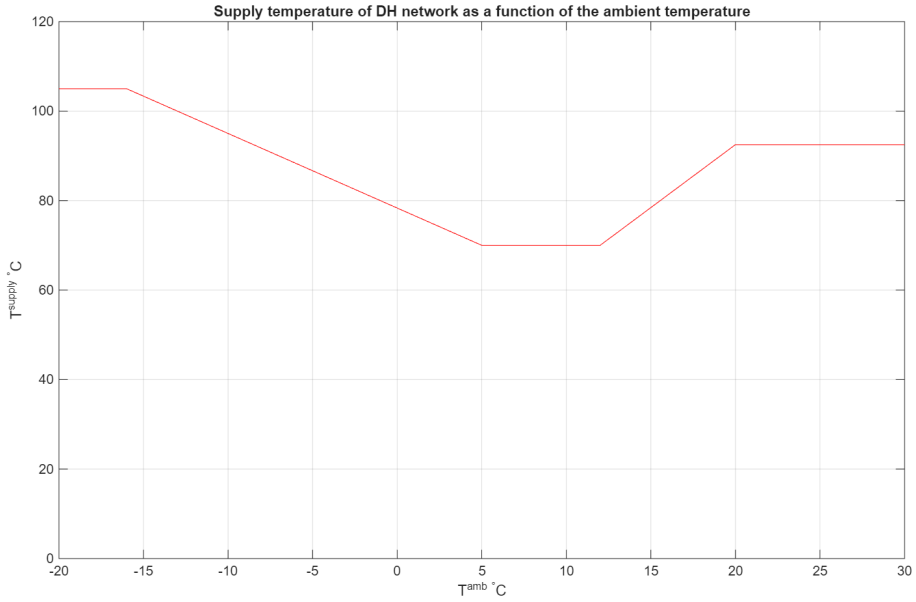

Figure 2.2: How the supply temperature of the Gothenburg DHn varies with the outdoor temperature.

Mathematically this can be described as

$$\begin{cases} T_t^{supply} = 70°C \ \forall \ T_t^{amb} \in [5°C, 12°C] \\ T_t^{supply} = 92.5°C \ \forall \ T_t^{amb} \in [20°C, \infty°C) \\ T_t^{supply} = 105°C \ \forall \ T_t^{amb} \in (-\infty°C, -16°C] \\ T_t^{supply} = 105°C \ - \ (T_t^{amb} - (-16°C)) \cdot 1.67 \ \forall \ T_t^{amb} \in (-16°C, 5°C) \\ T_t^{supply} = 70°C \ + \ (T_t^{amb} \ - \ 12°C) \cdot 2.81 \ \forall \ T_t^{amb} \in (12°C, 20°C) \end{cases}$$

where (T_t^{supply}) is the supply temperature of the DHn and (T_t^{amb}) is the ambient temperature at time step t. The multiplication factors of 1.67 and 2.81 describe the slopes of the supply temperature between the ambient temperatures of -15 to 5 °C and 12 to 20 °C respectively. The increased DH supply temperature during higher ambient temperatures originates from the need of absorption HPs for district cooling (DC) that require DH water at a temperature level of above 90 °C to function effectively [33].

A similar simplified relation can be generated for the relation between the ambient temperature and the return temperature of the DHn in 2019 [33]. This is seen in figure 2.3.

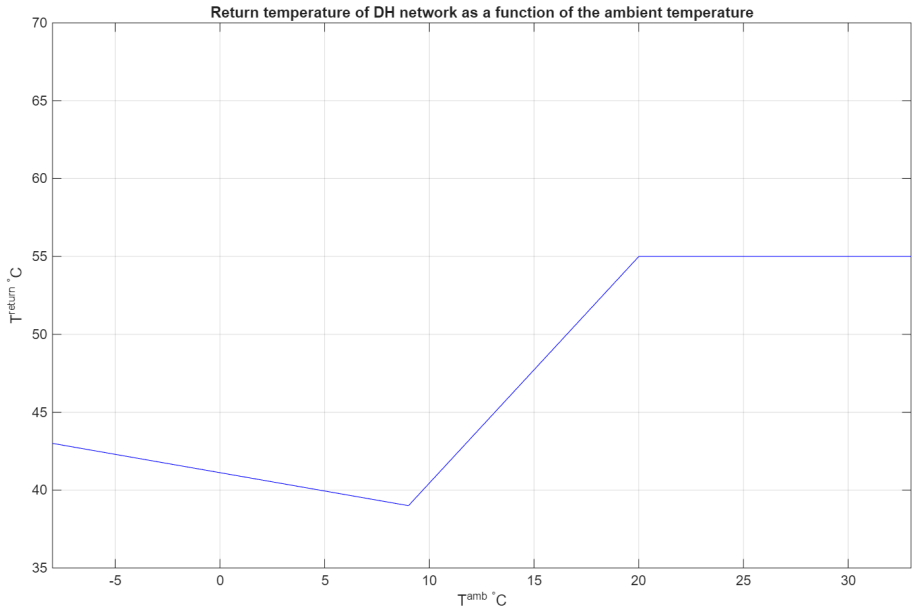

Figure 2.3: How the return temperature of the Gothenburg DHn varies with the outdoor temperature.

As for the DH supply temperature, the impact of the ambient temperature on the return temperature of the DHn can be represented mathematically as:

$$\begin{cases} T_t^{return} = 43°C \ - \ (T_t^{amb} - (-8°C)) \cdot 0.235 \ \forall \ T_t^{amb} \in (-\infty°C, 9°C) \\ T_t^{return} = 39°C \ + \ (T_t^{amb} - \ 9°C) \cdot 1.45 \ \forall \ T_t^{amb} \in [9°C, 20°C] \\ T_t^{return} = 55°C \ \forall \ T_t^{amb} \in (20°C, \infty°C) \end{cases}$$

In reality however, the temperature levels fluctuate over the year and are different for different regions inside of Gothenburg [33]. These levels should therefore be seen as states of ideal operation.

2.6.2 Production Units

Gothenburg has a mix of production units to supply both heat and electricity. These units have their own technical lifetime, which tells the model when to invest in new capacity. During normal operation, around 90 % of the electricity used in Gothenburg is imported from the Northern European system, but when the demand increases the locally produced electricity increases from 10- to 30% [38]. This increase in local production mainly comes from Rya KVV.

The existing capacities for production units are seen in table 2.1 for year 2035. It is assumed that the existing capacity in 2035 is the same as for year 2026. The combined heat and power (CHP) plants are a mix of wood chips and waste wood of roots and tops (RT). Rya KVV is a CHP plant with a combined cycle gas turbine with back-pressure (CCGT-BP). Also seen in the same table is a large supply in waste heat from the refineries and Renova waste incineration plant. The heat output from these two sources is not large compared to the whole system's heat capacity,

only 18 %. However, the production from these is almost always maxed out, meaning that the total heat production from these is large compared to the whole system. The total supply from the waste heat was 2360 GWh in the year 2019 [33].

Table 2.1: Existing production units in Gothenburg in year 2035 until 2050. Year 2060, all existing production units have been decommissioned [41].

Plant	Unit type	Fuel type	GW_{th} ** year 2035	GW_{th} ** year 2050	α ***
Renova WH	CHP	MSW	0.180	0.180	0.22
Refineries WH	-	-	0.170	0.170	-
Rya ÅP4	CHP	Wood chips/RT	0.140	0.140	0.29
Rya KVV *	CCGT-BP	Biogas	0.292	-	0.50
Ris P3	CHP	Wood chips/RT	0.030	-	0.29
Säv HP3	CHP	Wood chips	0.100	-	0.12
Rya HPs	HP	Electricity	0.150	0.050	3.33
Pellet boilers	HOB	Pellets	0.176	0.176	-
Gas boilers	HOB	Biogas	0.264	-	-
Bio-oil boilers	HOB	Bio-oil	0.272	0.026	-
Oil boilers	HOB	Fossil oil	0.200	-	-

* The existing plant is named Rya KVV, which stands for Rya CHP in English. However the plant is a CCGT-BP.

** During heating season.

*** Written as COP for HPs and not α.

Seen in table 2.1 is that most of the CHP plants have been decommissioned by 2050 due to their technical lifetime running out. Most heat-only boilers (HOBs) with bio-oil and all HOBs with fossil oil combustion have also been decommissioned until 2050. It is assumed that all capacity from Renova and the refineries are the same year 2050 as in year 2035. These values are changed in 4 main scenarios presented in section 3.8.

2.6.2.1 CCS Renova

Renova announced a goal to install carbon capture and storage (CCS) into their production in order to mitigate their carbon footprint by 2030 [42]. Out of the 540 000 tCO2 released year 2024, around 40 % was of fossil origin mainly coming from the incineration of plastic fractions [43]. This means around 200 000 tCO2/year has to be captured in order to acquire CO2 neutrality. Plans from Renova however is to install CCS to only 100 000 tCO2, which would result in a 50 % decrease [42] [43] [44].

Depending on the technology used for Renova to capture CO2, penalties in DH heat and electricity might come as a result. The following studies have been performed on the plant. Using monoethanolamine (MEA) will result in a 99% heat delivery and 80% electricity of normal operation [44]. Using hot potassium carbonate (HPC) will result in 107% heat and 56% electricity [44]. Another study looked into the possibility to use dry hydrated potassium carbonate (DHPC), which is a theoretical method not commercially available [43]. This method will give approximately 103%

in DH heat and 91.5-98% electricity production. The studies indicate that the DH supply from Renova won't be affected much from the CCS.

2.6.3 Storage Units

Physical properties for different storage types are presented in table 2.2. In Gothenburg, there is currently one accumulator tank installed (RyaTTES), with another accumulator tank planned to be installed (GasklTTES). The potential for TES in Gothenburg is limited for the different storage technologies. After consultation with Chalmers and Göteborg Energi, it was concluded that there is potential to use BTES, TTES and a CTES [33].

Table 2.2: Capacities and physical properties of TES in Gothenburg.

Storage Technology	Abbreviation	Maximum Capacity [GWh]	Injection-/ Extraction Rate [hours]	Temperature In/Out [°C] *	Source
Borehole storage with HP	HPBTES	792	4500/4500	50/60	[33]
Cavern storage with HP	HPCTES	35	350/350	40/80	[33]
Tank thermal energy storage **	TTES	-	60/60	Supply	[45]
Rya accumulator tank ***	RyaTTES	1	8.33/8.33	Supply	[33]
Gasklockan accumulator tank ***	GasKlTTES	1.45	14.5/19.33	Supply	[33]

* Temperatures are in/out of storage independent of HP. For TTES only the supply temperature of DH is stored.

** The maximum capacity is unbound.

*** These are already existing capacities in Gothenburg, therefore the capacity is already fixed.

There are currently five locations where BTES can be installed in Gothenburg [41]. Each 1 MW of discharge capacity gives a storage capacity of 4.5 GWh. This is independent of the HP installed. The storage temperature only reaches 60 °C, thus the temperature has to be upgraded before being supplied to the DHn, potentially through a HP.

In Gothenburg, there is currently potential for one CTES [33]. This storage comprises of two, 500 m long tunnels, each being 30 m high and 20 m wide. These have the potential to store 750 000 m^3 of hot water [46]. The 35 GWh of energy is assumed from a 40 °C temperature difference in the storage due to stratification (see section 2.4.1). The HPCTES was previously investigated and deemed non-profitable in earlier investigations [46]. The storage option is still allowed in this model to see if cost-effectiveness can be found under any operating conditions in the used model.

3
Method

In the first section the optimization model is presented after which the data collection and assumptions are introduced. Following this, the studied heat sources are explained and limitations in new capacity are presented. This is then followed up by the COP estimation model. Toward the end of the methodology, limitation of the HPs providing energy to the DHn is applied as availability profiles after which the thermal energy storages are explained in more detail and calculations regarding cost of producing heat are described. The section ends with a description of the different cases chosen to be studied further.

3.1 Model

This study used a LP optimization model to investigate the future potential of different kinds of large scale HPs in the Gothenburg DHn. The model used is a brownfield model of the energy system of Gothenburg, made at Chalmers. The model was first introduced by Heinisch et. al [47] in 2019 to correlate DH and electricity production in Gothenburg, and was further developed in 2021 by Heinisch et. al [48] to accommodate electric vehicle (EV) demand. In 2026, the model was extended by Rosén [49] to investigate how different transition pathways affect the cost-optimal solution. The model prior to this study, had a simplified representation of the HPs, with only one type of HP with constant COP. The heat sources were also set to be limitless, and no considerations of temperature levels or placement of the HPs were taken into account. The main additions to the model in this study are: a better representation of HPs in the city, with a wider variety of HP options with limitations in heat source availability and DHn transmission capacities for the different options. COP will be time dependent using hourly temperature data for the heat sink and the heat source. COP varies to different extents during the year for the different HPs. Using time dependent COP will give the model more flexibility to optimize production as explained in section 2.3.

The model has an objective function to minimize the total system costs over the years 2030-2080. The model runs using hourly time resolution over several years, modeling each 5th year between 2030-2050 and each 10th year between 2050-2080. Each year has the same normalized electricity- and heat demand profile. However, different time dependent parameters, such as the demand for electricity, are scaled to growth throughout each year, meaning the amplitudes change. The objective function is seen in equation (3.1) where c_{tot} is the total system cost over all years.

$C^{inv}_{y,p}$ and $C^{OM_{fix}}_{p}$ are the investment costs and the fixed operational and maintenance costs respectively, for each technology or plant, which are related to the new installed capacity ($i_{y,p}$) for each technology. The variable running costs (C^{run}_{p}) are dependent on the year- and time dependent (y,t) generation from the different technologies ($g_{y,p,t}$), which includes both invested in technologies and already existing capacities. Other costs included in the variable running costs are startup- ($c^{start}_{y,p,t}$) and part-load costs ($c^{partload}_{y,p,t}$) for the different thermal power plants. Lastly, the costs for imported electricity are summarized over the electricity price ($C^{el}_{y,t}$) and the actual time dependent imports/exports ($w_{y,t}$), where $w_{y,t}$ can act as positive numbers for imports and negative for exports. All of these are annualized with discount rate (r) of 5% and start year (Y_{start}). The model Rosén [49] made was also dependent on costs associated with H2 pipelines, which are not included in this version. For further details of the model the reader is referred to [49].

$$\min c_{tot} = \sum_{y \in Y} \left(\left(\sum_{p \in P} \left(\left(C^{inv}_{y,p} + C^{OM_{fix}}_{p} \right) \cdot i_{y,p} + \sum_{t \in \tau} \left(C^{run}_{p} \cdot g_{y,p,t} + c^{start}_{y,p,t} + c^{partload}_{y,p,t} \right) \right) + \sum_{t \in \tau} C^{el}_{y,t} \cdot w_{y,t} \right) \cdot \frac{1}{(1+r)^{y - Y_{start}}} \right) \quad (3.1)$$

Equations (3.2) and (3.3) describe the balances of producing electricity and heat with the corresponding demands. In equation (3.2), the electricity demand each hour for the different years ($D^{el}_{y,t}$) is combined with charging of stationary batteries ($b^{ch}_{y,P_{ElSt},t}$), charging of electric vehicles ($ev^{ch}_{y,e,t}$), electricity to heating technologies ($g_{y,P_{P2H},t}$)/($\mathrm{COP}_{p,t}$) where $\mathrm{COP}_{p,t}$ is the time dependent efficiency of the technology p, electricity to produce H2 in electrolyzers ($g_{y,PEM,t}$), electricity for compressors into storage ($K \cdot b^{ch}_{y,P_{H_2St},t}$), the electricity used to discharge heat storages involving HPs ($b^{dch}_{y,P_{HStHP},t}$) and the corresponding $\mathrm{COP}_{p,t}$ of their integrated HP. The discharge from the storage is defined as before the HP, visualized in figure A.11. These must in each time step be less than or equal to generation of electricity ($g_{y,P_{El},t}$), stationary battery discharge ($b^{dch}_{y,P_{ElSt},t}$), vehicle-to-grid (V2G) discharge ($ev^{dch}_{y,e,t}$) and electricity imports/exports ($w_{y,t}$). The generation from the P2H technologies is expressed in thermal energy, so the value has to be divided with the COP, in order to convert it into electricity used.

$$D^{el}_{y,t} + \sum_{p \in P_{ElSt}} b^{ch}_{y,p,t} + \sum_{e \in E} \mathrm{ev}^{ch}_{y,e,t} + \sum_{p \in P_{P2H}} \frac{g_{y,p,t}}{\mathrm{COP}_{p,t}} + g_{y,PEM,t} + \sum_{p \in P_{H2St}} K \cdot b^{ch}_{y,p,t} + \sum_{p \in P_{HStHP}} \frac{b^{dch}_{y,p,t}}{\mathrm{COP}_{p,t} - 1} \leq \sum_{p \in P_{El}} g_{y,p,t} + \sum_{p \in P_{ElSt}} b^{dch}_{y,p,t} + \sum_{e \in E} \mathrm{ev}^{dch}_{y,e,t} + w_{y,t} \quad \forall\, y \in Y, \forall\, t \in \tau \quad (3.2)$$

In equation (3.3) the heat demand each hour ($D^{heat}_{y,t}$) is coupled with stored heat ($b^{ch}_{y,P_{HSt},t}$). These are in every time step less than or equal to the produced heat from HPs, HOBs etc. ($g_{y,P_H,t}$), heating from CHP plants ($g_{y,P_{CHP},t}/\alpha_p$) with electricity-to-heat ratio (α_p), discharged heat in storages ($b^{dch}_{y,P_{HSt},t}$) and available waste heat ($X_{y,t}$) from the refineries and the waste incineration plant.

$$D_{y,t}^{heat} + \sum_{p \in P_{HSt}} b_{y,p,t}^{ch} \leq \sum_{p \in P_H} g_{y,p,t} + \sum_{p \in P_{CHP}} \frac{g_{y,p,t}}{\alpha_p} + \sum_{p \in P_{HStTank}} b_{y,p,t}^{dch} + \sum_{p \in P_{HStHP}} \frac{b_{y,p,t}^{dch}}{1 - \frac{1}{\mathrm{COP}_{p,t}}} + X_{y,t} \quad \forall\, y \in Y, \forall\, t \in \tau \quad (3.3)$$

3.1.1 Data and Assumptions

This subsection presents the data that has been used as input to the model and assumptions that have been made.

3.1.1.1 Electricity- and Heat Demand Profiles

The electricity demand profile in 2019 is based on actual consumption data in Gothenburg. To account for the expected population growth in Gothenburg, it has been assumed that the electricity demand in 2050 is 20% larger compared to the 2019 level as explained by Bertilsson et al. [12]. Since this model includes multiple years reaching from 2030 to 2080 (with 5-years intervals between 2030-2050 and 10 years intervals between 2050-2080) the electricity demand growth for each time period has been scaled linearly in relation to the 2050 level, such that each 5-year time period implies a 4% increase in relation to the 2019 level. The same growth is also expected after 2060, but for 10 years intervals instead, due to the assumption of increased energy efficiencies resulting in a lower demand growth. The electricity demand origins from the demands of the residential, commercial and industry sectors [50]. The electricity demand for each studied year in relation to the 2019 level is given in table 3.1.

Table 3.1: Electricity demand in relation to the 2019 level.

Year	Electricity demand profile
2030	$1.04 \cdot D_{2019,t}^{el}$
2035	$1.08 \cdot D_{2019,t}^{el}$
2040	$1.12 \cdot D_{2019,t}^{el}$
2045	$1.16 \cdot D_{2019,t}^{el}$
2050	$1.20 \cdot D_{2019,t}^{el}$
2060	$1.28 \cdot D_{2019,t}^{el}$
2070	$1.32 \cdot D_{2019,t}^{el}$
2080	$1.36 \cdot D_{2019,t}^{el}$

The heat demand profile has a similar temporal resolution as the electricity demand profile and is based on actual data of Gothenburg in 2019. It includes the heating demands from the residential-, commercial- and industrial sectors, but does not take into account demand for high temperature process heat [50]. The heat demand is assumed to remain constant over the years as a result of the opposing effects between

increased energy efficiencies and warmer climate which reduce the heat demand, and the population growth which increases the demand [12]. The heat demand in Gothenburg for year 2019 is seen in figure 3.1, where also the two demand peaks during the year are shown by the arrows.

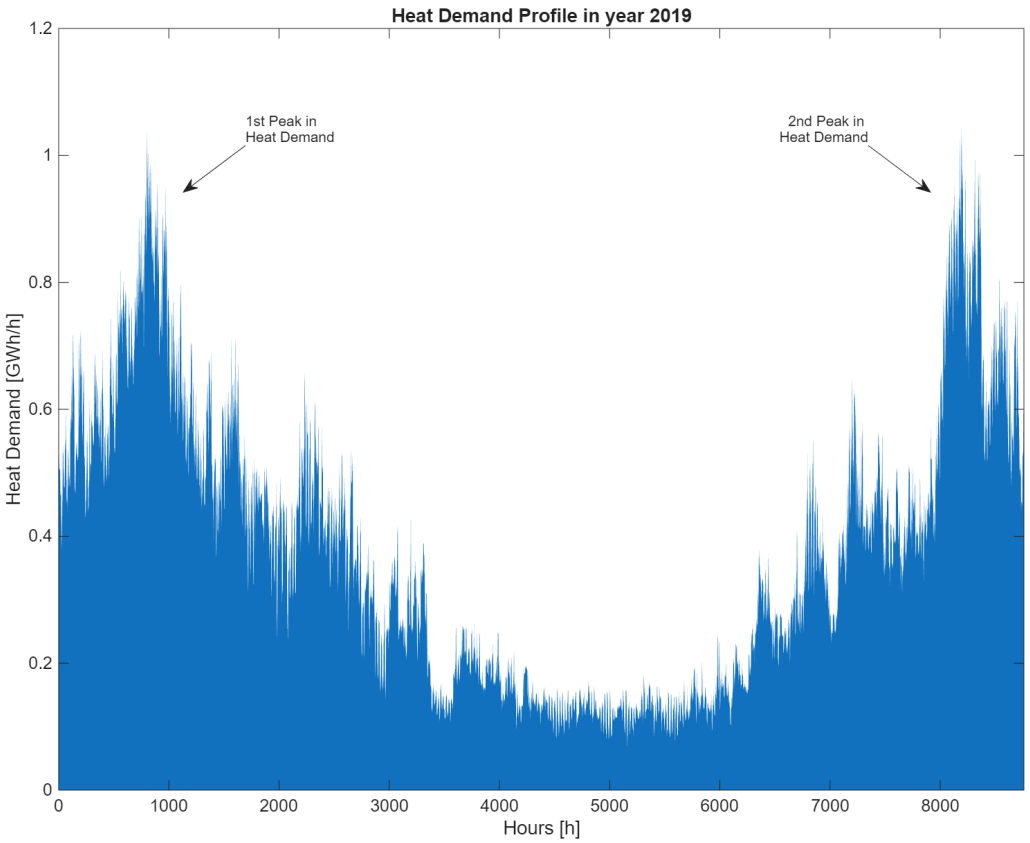

Figure 3.1: Heat demand profile for the year 2019, showing two peaks in heat demand during the year.

3.1.1.2 Electricity Prices

The electricity prices used as input in this model originates from a model conducted by Göransson et al. [16] called ELLI (ELectricity Long-term Investment), where a linear optimization investment model for minimizing the total system costs of the northern Europe's energy mix was developed. The model accounts for the expected growth of demand in the time period 2030-2065, taking into account the projected growth of energy usage in sectors such as new industries, electricity for H2, transport, and the DHn, and proposes energy mixes which meet these constraints at the lowest cost. As this study includes an investment period reaching up until year 2080, it has been assumed that the electricity price profile, from year 2065 and onward, is that of year 2065. This means that the years 2070-2080 have the same electricity prices, due to the investment periods defined in the model.

The ELLI model also has a high temporal resolution with a large spatial scope to capture the intermittency patterns of renewable sources, flows of trade between

countries and investments over time reflecting an increasing energy demand. It is the long-term marginal cost resulting from the different energy mixes, mainly consisting of wind power, solar photovoltaics (PVs) and hydropower, that is used as input to the model to represent future electricity prices in the price region SE3. The ELLI model has been run using the weather year of 2019 to match the heat- and electricity profiles that are used in this model. An example of how the marginal cost of electricity changes over the year 2050 in the price region SE3 can be seen in figure 3.2. The rapid increase in electricity price around hour 600 is due to new investments in peak units having to operate with a high marginal cost. For more information, the reader is referred to [16]. How the average electricity prices varies over each studied year in the model, compared to real data for year 2019 and year 2025, can be seen in figure A.1 in appendix A.1.

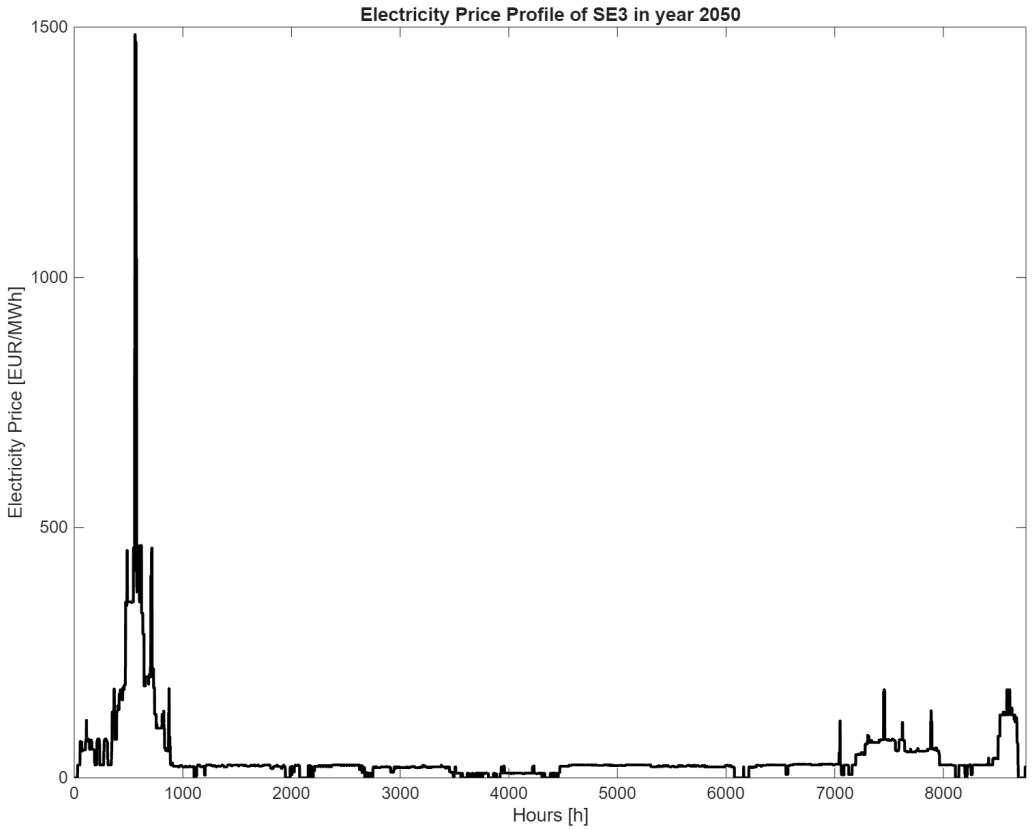

Figure 3.2: Electricity price for 2050 in price region SE3. Price originates from another model called ELLI.

Seen when comparing heat demand and electricity price is that the 1st heat demand peak will align with the high electricity prices in the beginning of the year. The 2nd heat demand peak will align with a comparably low electricity price. This can partly be explained with high penetration of wind during the 2nd heat demand peak. An averaged, weekly, wind profile for the west coast of Sweden can be seen in figure A.2 in appendix A.1.

3.1.2 Costs of Technologies

Most of the costs associated with the different types of technologies have been retrieved from the Danish Energy Agency (DEA) [51] for different years to account for technological learning. As the DEA recommends costs based on a heat sink temperature of 75 °C for HPs, an additional factor of 5% has been added to the investment costs as higher temperature lifts might require components that are suitable for higher pressures. For HPs not included in the DEA, the costs have been assumed equal to the most similar type of HP. Costs for technologies not included in the DEA have been taken from projects and plans Göteborg Energi have done previously. A summary of the technologies, their technical lifetime and CAPEX in 2050 is shown in table 3.2. A total list of the costs including the CAPEX and the variable- and fixed O&M over the modeled years are summarized in table A.1 in appendix A.2. Fuel costs associated with the different technologies are given in table A.2 in appendix A.2.

Table 3.2: Investment costs and technical lifetime of technologies included in the study.

Technology	Abbreviation	Technical lifetime (years)	CAPEX [EUR/kW] year 2050
Offshore wind	WOFF	30	1640
Optimal tilt Solar PVs	PVOpt	40	290
Rooftop Solar PVs	PVRoof	40	636
Gas turbine biogas	Peak_{WG}	25	550
Combined-cycle gas turbine biogas	CCGT_{WG}	25	850
Combined-cycle backpressure gas turbine biogas	$\text{CCGT}_{BP,WG}$	25	1168
Combined heat and power biomass	CHP_{W}	25	3360
Heat only-boiler biomass	HOB_{W}	25	430
Heat only-boiler biogas	HOB_{WG}	25	50
Heat only-boiler pellets	$\text{HOB}_{Pellets}$	25	650
Heat pump seawater	HP_{Sea}	25	420
Heat pump sewage water	HP_{Sew}	25	420
Heat pump air	HP_{Air}	25	851
Heat pump hydrogen PEM	HP_{H2}	25	641
Heat pump battery factory	HP_{BF}	25	641
Electric boiler	EB	25	60
Electrolyzer	PEM	25	325
Cavern storage with heat pump	HPCTES	55	1.1
Borehole storage with heat pump	HPBTES	55	0.5
Tank thermal energy storage	TTES	55	3
Hydrogen storage	H2_{tank}	25	22

3.2 Heat Sources of Heat Pumps

This section presents the heat sources that have been analyzed together with descriptions regarding data gathering and other specifics.

3.2.1 Seawater

The temperature profile for seawater was gathered from the Swedish meteorological- and hydrological institution (SMHI) [52] from the station Göteborg-Krossholmen as

this was one of few stations located in Gothenburg that had measurements for the year 2019. It did however not have measurements for all hours during 2019 and thus, 10 data points from the beginning of the year 2020 have been used as a complement to have a full profile of the seawater temperature. The values are measured at a depth of 1 meter, meaning that the temperatures follows the same seasonal dependencies as the ambient air. The temperatures of the surface layers are more volatile compared to the temperature levels at deeper depths where the temperature levels are more consistent [53]. From a producer point of view it would become more beneficial to use water at a deeper depth to enable the HPs to run during more time periods over the year as the risk of freezing is lower. However, since no data was commercially available at deeper depths, the depth of one meter is a limitation in this study. Due to the risks of freezing at too low seawater temperatures, there is a lower limit to when seawater HPs can operate. In this model, it is set at an inlet temperature of 2.5 °C based on the limit of an already existing seawater HP in Stockholm [54].

3.2.2 Ambient Air

Data for hourly temperature measurements in 2019 was acquired from SMHI [55] from three different stations scattered around Gothenburg. The three stations were Göteborg-Rya, Göteborg-Rosenlund and Göteborg A. The data from the different stations were aggregated and a mean value was calculated. This was necessary as neither of the stations had hourly data for all hours of 2019, but by aggregating them and calculating a mean value, a complete profile with hourly resolution was generated. For clear outliers in the data indicating errors in the measuring devices (temperatures reaching -25 °C during the middle of the day in the summer), the temperatures for these hours were approximated as the mean of the hours before and after, or as having the same profile as the day before in the case that multiple errors happened sequentially. Due to this, the measurements of the ambient temperature become a source of uncertainty in the current study, but as the temperatures come from an open source, it would be easier to generalize the method for other cities, motivating that these measurements should be used.

Air does not have the problem of freezing as for instance seawater, but as air consists of water there is a risk for formations of frost on the evaporator surface at ambient temperatures reaching below 7 °C [56]. The formation of frost will reduce the COP-value of the air-source HPs by approximately 15%, which is what has been used in this study.

3.2.3 Sewage Water

The HPs at Rya are connected with Gryaab, which provides treated sewage water that is used as input to the evaporators of the HPs [57]. Treated sewage water has a relatively more stable temperature profile compared to seawater and ambient air and was collected by Göteborg Energi for 2019. Due to the risk of melted snow mixing with the sewage water during colder periods, it becomes hard for the HPs to operate at sewage water temperatures below 8 °C as there is a risk of ice blocks

entering the evaporator [58].

3.2.4 Heat from Electrolyzers Producing Hydrogen

One way to increase the overall efficiency of electrolyzers is to recover the heat that is generated in the electrolyzer stack. For each unit of electricity that is used to generate H2, a certain share of that electricity (η^{WH}) is converted into useful heat [59]. Depending on the type of electrolyzer configuration, the temperature of the water leaving the electrolyzer varies, meaning that a HP is necessary to lift the temperature to the required DH temperature. The electrolyzers that have been included in this analysis are proton-exchange membrane (PEM) electrolyzers. The hot water from the electrolyzer therefore becomes the inlet stream to the evaporator of the HP. The upper limit of the heat leaving the HP_{H2} is thus constrained by the electricity used to produce H2 in the electrolyzer. The modeling constraint becomes:

$$g_{y,HP_{H2},t}\left(1 - \frac{1}{\text{COP}_{HP_{H2},t}}\right) \leq \eta^{WH} \cdot g_{y,PEM,t} \;\forall\; y \in Y,\; \forall\; t \in \tau \tag{3.4}$$

This is however the theoretically maximum amount of waste heat that can be recovered, but with the current DHn constraints the recoverable waste heat is lower since the HPs recovering waste heat from electrolyzers are assumed to be placed next to the refineries which have limited transmission capacities. The temperature level for PEM electrolyzers has been assumed constant at 60 °C, as this is the temperature level that has been used in previous studies at Göteborg Energi [41]. It is further assumed that the temperature difference of the heat source is 10 °C as proposed by Tommasini et al. [59].

3.2.5 Heat Recovery from Battery Factory

In 2022, there was a decision that a large battery factory (BF) would be introduced in Gothenburg which was expected to be finished in 2026 [60], but previously this year it was stated that the operation of the factory was put on halt [61] until a new technology partner is approved. In this study however, it is assumed that the production of the factory will be online in 2035, meaning that the excess heat produced by the factory will be handled by Göteborg Energi to produce heat for the DHn [60].

The battery production facility is expected to use around 1-2 TWh of energy annually, and in this case the upper value has been used. It is further assumed to be of constant load, resulting in an electricity increase of 228 MW. In the case that the factory becomes active, the flow of the water entering the HP facility is expected to have a temperature of around 30 °C [62], depending on the battery technology that NOVO choose to pursue [58]. The temperature difference over the evaporator for the heat source is 10 °C as a higher temperature difference reduces the necessary mass flow [58]. The maximum capacity of the HP is 50 MW_{th}. In case the battery factory is not introduced, it is assumed that another industry will use the pipes instead with a similar cooling demand such that the temperatures remain the same.

3.3 Limitations in New Capacity

New investments in Gothenburg are limited for the different generation technologies and storages. The constraints defined are either: geographically- or technically limited. Each technology can have one or both types. A geographical constraint is coupled with transmission capacity with more- or less resolution. Meaning, sometimes equations are specific to individual pipes (high resolution), meaning that neighboring production might not be included. Sometimes the equations have an unspecified cluster of pipes within a geographical area (low resolution). There are also technical constraints coupled with the actual potential of a technology without transmission constraints. For example: maximum heat source available for HP_{Sew}.

The constraints come from Göteborg Energi [33] and the ones presented below are relevant for a specific scenario (*Scenario 2*) described in more detail in section 3.8. Some constraints change with years, some are also influenced by the scenario studied. The limits coupled with different constraints and how they change between years for the main 4 scenarios are presented in table 3.4 in section 3.8.

Important to clarify is that the model uses one aggregated demand, meaning the model is treated as one node. This means that the generation combined from all technologies is bound by the total demand, not by individual demands for certain regions. This means that the geographical constraints become limited in their implementation. The equations presented are thus a translation from actual geographical- and technical constraint onto individual technologies, meaning there is actually no geographical resolution in the model. In this study, two areas of interest have been in focus, in order to correctly limit the current- and future potential of HPs in the DHn of Gothenburg. One area is North-West Gothenburg, where the largest potential for HPs is located, together with the two refineries previously mentioned. The other area of focus is the geographical area of Rya, included into North-West Gothenburg, where HP_{Sew} is currently located.

Firstly, the constraint in Rya is defined, where two technologies constrain each other in a geographical constraint with high resolution. This constraint only defines two HP-types, presented in equation (3.5) as:

$$\sum_{p} g_{y,p,t} \leq 0.16 \text{ [GW]} \; \forall \; y \in Y, \; \forall \; p \in \{HP_{Sew}, HP_{BF}\}, \forall \; t \in \tau \tag{3.5}$$

Geographically, other technologies are in close proximity, but do not share the same pipes. Individually, HP_{Sew} and HP_{BF} also have technical constraints of maximum heat source availability, denoted in equations (3.6) and (3.7) as:

$$g_{y,p,t} \leq 0.16 \; [GW] \; \forall \; y \in Y, \forall \; p \in HP_{Sew}, \forall \; t \in \tau \tag{3.6}$$

$$g_{y,p,t} \leq 0.05 \text{ [GW]} \; \forall \; y \in Y, \forall \; p \in HP_{BF}, \forall \; t \in \tau \tag{3.7}$$

HP_{Sew} and HP_{BF} are part of a larger constraint binding more technologies out of North-West of Gothenburg. The technologies also included are: $\text{HP}_{Sea,Rya}$, HP_{H2}, RyaTTES and HPCTES. This limitation is stated as:

$$\sum_{p \in \{HP_{Sew}, HP_{BF}, HP_{Sea,Rya}, HP_{H2}\}} (g_{y,p,t}) + b^{dch}_{y,RyaTTES,t} + \frac{b^{dch}_{y,HPCTES,t}}{1 - \frac{1}{\text{COP}_{HPCTES,t}}} \leq 0.21 \text{ [GW]} \ \forall \ y \in [2030], \forall \ t \in \tau \quad (3.8)$$

Equation (3.8) will vary with scenarios studied. The constraint will also become more relaxed with each year, when capacity in the area is decommissioned, seen in table 3.4.

Another constraint not directly implemented into North-West Gothenburg is how HP_{Sea} is constrained. There are two locations possible in Gothenburg with transmission capacity, one in Rya ($\text{HP}_{Sea,Rya}$) and one in Rosenlund ($\text{HP}_{Sea,RL}$). Seen in equation (3.8), $\text{HP}_{Sea,Rya}$ will be constrained by the other technologies together by its own constraints defined by equations (3.9) and (3.10) as:

$$g_{y,p,t} \leq 0 \text{ [GW]} \ \ \forall \ y \in [2030, ..., 2045], \ \forall \ p \in HP_{Sea,Rya}, \ \forall \ t \in \tau \quad (3.9)$$

$$g_{y,p,t} \leq 0.292 \text{ [GW]} \ \ \forall \ y \in [2050, ..., 2080], \ \forall \ p \in HP_{Sea,Rya}, \ \forall \ t \in \tau \quad (3.10)$$

The freed capacity from year 2050 is due to Rya KVV being decommissioned. $\text{HP}_{Sea,RL}$ is constrained by a transmission constraint in Rosenlund in equation (3.11) as:

$$g_{y,p,t} \leq 0.1 \text{ [GW]} \ \forall \ y \in Y, \forall \ p \in HP_{Sea,RL}, \forall \ t \in \tau \quad (3.11)$$

HP_{H2} is constrained due to transmission capacity available from existing pipes from the refineries. As waste heat disappears with electrification, that transmission capacity can be used by the HPs instead, defined in equation (3.12) as:

$$g_{y,p,t} \leq 0.06 \text{ [GW]} \ \forall \ y \in Y, \forall \ p \in HP_{H2}, \forall \ t \in \tau \quad (3.12)$$

This constraint is a transmission constraint. In sensitivity analysis when transmission constraints are removed, the maximum production from HP_{H2} is instead constrained by a technical constraint, defined in equation (3.4).

The last constraint in North-West Gothenburg is associated with the potential location of a HPCTES. This constraint is a technical one, defined in equation (3.13) as:

$$\frac{b^{dch}_{y,p,t}}{1 - \frac{1}{\text{COP}_{p,t}}} \leq 0.100 \text{ [GW]} \ \forall \ y \in Y, \forall \ p \in HPCTES, \forall \ t \in \tau \quad (3.13)$$

The maximum potential for HPBTES is a transmission constraint, due to four possible locations with an accumulated maximum discharge defined in equation (3.14) as:

$$\frac{b^{dch}_{y,p,t}}{1-\frac{1}{\mathrm{COP}_{p,t}}} \leq 0.180 \text{ [GW]} \; \forall \; y \in Y, \forall \; p \in HPBTES, \; \forall \; t \in \tau \tag{3.14}$$

There are also previously defined constraints already in the model, which still apply. The maximum capacity for on-shore wind is zero in all scenarios, as on-shore wind has no potential to develop in the region. For off-shore wind, a maximum potential of 1 GW in the Gothenburg area has been assumed based on a project called Västvind [63]. The maximum deployment of solar PVs, optimal tilt and rooftop, is 0.1 GW and 1.9 GW respectively. The available area for rooftop solar PVs is based on a model presented by Wiginton et al. [64] that depends on population size and an assumption of power output per capita of crystalline solar PVs. The import capacity currently in Gothenburg is 0.895 GW, but is assumed to increase up to 1.545 GW by 2030 [49].

3.4 COP Estimation of Heat Pumps

The method chosen for approximating the time-dependent COP values, is the method proposed by Jensen et al. [26] as it has been shown that this model gives results that are similar to those of thermodynamic models [25]. The calculations for the COP is shown in equation (3.15) where COP_J is the corrected Jensen COP. The COP depends on the logarithmic mean temperature of the hot and cold streams ($\bar{T}_H$ and $\bar{T}_c$), the COP of a Lorenz cycle (COP_L), the logarithmic pinch point temperature difference of the heat exchanger ($\Delta\bar{T}_{pp}$), specific compressor features ($\eta_{is,c}$ and F_Q), and characteristics of the refrigerant ($\Delta\bar{T}_{r,H}$, $\Delta\bar{T}_{r,C}$, $\frac{w_{is,e}}{w_{is,c}}$). For ammonia and isobutane, relationships are found for calculating the refrigerant specific parameters, and thus ammonia has been assumed as the refrigerant in this study. Ammonia is a widespread refrigerant that is commonly used in large-scale HPs for DH [65] [22] [66], and its usage is expected to increase in large-scale HPs in Europe [67]. One drawback of ammonia however is its toxicity, but for larger systems this can be handled relatively simple through precautionary safety measures [22]. With this said, ammonia has been assumed in this work.

$$\mathrm{COP}_L = \frac{\bar{T}_H}{\bar{T}_H - \bar{T}_C}$$

$$\mathrm{COP}_J = F_{corr}\left(\mathrm{COP}_L \frac{1+\frac{\Delta\bar{T}_{r,H}+\Delta\bar{T}_{pp}}{\bar{T}_H}}{1+\frac{\Delta\bar{T}_{r,H}+\Delta\bar{T}_{r,c}+2\Delta\bar{T}_{pp}}{\bar{T}_H-\bar{T}_C}}\eta_{is,c}\left(1-\frac{w_{is,e}}{w_{is,c}}\right)+1-\eta_{is,c}-F_Q\right) \tag{3.15}$$

The cold source is assumed to be cooled 5 K for all heat sources apart from seawater where it was assumed that it could be cooled 3 K, unless specific temperature differences have been stated. The reason for having a lower ΔT for seawater is to

decrease the risks of having problems with freezing. It becomes beneficial to increase the mass flow, which means that a lower temperature difference can be designed for [68]. Having a lower temperature difference at the heat source heat exchanger also means that the seawater HPs can be utilized for more hours since the water is cooled less and can as a result be utilized even at lower temperatures. To account for the fact that higher temperature lifts might require a two-stage cycle, a correction factor, F_{corr}, of the COP-value of 1.05 has been assumed as presented in Pieper et al. [69]. An explanation of the input parameters used for the COP estimations is given in table 3.3.

Table 3.3: Input parameters in equation (3.15)

Parameter	Value	Unit
F_{corr}	1.05	[-]
$\Delta\bar{T}_{pp}$	ΔT_{pp}	[K]
$\Delta\bar{T}_{r,H}$	Estimated from [26]	[K]
$\Delta\bar{T}_{r,C}$	$\frac{1}{2} \cdot \Delta T_c$	[K]
$\eta_{is,c}$	0.8	[-]
$\frac{w_{is,e}}{w_{is,c}}$	Estimated from [26]	[-]
F_Q	0	[-]
$\bar{T}_H$	$\Delta T_H / ln(T_{H,o}/T_{H,i})$	[K]
$\bar{T}_C$	$\Delta T_C / ln(T_{C,i}/T_{C,o})$	[K]

The pump work coupled with the heat sink and heat source is not included when calculating how much electricity is needed for the HPs. The pump work is accordingly not associated with the HP, but rather to the DHn, so the assumption is that the pump work is allocated into the already existing electricity demand.

3.5 Availability Profiles of Heat Pumps in the District Heating System

As the temperature lift is dependent on the refrigerant being used, as explained in section 2.2.1, this means that the HPs can only lift the supply temperature to a certain temperature level.

Since the supply temperature of the DHn fluctuates over the year, it further means that there will be some hours of the year where the HPs cannot supply all the heat necessary to the heat sink. For ammonia, the upper limit of condensing temperature for safe operation is around 87 °C [70]. With the assumed pinch point temperature of 5 °C in the condenser, this means that the maximum supply temperature of the DHn possible from large-scale HPs using ammonia is 82 °C. This can be explained by the diagram in figure 3.3.

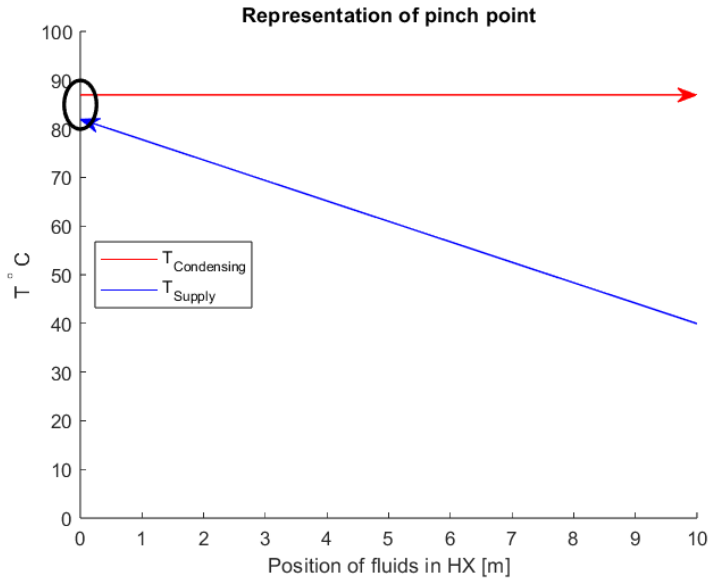

Figure 3.3: Representation of pinch point and maximum supply temperature. The values on the x-axis represents how the temperature of the DH water changes as it passes the heat exchanger, but the values have no significance. The input supply temperature also varies so this is just an example representing how the pinch point affects the maximum supply temperature.

The implication this has in the model is that constraints have to be set limiting the total demand of heating that can be fulfilled by the HPs. This was done by calculating the ratio between the energy needed to lift the DH water to the wanted temperature and the possible amount of energy that the HPs could provide at each time step. The energy required to lift the DH water to its set supply temperature is given in equation (3.16), where ($\dot{Q}^{needed}$) represents the energy needed, and is dependent on the mass flow ($\dot{m}$), the specific heat capacity of water (c_p) and the difference between the temperature at the inlet (T^{return}) and the temperature at the outlet (T^{supply}).

$$\dot{Q}_t^{needed} = \dot{m}_t \cdot c_p \cdot (T_t^{supply} - T_t^{return}) \; \forall \; t \in \tau \tag{3.16}$$

The maximum temperature the HPs can provide is 82 °C, which is referred to as (T^{max}). The total amount of energy ($\dot{Q}^{HP}$) that the HPs can provide to the DH water in the condenser can thereby be calculated according to equation (3.17).

$$\dot{Q}_t^{HP} = \dot{m}_t \cdot c_p \cdot (T^{max} - T_t^{return}) \; \forall \; t \in \tau \tag{3.17}$$

As a result of this, the ratio (γ) between the heat flows only becomes a function of the temperatures, shown in equation (3.18). This is under the assumption that the specific heat capacity of water stays constant for small temperature differences.

$$\gamma_t = \frac{\dot{Q}_t^{HP}}{\dot{Q}_t^{needed}} = \frac{\dot{m}_t \cdot c_p \cdot (T^{max} - T_t^{return})}{\dot{m}_t \cdot c_p \cdot (T_t^{supply} - T_t^{return})} = \frac{(T^{max} - T_t^{return})}{(T_t^{supply} - T_t^{return})} \; \forall \; t \in \tau \tag{3.18}$$

By calculating the ratio between the energy from the HPs to the energy needed for the DH water, availability profiles could be created that limit the total supply that the HPs can provide to the DHn. This is necessary to not overestimate the potential of HPs since in the cases that the ratio is smaller than one, other heat generating facilities such as EBs or biogas heat only-boilers (HOB_{WG}) need to provide the remaining energy to lift the supply temperature to the required value [33]. The total amount of energy that the HPs can provide in each time step is therefore limited by equation (3.19).

$$\sum_{p \in P_{HP}} g_{y,p,t} + \sum_{p \in P_{HStHP}} \frac{b^{dch}_{y,p,t}}{1 - \frac{1}{\mathrm{COP}_{p,t}}} + \sum_{p \in P_{HStTank}} b^{dch}_{y,p,t} + X_{y,t} \leq \gamma_t \cdot D^{heat}_{y,t} \quad \forall\ y \in Y,\ \forall\ t \in \tau_{winter} \tag{3.19}$$

There are of course certain limitations that need to be mentioned when it comes to estimating the heat supply that the HPs can cover. This method assumes that the temperature of the DHn remains constant across the city, which in reality is not the case. If HPs hence are placed at geographically strategic locations, the possibilities of providing energy over a larger period of the year increase. It is further assumed that existing HPs can lift the temperatures to similar levels which also in reality might differ slightly.

3.6 Modeling of TES

Modeling of the heat storages looks different, depending on which type of storage that the model invests in. The differences are mainly related to how the storage utilizes the energy stored, through different configurations depending on the temperature range in the storage. For example, the CTES works with lower temperatures, and thereby needs a HP to upgrade the temperature. Accumulator tanks work with higher temperature, meaning that they only use heat exchangers to utilize the energy stored. As data is limited from DEA [45] to only PTES (not possible in Gothenburg) and TTES, the costs for other storage types had to be calculated independently. More information regarding modeling assumptions can be found in appendix A.10.

3.6.1 Modeling of CTES

The CTES potential in Gothenburg was assumed 35 GWh, depending on a temperature lift of 40 °C with a hot side of 80 °C and a cold side of 40 °C. As 80 °C is sometimes higher than the supply temperature of the DHn, the COP calculations became problematic, and therefore the hot side was lowered to 70 °C. In order to keep the same temperature difference in the storage, the cold side was also lowered by 10 °C to 30 °C. The temperatures in the storage was assumed to be constant, leading to perfect stratification, explained in section 2.4.1. In real life operation however, the temperature on the hot- and cold side change with storage volume. To

simplify and guarantee that discharge is feasible in all time steps, the discharge of the storage is done with a HP, resulting in a need for electricity. Charging of the storage is made through a heat exchanger.

3.6.2 Modeling of BTES

BTES is assumed to only be able to invest in the configuration with combination of a HP. As the temperature of the storage is lower on average (60 °C) than the supply temperature needed, the storage would not have sufficient temperature to discharge the energy stored. In reality the storage would have a temperature gradient over the year, however for this project, it was advised by Göteborg Energi [41] to only use the HP option. For the COP, the same method was used as other HPs, where the COP would vary throughout the year.

3.6.3 Modeling of TTES

TTES information was available from DEA [45] and already implemented into the model. Unlike the other storage types, TTES doesn't use a HP to supply heat. The storage is assumed to not be dependent on temperatures, only state of charge (SOC).

3.6.4 State of Charge

The SOC-equation defines the storage energy level in each individual TES in the model. The temperatures in the storages are not included in the model, only the total energy. All TES follows the SOC-equation defined in equation (3.20) as:

$$soc_{y,p,t+1} = soc_{y,p,t} \cdot (1 - L_{y,p}) + b^{ch}_{y,p,t} \cdot \eta^{ch}_{y,p} - \frac{b^{dch}_{y,p,t}}{\eta^{dch}_{y,p}} \; \forall \; y \in Y, \; \forall \; p \in P_{HSt} \; , \forall \; t \in \tau \tag{3.20}$$

The equation includes SOC for the current time step ($soc_{y,p,t}$), plus the next time step ($soc_{y,p,t+1}$). The SOC in the current time step has a loss term depending on the amount of stored energy ($L_{y,p}$), losses during charging (η^{ch}) and losses during discharging (η^{dch}). The charged- and discharged energy is defined as b^{ch} and b^{dch}.

The equation works both for TES with- and without a HP, as the boundary of the equation is defined before the HP. The HP is instead accounted for in the heat-equation for the whole system (equation (3.3)). In appendix A.10, a more detailed explanation is given, together with a visualization of the boundary in figure A.11.

3.7 Cost of Producing Heat

It is of interest to study how the costs of producing heat via DH compares to the costs of producing heat for an individual household. The costs for producing DH

were calculated based on a Greenfield model as not enough time was left to apply it to the Brownfield model. The annual costs (c_N) were normalized to the heat produced such that an average cost of producing heat over the year was calculated. This was necessary as the heat produced from DH is much larger than the heat produced for an individual household, but by normalizing both of the calculations a comparison was possible on a common scale. The P2H technologies are dependent on the generation, the efficiency and the electricity price at all time steps in the different years. The remaining heating technologies are divided by their thermal efficiencies (η^{th}) and multiplied by the cost of the fuel (C^{fuel}). For the CHP plants the cost of heat was allocated to the share of fuel used to produce heat given by the cost of the fuel minus the revenue from producing electricity. The costs for the fuel were calculated using the generated electricity divided by the electrical efficiency (η^{el}). The calculations are shown in equation (3.21).

$$c_{N,y}^{DH} = \frac{\sum_t \left(\sum_{p \in P_{P2H}} \frac{g_{y,p,t}}{\mathrm{COP}_{p,t}} \cdot C_{y,t}^{el} + \sum_{p \in P_H \setminus \{P_{P2H}\}} \frac{g_{y,p,t}}{\eta_p^{th}} \cdot C_p^{fuel} + \sum_{p \in P_{CHP}} \left(\frac{g_{y,p,t}}{\eta_p^{el}} \cdot C_p^{fuel} - g_{y,p,t} \cdot C_{y,t}^{el} \right) \right)}{\sum_t \left(\sum_{p \in P_H} g_{y,p,t} + \sum_{p \in P_{CHP}} \frac{g_{y,p,t}}{\alpha_p} + X_{y,t} \right)} \quad \forall\, y \in Y \tag{3.21}$$

For the individual HPs it has been assumed that these are used for hot water preparation at 55 °C and that they use ambient air as the heat source. Hourly COP values could therefore be calculated using the method described in section 3.4. It was further assumed that the household follows the same normalized heat demand profile (ϕ_t) as the DHn. The normalized annual costs for an individual household are thus only dependent on the heat profile, the COP-value and the electricity price as given in equation (3.22).

$$c_{N,y}^{Ind} = \frac{\sum_t \phi_t \cdot \frac{1}{\mathrm{COP}_t} \cdot C_{y,t}^{el}}{\sum_t \phi_t} \;\forall\, y \in Y \tag{3.22}$$

For the calculations, both the regional price of electricity and the local marginal cost of electricity was used.

3.8 Model Scenarios

In the context of Gothenburg, important actors in the heating system are the two refineries and Renova as they provide medium-grade waste heat to the DHn. However, to reach the goal of climate neutrality for Gothenburg, the refineries and Renova also need to reach climate neutrality. This will impact the availability of the waste heat and impact the electricity sector, as electricity will be used to produce H2 that will be utilized in the different sectors [38]. For the refineries this might mean producing biobased- or electrofuels for the transport industry whereas for Renova it might mean implementing CCS to capture the CO_2 emissions originating from the incineration of plastic fractions in the waste.

In this work, four different pathways will be analyzed as a base and sensitivity analyses will be applied to some of them. A summary of the differences between the scenarios in terms of H2 demand, waste heat availability and maximum allowed installed capacities (with current DHn transmission capacity limits between different parts of the city) measured in GW are seen in table 3.4. Limitations that were presented in section 3.3 that are not shown in the table are the same for all scenarios. For a more detailed description of the scenarios and waste heat availability the reader is referred to appendix A.3. In figure 3.4 the main differences between the scenarios are shown. Seen in the figure, the refineries are decreased with each scenario together with their corresponding H2 demand. Renova is assumed to be active in every scenario except *Scenario 4*.

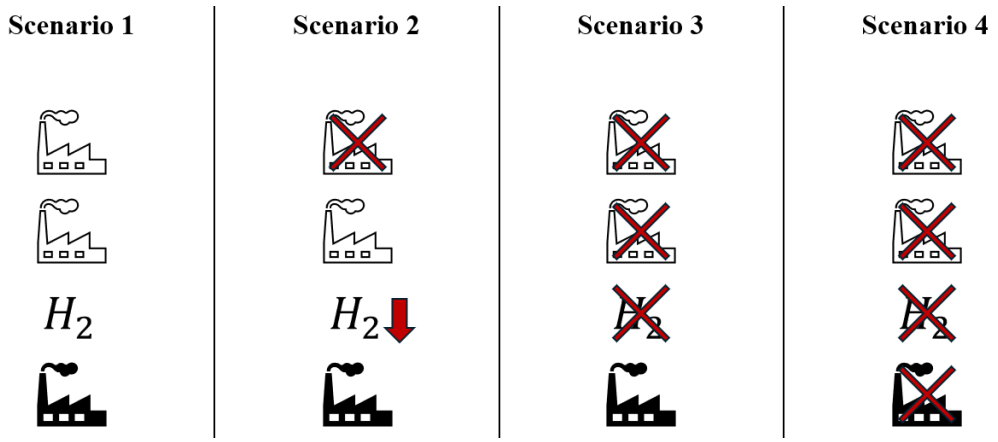

Figure 3.4: Main differences between the four main Scenarios 1-4, showing the level of refineries, H2 demand and waste incineration for each scenario.

The main difference between them are related to the estimated H2 demand, which will impact both the electricity system and the DH system through reduced waste heat availability. The maximum annual demand of H2 of 5 TWh is based on a report from Edvall et al. [71] and is assumed to be allocated equally between the two refineries. This is because no information is given about their future plans or other industries that might require H2. The reduction in available waste heat is related to the reduction in production volume from Preem, where they have announced plans

to reduce fuel production to one third of today's level [72]. The reduced waste heat production is added onto the current dispatch constraint of 210 MW in the Rya area, see equation (3.8), for all of the different scenarios as it is assumed that a reduction in waste heat frees up space in the current transmission network without investments in increased infrastructure. The same goes for when existing capacities are decommissioned in the same area.

Table 3.4: Summary of differences in H2 demand, waste heat availability and discharge constraints for the main scenarios in GW.

	2030	2035	2040	2045	2050	2060	2070	2080
				Refineries [GW]				
Scenario 1: Electrified Refineries	0.17	0.051	0.051	0.051	0.051	0.051	0.051	0.051
Scenario 2: Renova + One Refinery	0.17	0.0255	0.0255	0.0255	0.0255	0.0255	0.0255	0.0255
Scenario 3: Renova + No Refineries	0.17	0	0	0	0	0	0	0
Scenario 4: No Renova + No Refineries	0.17	0	0	0	0	0	0	0
				Waste Incineration [GW]				
Scenario 1: Electrified Refineries	0.18	0.18	0.18	0.18	0.18	0.18	0.18	0.18
Scenario 2: Renova + One Refinery	0.18	0.18	0.18	0.18	0.18	0.18	0.18	0.18
Scenario 3: Renova + No Refineries	0.18	0.18	0.18	0.18	0.18	0.18	0.18	0.18
Scenario 4: No Renova + No Refineries	0.18	0	0	0	0	0	0	0
				Rya HP_{H2} * [GW]				
Scenario 1: Electrified Refineries	0	0.119	0.119	0.119	0.119	0.119	0.119	0.119
Scenario 2: Renova + One Refinery	0	0.0595	0.0595	0.0595	0.0595	0.0595	0.0595	0.0595
Scenario 3: Renova + No Refineries	0	0	0	0	0	0	0	0
Scenario 4: No Renova + No Refineries	0	0	0	0	0	0	0	0
				H2 Demand [TWh]				
Scenario 1: Electrified Refineries	0	5	5	5	5	5	5	5
Scenario 2: Renova + One Refinery	0	2.5	2.5	2.5	2.5	2.5	2.5	2.5
Scenario 3: Renova + No Refineries	0	0	0	0	0	0	0	0
Scenario 4: No Renova + No Refineries	0	0	0	0	0	0	0	0
				North-West constraint ** [GW]				
Scenario 1: Electrified Refineries	0.21	0.329	0.329	0.329	0.621	0.761	0.761	0.761
Scenario 2: Renova + One Refinery	0.21	0.355	0.355	0.355	0.647	0.787	0.787	0.787
Scenario 3: Renova + No Refineries	0.21	0.38	0.38	0.38	0.672	0.812	0.812	0.812
Scenario 4: No Renova + No Refineries	0.21	0.38	0.38	0.38	0.672	0.812	0.812	0.812

* The recyclable heat is limited by the refineries existing transmission capacities and maximum recyclable heat.

** When the available waste heat from the refineries is reduced or existing capacities are decommissioned these are added onto the dispatch constraint explained by equation (3.8).

3.9 Sensitivity Analysis

This section will present the sensitivity analyses that have been chosen to be investigated further. Most of the sensitivity analyses have been applied to *Scenario 2* as it was deemed to have a more realistic H2 demand, while still containing characteristics affecting the energy system more than the remaining scenarios in terms of electricity demand.

3.9.1 No Investments in Offshore Wind

The current limit of 1 GW offshore wind capacity is assumed to be available for investments in 2035. However, there have been multiple projects that during the recent years have been rejected due to various reasons. It is thus of interest to analyze how the role of P2H technologies changes if the planned offshore wind farm is not implemented.

3.9.2 Biomass Prices

To test the effects of varying biomass prices in the future a sensitivity analysis was performed where the biomass price was varied from the reference value of 40 EUR/MWh to 20 EUR/MWh. The values were chosen to enable a fair comparison between different price levels while not underestimating the future prices.

3.9.3 Taxes and Tariffs on Generation Units

An important aspect of the study is to analyze the effects of taxes and tariffs on the P2H technologies and HOB_{WG}.

3.9.3.1 HP- and EB Tax and Cap

The taxes evaluated are related to production per Wh (energy-tax) and are included in the objective function for P2H technologies per Wh energy they consume during each time step. The tax used is the one active from 2026, which is approximately 45 EUR/MWh [73].

More relevant to the EBs are the tariffs related to installed capacity, as these hit much harder on the profitability of the producer with few FLHs. Even if installed capacity tariffs are not included, it is still relevant to constrain how much EB capacity is allowed, as the system will not be reasonable with too much EBs with the current tariffs in place in a real electricity system. To test the system on this, the allowed installed capacity will be capped to 100 MW to see how the system handles the capacity constraint.

3.9.3.2 Tariffs on Biogas Heat-Only Boilers

Other taxes and tariffs included are related to the usage of gas from a gas-network. To see taxes and tariffs related to the HOB_{WG}, see source from Göteborg Energi

[74]. Instead of inserting tariffs directly into the model, as these are very volatile, additional costs were added if a biogas storage is instead connected to the gas-network. The idea would be to connect a storage and reduce maximum demand against the network, meaning the tariffs would theoretically reduce. An extra cost of 14.81 EUR/MWh was therefore added to the variable O&M costs of biogas fueled production units. More information regarding the calculations can be found in appendix A.4.

3.9.4 Removed DHn Transmission Limits

To analyze the impact that the existing DHn has on the cost-optimal solution, a sensitivity analysis has been performed where the existing DHn transmission limits are removed. The equations removed from the model are: (3.5), (3.8), (3.9), (3.10), (3.11) and (3.14). Equation (3.12) is not bound by transmission anymore, but instead to the technical constraint of maximum waste heat available from the electrolyzers producing H2. This is explained in section 3.2.4 and is constrained by equation (3.4).

4

Results

This section presents the results of the study and are chosen to answer the research questions mentioned in the introduction of the thesis. The first part considers the impacts of electrification of refineries on the energy system, after which the importance of the existing units is analyzed. This is then followed up by the results from the sensitivity analyses and at the end, storages will be presented.

4.1 Impact of the Electrification of the Refineries on the Energy System

To answer *RQ3*, the impact of the electrification of refineries on the energy system is analyzed by comparing the system composition for the different scenarios. This is visualized by the bars in figure 4.1 representing the total installed thermal capacities for the different heat generating units for the modeled years. What can be seen in the figure for *Scenario 2*, *Scenario 3* and *Scenario 4*, is that the new investments are dominated by HPs together with EBs and HOB_{WG}, indicated by the teal-, red- and yellow striped bars. *Scenario 1*, in which the highest H2 demand is assumed and the highest amount of waste heat is available, has unlike the other scenarios a mix of new CHP plants seen by the striped blue bar in the upper plot year 2060. *Scenario 4*, where no waste heat from the refineries or Renova is available, shows the highest total installed thermal capacities of heat generating units, since new investments needs to be made to cover up for the lost base-load production coming from the refineries and the waste incineration plant.

In 2035, it is assumed that the H2 demand is active in *Scenario 1* and *Scenario 2*. As a consequence, new investments are mainly made in HP_{H2} both since it becomes cost-effective to recover heat from the stack and that the relative efficiency is higher due to a higher source temperature. New investments in HPs are also made for *Scenario 3* and *Scenario 4*, with no H2 demand, indicated by the striped teal bars for the scenarios. This is mainly due to one of the existing CHP plants being decommissioned year 2035, requiring new investments. The largest difference in new investments between the scenarios becomes visible in year 2060, as that is when all existing capacity is decommissioned. For all of the main scenarios, new investments are made in EBs as early as year 2030.

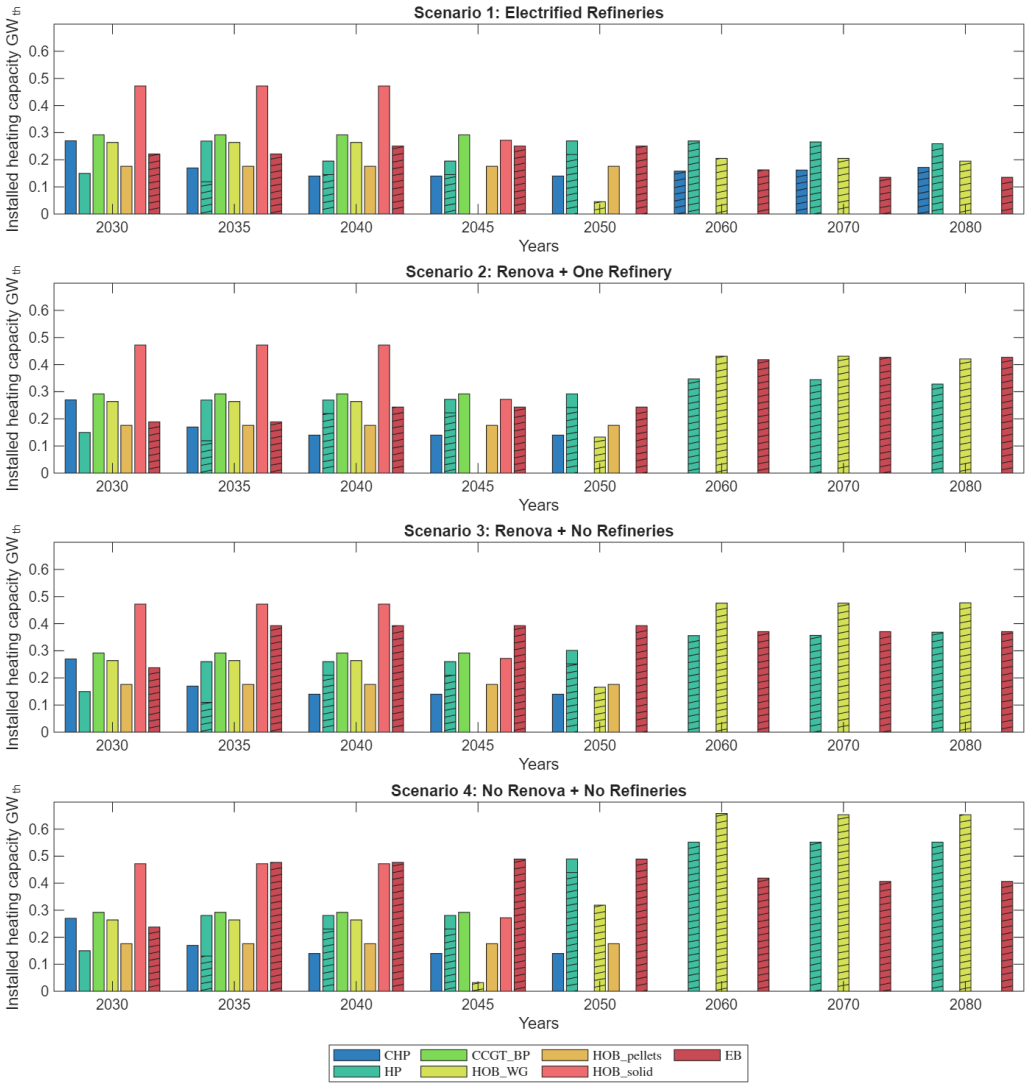

Figure 4.1: Total installed capacities for all studied scenarios and years. The striped lines represents the new investments that are still active in the different years.

In figure 4.2 the total installed thermal capacities for the HPs are divided into the different HP categories. Seen for *Scenario 1* and *Scenario 2*, the two upper plots, is that HP_{H2} is maxed from 2035 until 2080, showing new investments after each decommission. Common for all scenarios is near maximum investments in HP_{Sew}, which together with HP_{BF} fulfills the capacity governed by equation (3.5). As the options for higher COP HPs become more limited for each scenario, the model still sees cost-effectiveness to invest in lower COP HPs. In *Scenario 2*, the model invests in all capacity in $\text{HP}_{Sea,RL}$ in year 2060 where $\text{HP}_{Sea,Rya}$ also starts to be installed. As the model invests in a lot of HP_{Sea} by 2060, some of the invested HPs are decommissioned from earlier investments. In *Scenario 3* and *-4* shown in the bottom two plots in the figure, $\text{HP}_{Sea,RL}$ is maxed to the capacity constraint of 0.1 GW. Seen in *Scenario 4*, the model invests in as much HP_{Sea} as possible from 2060 until 2080. It is only in *Scenario 4* where investments in HP_{air} are present since all other types of HPs included in this study already are maximized with respect to the current DHn

transmission capacities between different parts of the city. HP_{air} is only invested in for one investment period, being decommissioned in year 2060.

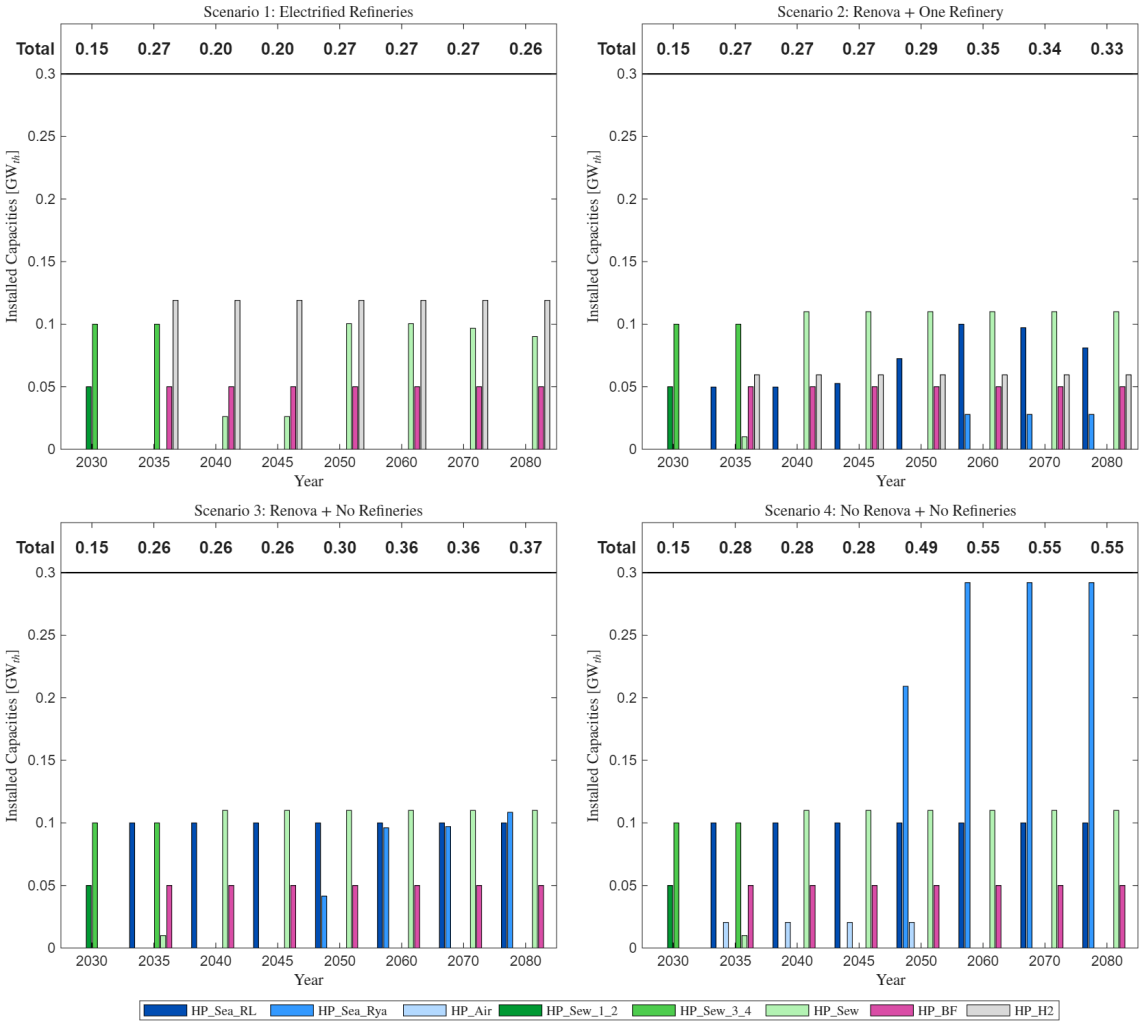

Figure 4.2: Total installed capacities for all existing- and new heat pumps for Scenario 1-4.

It is only in *Scenario 1*, where the full H2 demand is active, that new investments in CHP plants are preferred in the model. This can be explained by looking at the difference between the local marginal cost of producing electricity and the regional cost arising from price area SE3 together with the amount of hours that the import capacity constraint becomes binding, as visualized in figure 4.3. In the figure, the x-axis shows the share of hours where the import constraint becomes binding and the y-axis shows the average difference between the marginal cost of electricity and the regional electricity price for the year 2060.

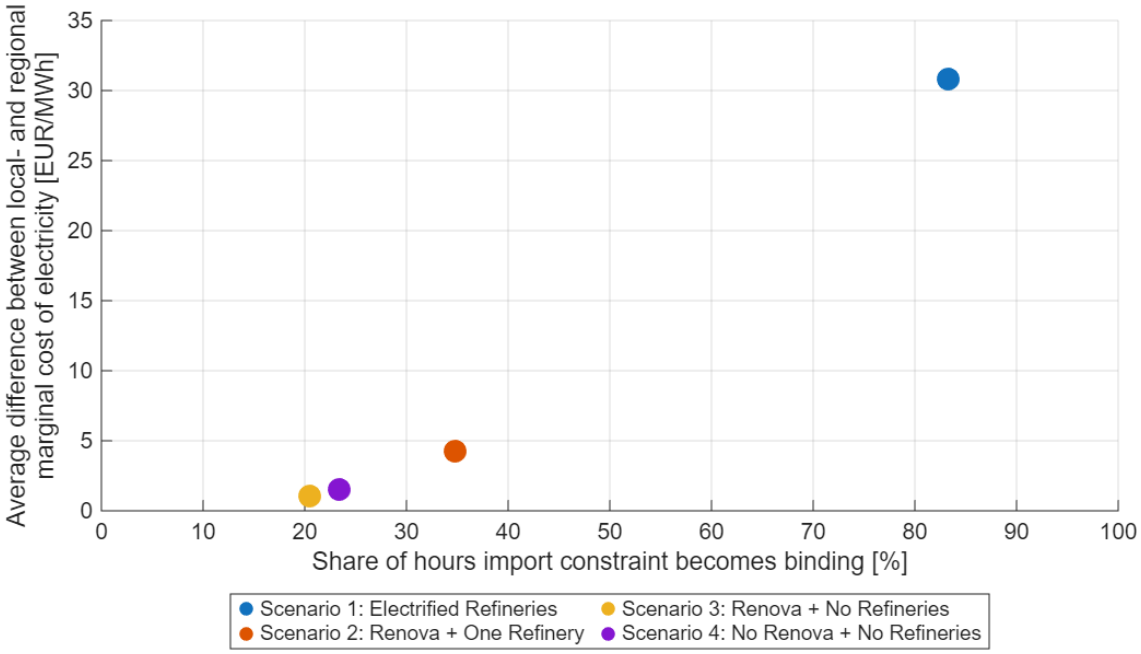

Figure 4.3: Average difference between local- and regional marginal cost of electricity as a function of share of hours with maximum import for the year 2060.

As the import constraint becomes binding for a large share over the year for *Scenario 1*, it indicates that electricity grid congestion is prevalent and access to cheap electricity is limited. This is visible on the x-axis where the import is maximized for 83% of the year in *Scenario 1*, which can be compared to *Scenario 2* where it only becomes constrained for 35% of the year. As a result, CHP investments are justified in *Scenario 1* as these have the benefit of producing both heat and electricity at the same time and the high investment costs can be motivated due to the high amount of hours needed over the year where electricity cannot be imported and has to be produced locally. However, it can also be seen that the average difference between the local- and regional marginal cost of electricity is around six times larger in *Scenario 1* compared to the other scenarios with an increase from below 5 EUR/MWh, to 32 EUR/MWh. Thus, when the grid is more congested the cost of producing electricity locally becomes higher than the cost of import as more expensive units needs to operate to fulfill the electricity supply- and demand balance.

As seen by the bars representing the annual share of different electricity generating units in figure 4.4 for *Scenario 1* and *Scenario 2*, local investments are most prevalent, as the two scenarios have a H2 demand, leading to higher electricity demand. For all the scenarios, the main source of electricity comes from imports indicated by the larger annual share of the total electricity supply, followed by investments in offshore wind, optimal tilt solar PV farms and generation from existing units. There is also a higher investment in peak biogas turbines in *Scenario 1* to handle fluctuations with higher amplitude but lower duration as these become cost-effective when running on few FLHs due to their low investment cost. In *Scenario 3* and *Scenario 4*, where no new electricity demand is allocated to H2 production, the electricity demand is mainly met by import and production from already existing

units. *Scenario 4* has a slightly larger share of hours where import becomes binding compared to *Scenario 3*, shown in figure 4.3, as no waste heat is available. Thus 60 MW of offshore wind capacity is invested in to cover up local electricity production.

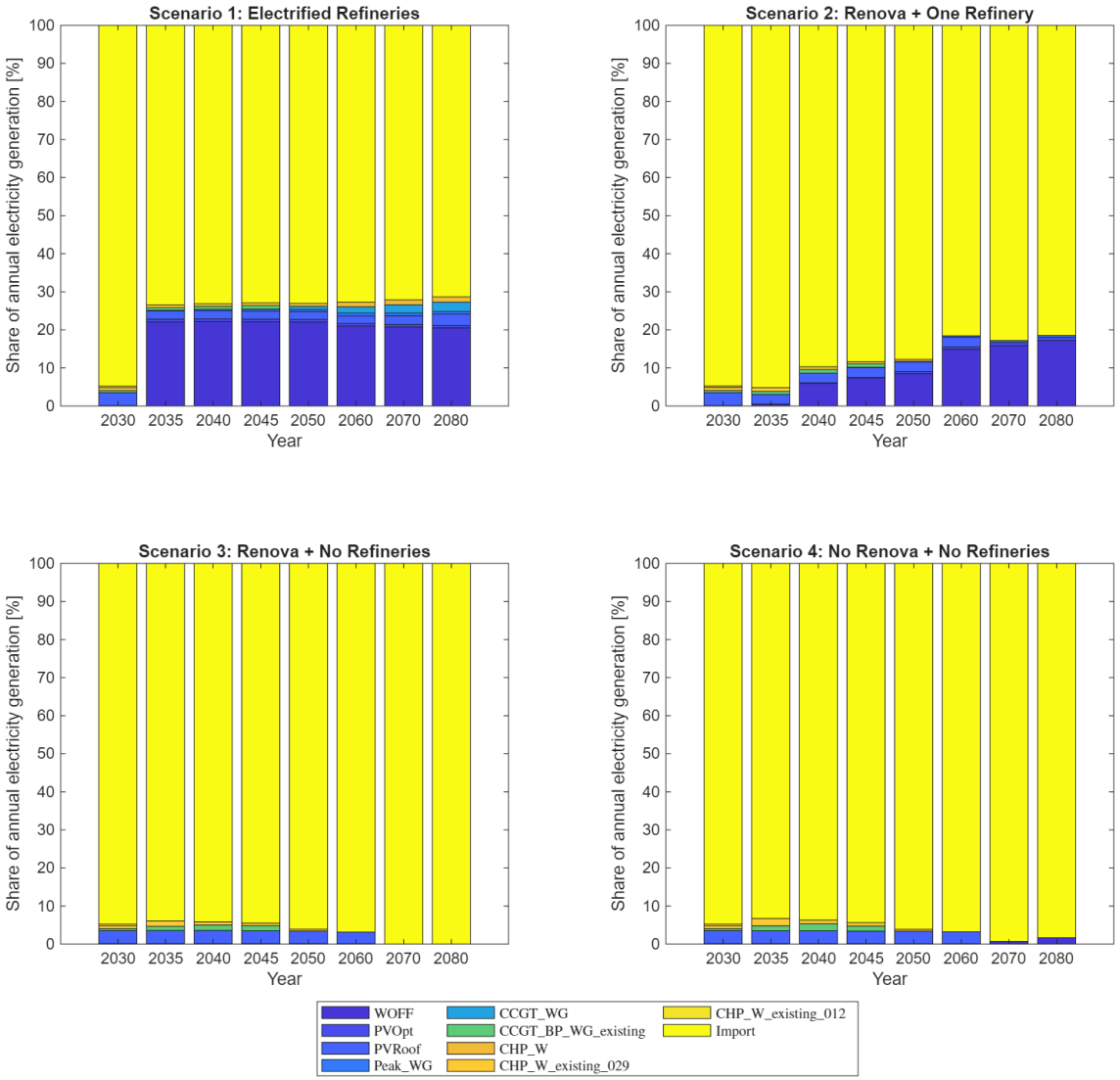

Figure 4.4: Shares of yearly electricity dispatch for Scenario 1-4 from different electricity generating units and imports.

4.2 Importance of Existing Units

As the current energy system is mainly based on waste heat and bio-based production units, it is important to analyze the role of existing units in the energy transition. This was done by looking at the heat dispatch for the different years. Figure 4.5 shows the heat dispatch for all studied years for *Scenario 2* as this is the scenario that has mainly been used for the sensitivity analyses. The remaining dispatches for the other scenarios can be found in figures A.4 to A.6 in appendix A.5. The results in the following section are related to *RQ1* and *RQ2*.

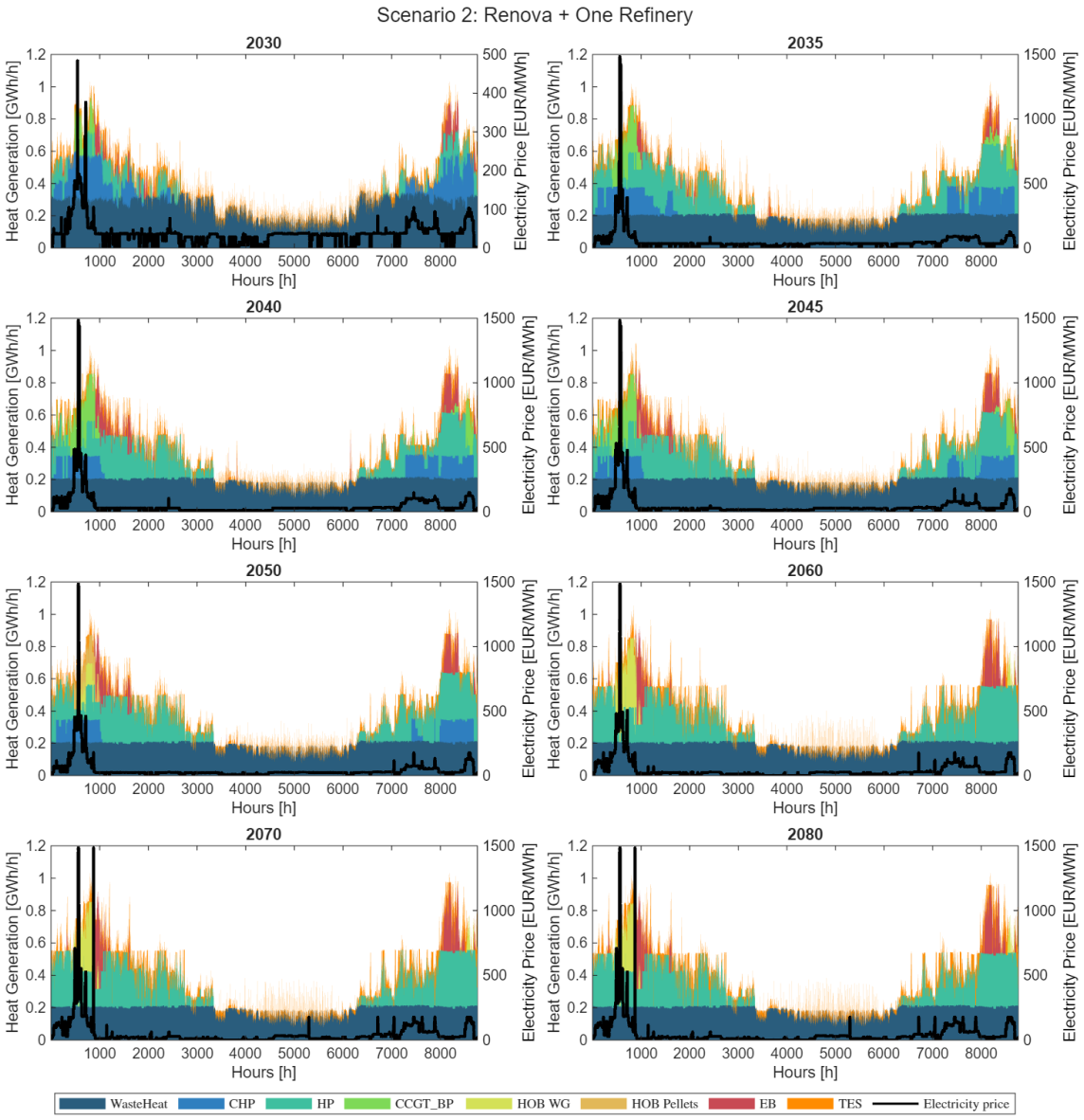

Figure 4.5: Heat dispatch of Scenario 2 for all studied years, compared to the electricity price.

For the first couple of years up until 2060, it can be seen that HPs are used in symbiosis with the existing CHP plants and the CCGT-BP plant as mid-load indicated

by the teal, blue and light green dispatches, where the thermal power plants ramp up their production during hours where the electricity price becomes expensive and the heat demand becomes higher due to colder temperatures during the winter. Up until 2050, new investments are mainly made in HP_{H2} and EBs, where EBs are used opportunistically as peak-load plants when there is an excess production of electricity corresponding to low prices.

In all years, HPs are being used as flexible mid-load plants that respond to electricity prices such that they flexibly increase and decrease their production as external price signals varies. The characteristics are more clearly visualized in figure 4.6 where the heat dispatch of the first 800 hours of the years are shown.

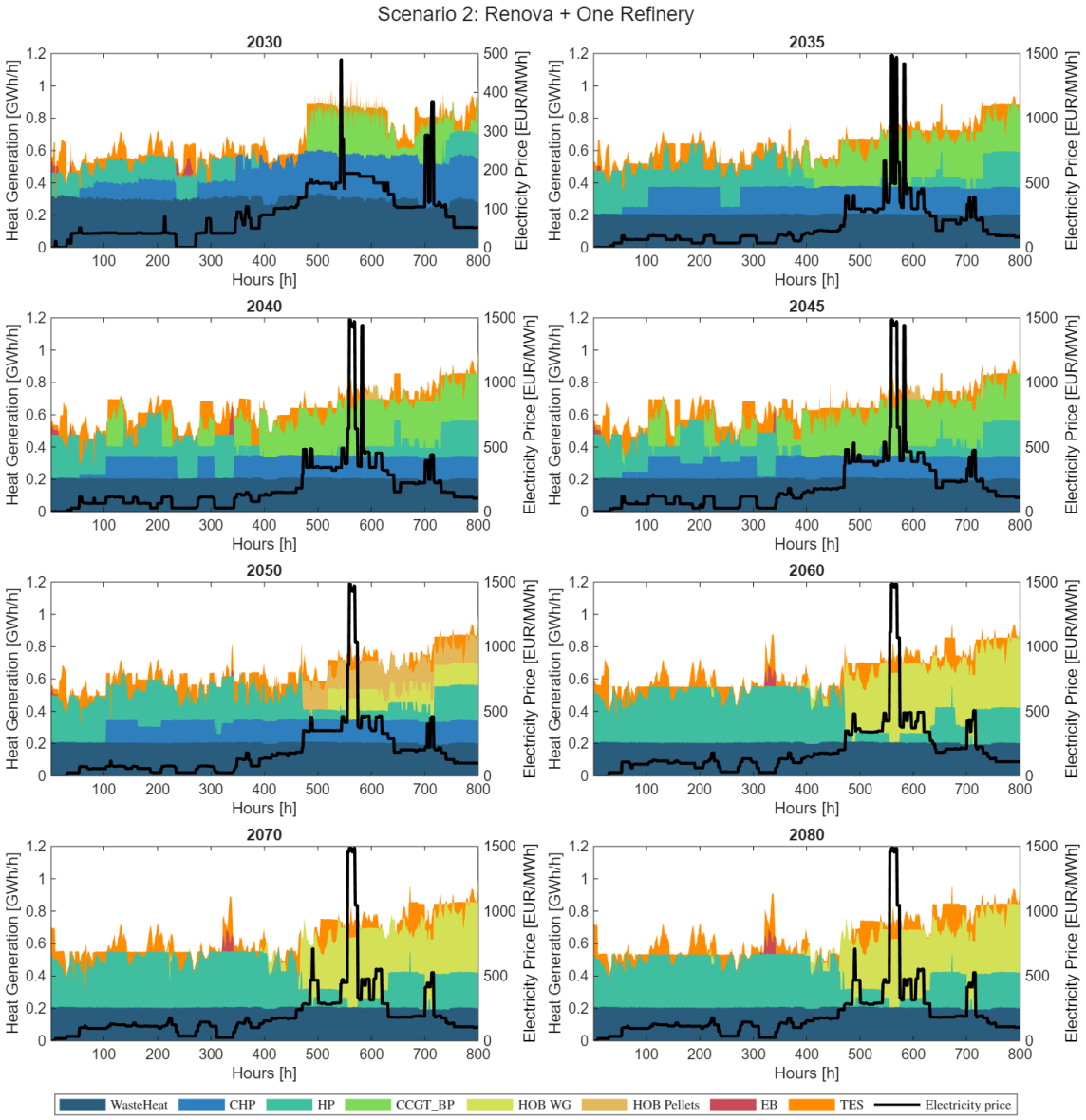

Figure 4.6: Heat dispatch of Scenario 2 the first 800 hours of the year for all studied years, compared to electricity price.

When the cost of importing electricity is amplified around the hours 500-600, the

P2H technologies reduce production and the heat demand is instead fulfilled with existing thermal production units. After 2050 it is instead HOB_{WG} that cover the heat demand when the electricity price spikes. In 2050, the existing CCGT-BP is decommissioned and thus existing HOBs running on pellets are used together with EBs and HOB_{WG} during the winter. The EBs are used when the electricity price is low indicating a surplus of electricity. From 2060 and onward, the production from CHP and CCGT-BP is replaced by a higher share of HOB_{WG} when the heat demand increases during winter, together with EBs as the electricity prices decrease. A comparison between the P2H technologies can be seen in figure A.7 in appendix A.6 where it is further visualized that EBs produce during low electricity prices, whereas HPs can produce during higher prices to act as mid-load.

To further study the influence of the existing units in the optimal system configuration the results from the Brownfield model were compared with a Greenfield optimization where all existing capacities were put to zero (not including refineries and Renova). This is shown by the installed thermal capacities of the different heat generating units in figure 4.7, where the striped lines represents new investments that are still active in the modeled years.

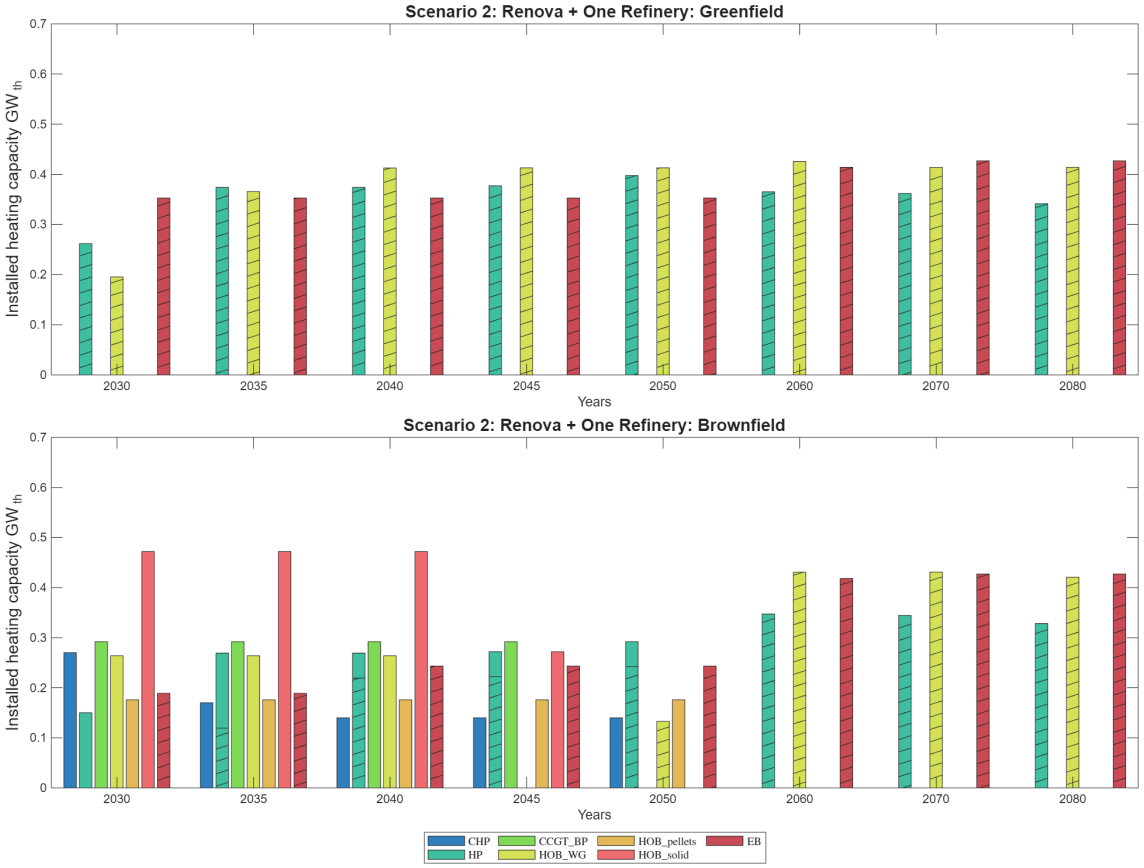

Figure 4.7: Total installed capacities for Scenario 2 with Greenfield and Brownfield. The striped lines represents the new investments that are still active in the different years.

When comparing the models, it can be seen that in the Greenfield model, a system

primarily based on P2H technologies together with HOB_{WG} offers the cheapest system configuration, whereas much smaller investments are made in the Brownfield model up until 2060 since existing capacities can be utilized instead. It can also be seen when comparing the two plots that the two cases converge in year 2060 indicating that irregardless of the current system configuration, the cheapest alternative from a techno-economic perspective is to have a system where HPs acts as mid-load and HOB_{WG} and EBs are used for peak-load depending on the electricity price. Fewer new investments are required in the Brownfield model up until 2060, indicating the importance of utilizing the existing capacities until their technical lifetime has run out.

Similar results can be seen in the annual share of electricity dispatch for the modeled years as visualized in figure 4.8 where the existing capacities are used in co production with new investments of mainly offshore wind, followed by peak biogas turbines and optimal tilt solar PVs, in the Brownfield model. Also here the two cases shows similar dispatch of electricity after the year 2060 when existing rooftop solar PV capacities are decommissioned.

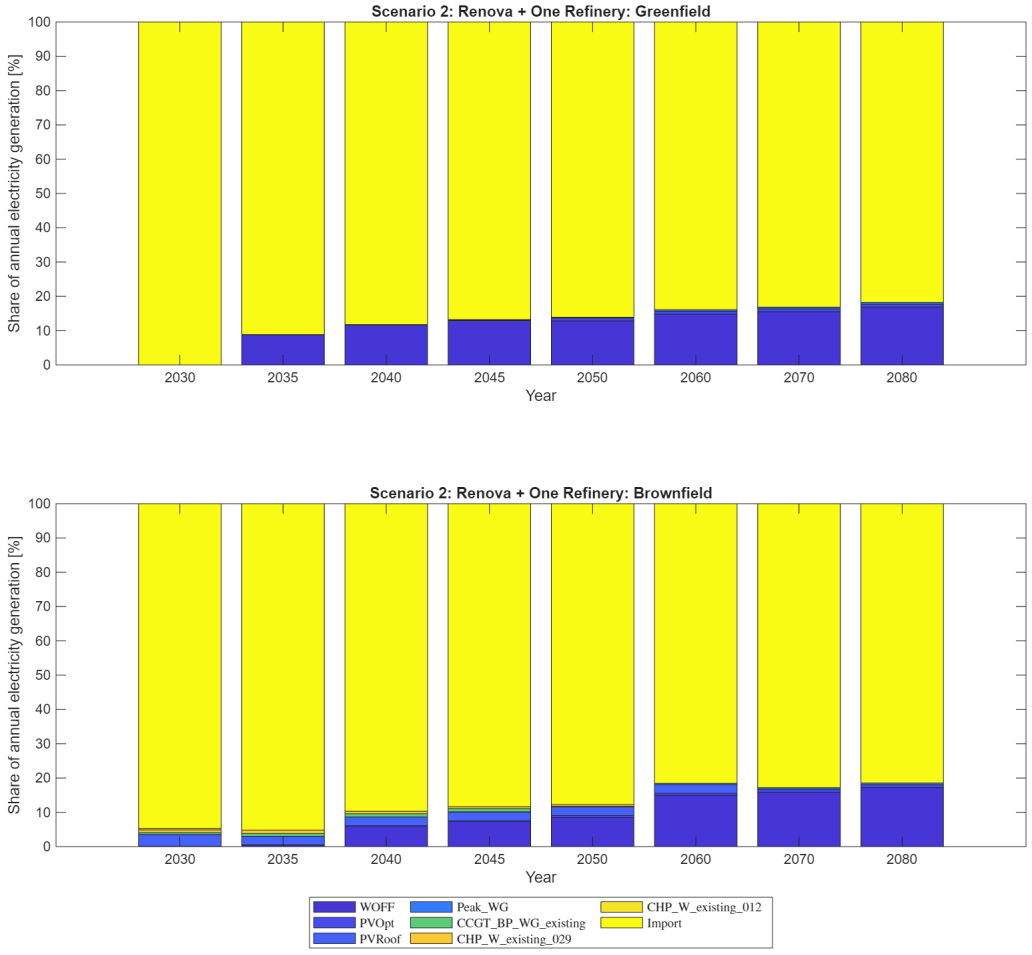

Figure 4.8: Shares of yearly electricity dispatch for Scenario 2: Greenfield and Brownfield, from different electricity generating units and imports.

4.3 DH vs. Individual HPs

The results of the differences in costs of producing heat between an individual household and the cost of producing DH per MWh of heat in the Greenfield model are shown in table 4.1. The table shows the cost of producing heat and therefore not the cost that the household owners experience, and does not include the costs of DH infrastructure or investment costs for individual HPs.

Table 4.1: Average cost of producing heat for an individual household and for DH with two different price signals.

	2030	2035	2040	2045	2050	2060	2070	2080	Unit
Local Electricity Prices									
DH cost	8.27	16.46	15.12	15.35	15.86	16.15	15.39	15.48	EUR/MWh
Individual HP cost	14.90	23.42	23.98	24.26	23.18	24.60	24.97	25.03	EUR/MWh
SE3 Electricity Prices									
DH cost	8.27	13.90	13.88	13.64	13.04	13.39	13.35	13.42	EUR/MWh
Individual HP cost	14.90	21.20	22.31	22.34	20.40	21.91	22.55	22.55	EUR/MWh

As seen in the table, the costs of producing heat from DH are lower during all years compared to the costs of producing heat with an individual HP with an average difference of around 8 EUR/MWh. The reason for this is that the individual HPs are more tightly linked to the consumer demand, meaning that these produce when the heating demand and also the electricity prices increase. In the DHn on the other hand, there is a larger mix in the energy portfolio such that the P2H technologies can reduce their production when the electricity prices increases and the heat demand can be covered by other production units like HOBs or CHP plants.

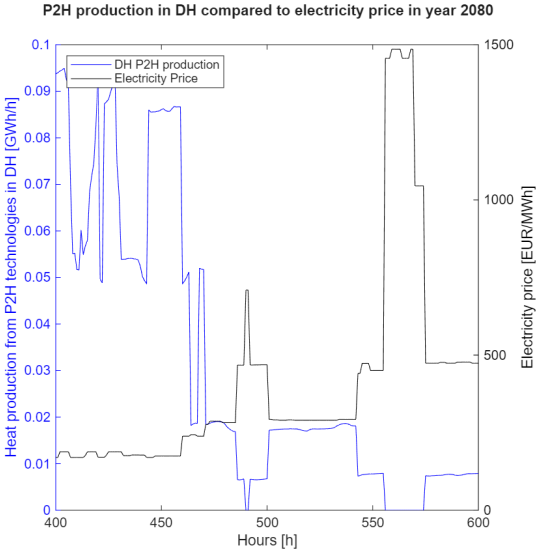

((a)) P2H production in the DHn compared to electricity price.

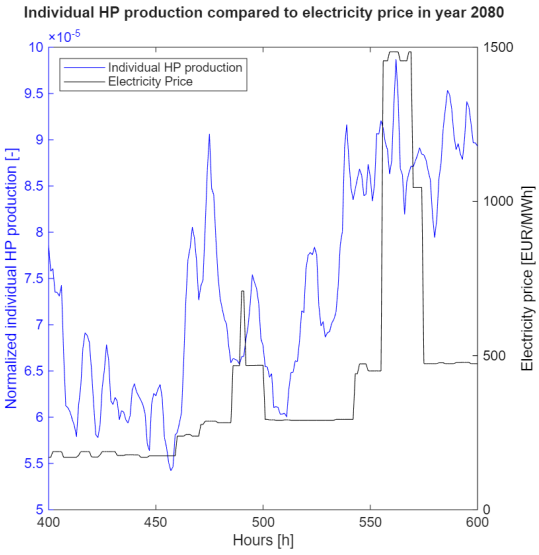

((b)) Individual HP production compared to electricity price.

Figure 4.9: Difference between production from P2H technologies in the DHn and production from individual HPs. The secondary axis shows the electricity prices, whereas the primary axis shows the production.

This is more clearly visualized in figure 4.9 showing the P2H dispatch in the DHn in subplot 4.9(a) compared to the electricity price, and the dispatch from individual HPs in subplot 4.9(b), between hour 400-600 in year 2080. What can be seen in subplot 4.9(a) is that the P2H technologies in the DHn reduce their production when the electricity prices increase. This can be compared with the individual HPs shown in subplot 4.9(b), where the HPs produce even when the electricity prices are increased as the heat demand must be fulfilled.

4.4 Sensitivity Analyses

In the following section, the results from the sensitivity analyses that have been made are given. All sensitivity analyses have been applied to *Scenario 2* with the same constraints shown in table 3.4.

4.4.1 Without Available Offshore Windfarm

This section is mainly related to *RQ2*. When no offshore wind is available in the system, the optimal system composition changes. In this scenario there is a higher share of CHP plants acting as mid-load to cover the local electricity demand originating from congestion in the electricity grid. This is shown in figure 4.10 where the blue color above the waste heat base-load still produces even though electricity prices go down in SE3.

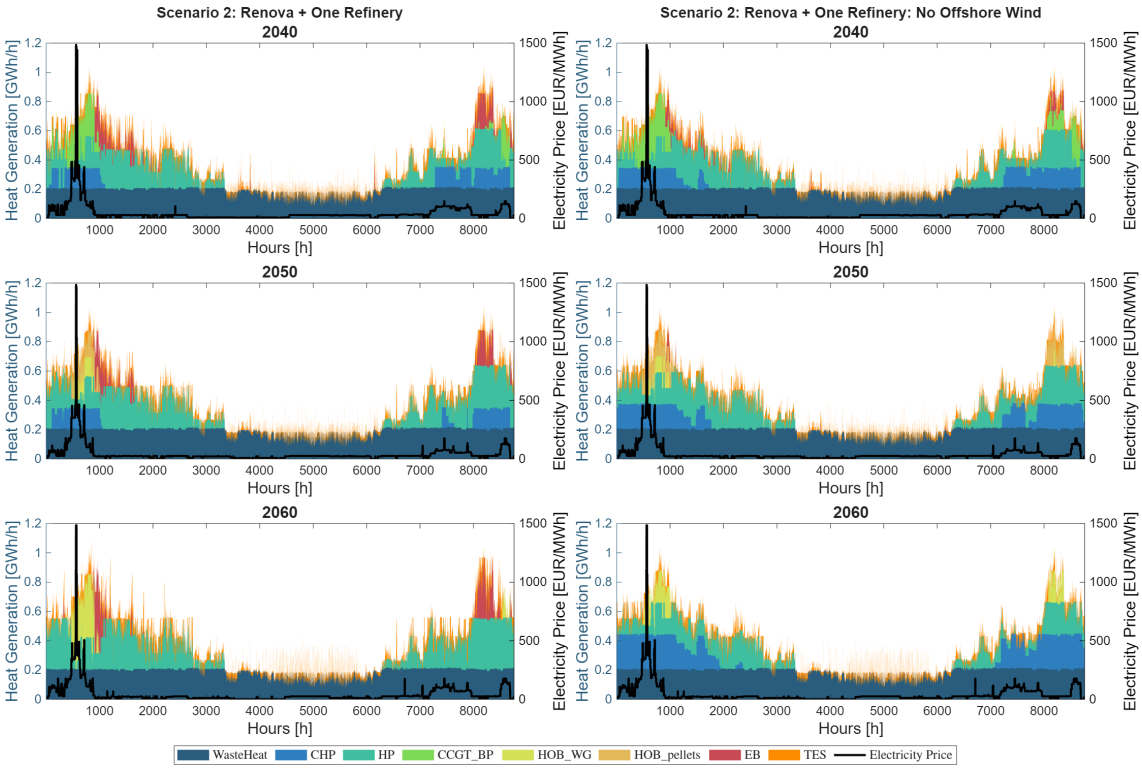

Figure 4.10: Heat dispatch comparison between base case Scenario 2 and no offshore wind park, for studied years 2040, 2050 and 2060, compared to the electricity price.

There are also lower investments in EBs as these are mainly used opportunistically when there is a high excess production of electricity. However, when there is limited access to electricity in the local node, the potential of the EBs is reduced as electricity to other units are prioritized, e.g. electrolyzers as the H2 demand must be satisfied which also means that electrolyzer HPs are preferred as well.

EB investments occur mainly only once in the system year 2030 in *Scenario 2: No Offshore Wind*, to be decommissioned by year 2060, seen by the difference in installed thermal capacities between the years in figure 4.11, as dark red color. The total investment of EBs in 2030 is 130 MW, compared to the base case of 148 MW. The main difference between the cases is that new investments occur in *Scenario 2* for 2060 (figure 4.1), meaning the total installed capacity increases for EBs. When looking at figure 4.10, the EB generation mostly stops as soon as 2050 with absence of red for the peak demands, meaning that the installed capacity is not utilized fully even though there is installed capacity available. This reduction can be explained by the increased electricity demand in the future indicating that the grid becomes even more constrained.

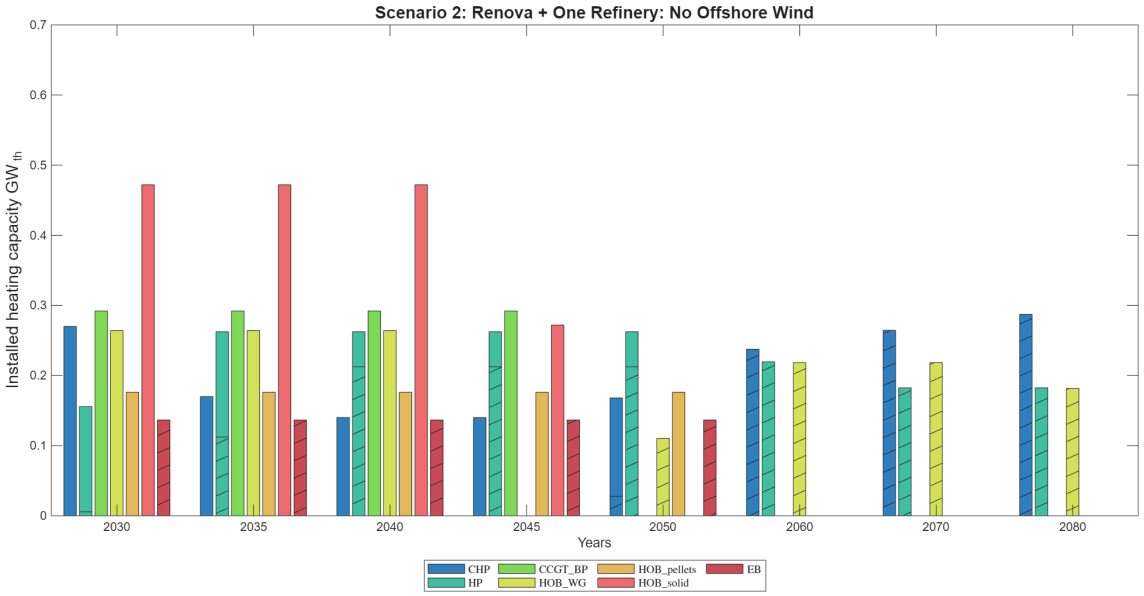

Figure 4.11: Total installed capacities for Scenario 2 with no offshore wind park. The striped lines represents the new investments that are still active in the different years.

Seen in figure 4.12, the difference between local- and regional marginal cost of electricity is compared to the import capacity constraint. Seen 2030 is that the difference between the two is zero, even though many hours of the year uses all the import available. This indicates not a restriction in import, rather that the model uses all import when electricity is cheap. Seen differently year 2040 and more so 2060, is that the difference between the two costs increases, and this occurs during hours where import is maximized, meaning the import becomes restrictive. This explains why the EBs stop generating heat after 2060. Even though the SE3 price of electricity is still low, the marginal cost of electricity becomes very high, resulting in that the EBs cannot produce opportunistically anymore.

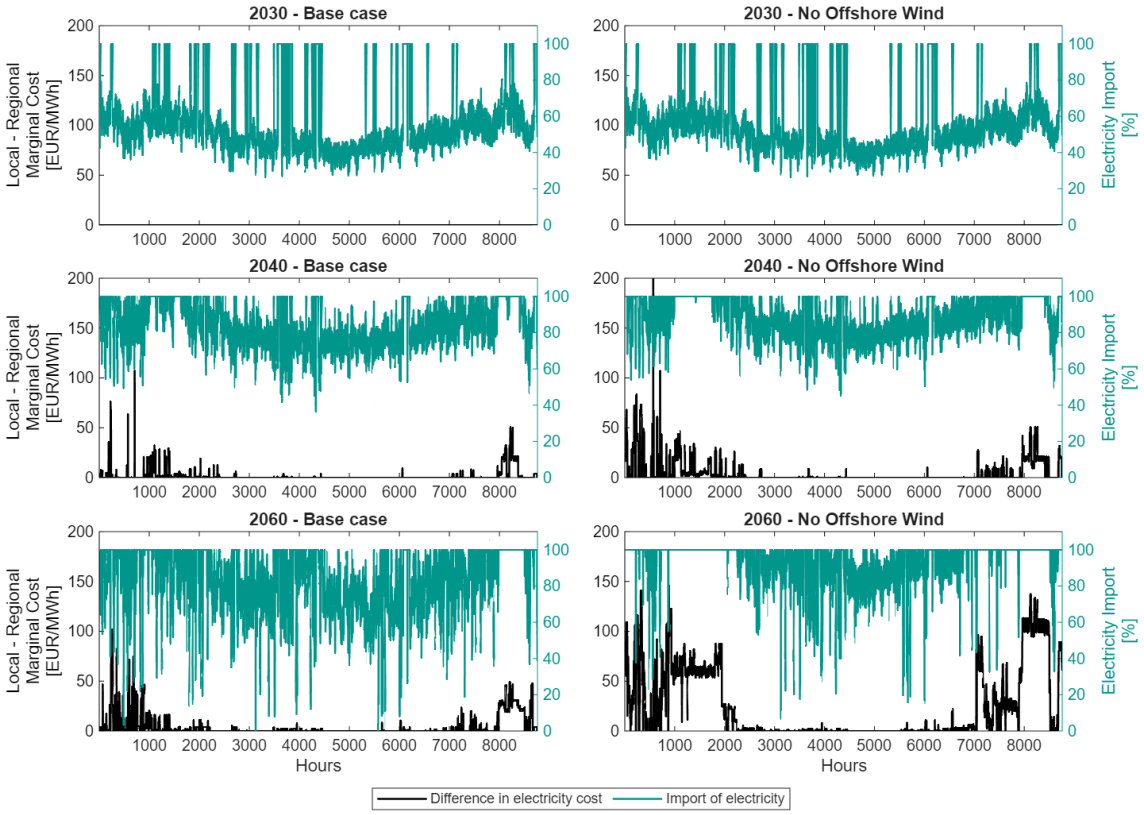

Figure 4.12: Difference in marginal cost of electricity for local- and SE3 electricity cost, compared to the percentage of imports used for Scenario 2 and sensitivity analysis with no offshore wind. Left axis shows difference in electricity cost, right axis shows percentage of electricity imports.

Also seen in figure 4.12 is that the difference between the two costs never become negative. This means that the local marginal cost will always be equal or higher than the regional cost. This is explained by looking at the import level of electricity. The city almost always has an import demand, thus seldom exports. The only way the local cost of electricity would be lower than the regional cost would be if export becomes constrained, meaning a reversed effect than constrained imports. This does not occur for any of the scenarios and years studied.

4.4.2 Changes in Biomass Price

Due to the increased competitiveness of biomass in different sectors and that the current system is highly based on bio-based generation, it is of interest to study the impact of a varying biomass price on the optimal system composition. This was done by varying the biomass price from 20 EUR/MWh to 40 EUR/MWh, where the reference case is based on a price of 40 EUR/MWh. In figure 4.13 the results show that when the biomass price is decreased to 20 EUR/MWh, the system favors new investments in CHP plants together with HPs as mid-load. This is seen as darker shades of blue dominating the system together with shades of green and orange for biomass price 20 EUR/MWh after year 2060. There is also a decrease in EB production, seen as dark yellow, of almost 50% compared to base case of 40 EUR/MWh.

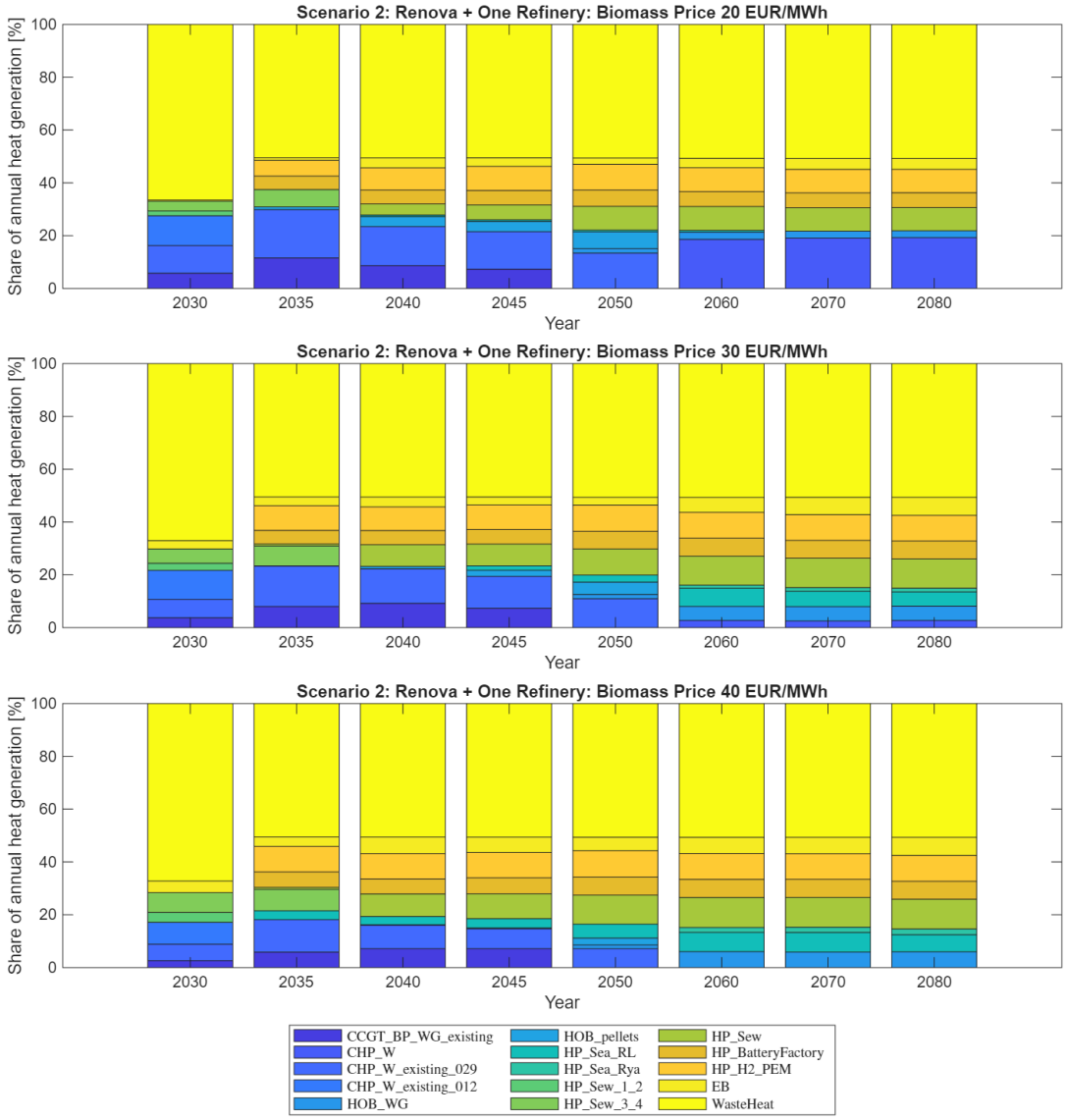

Figure 4.13: Normalized share of heat generation in Scenario 2 for different biomass prices.

When observing prices of 30 EUR/MWh and 40 EUR/MWh, there is color of turquoise, indicating HP_{Sea}, together with a lighter blue, indicating HOB_{WG}. The CHP plants essentially replace these two when the biomass price is decreased to 20 EUR/MWh. When combining this with less EB production, this scenario has less demand for peaking units.

For biomass prices of 40 EUR/MWh, there is still production from CHP plants, however this is only from already existing units. The production is motivated by the high electricity prices seen during peak demand periods. It is not cost-effective to invest in new CHP plants, due to the high investment costs. The tipping point of a system favoring new investments in CHP units seems to be around 20 EUR/MWh.

4.4.3 Impacts of Taxes and Tariffs on Generation Units

As current, Swedish, DH-systems include different taxes and tariffs on electricity, biogas and installed capacities, it is of interest to study the effects of these in the optimal system composition to answer *RQ4*. This is done by analyzing the average marginal cost of producing heat for each season and compare with the reference case where these different types of taxes and tariffs were not included. The reference case is compared to three different sensitivity analysis cases. For further explanation on how the analysis is constructed, see section 3.9.3. The results are presented in figure 4.14.

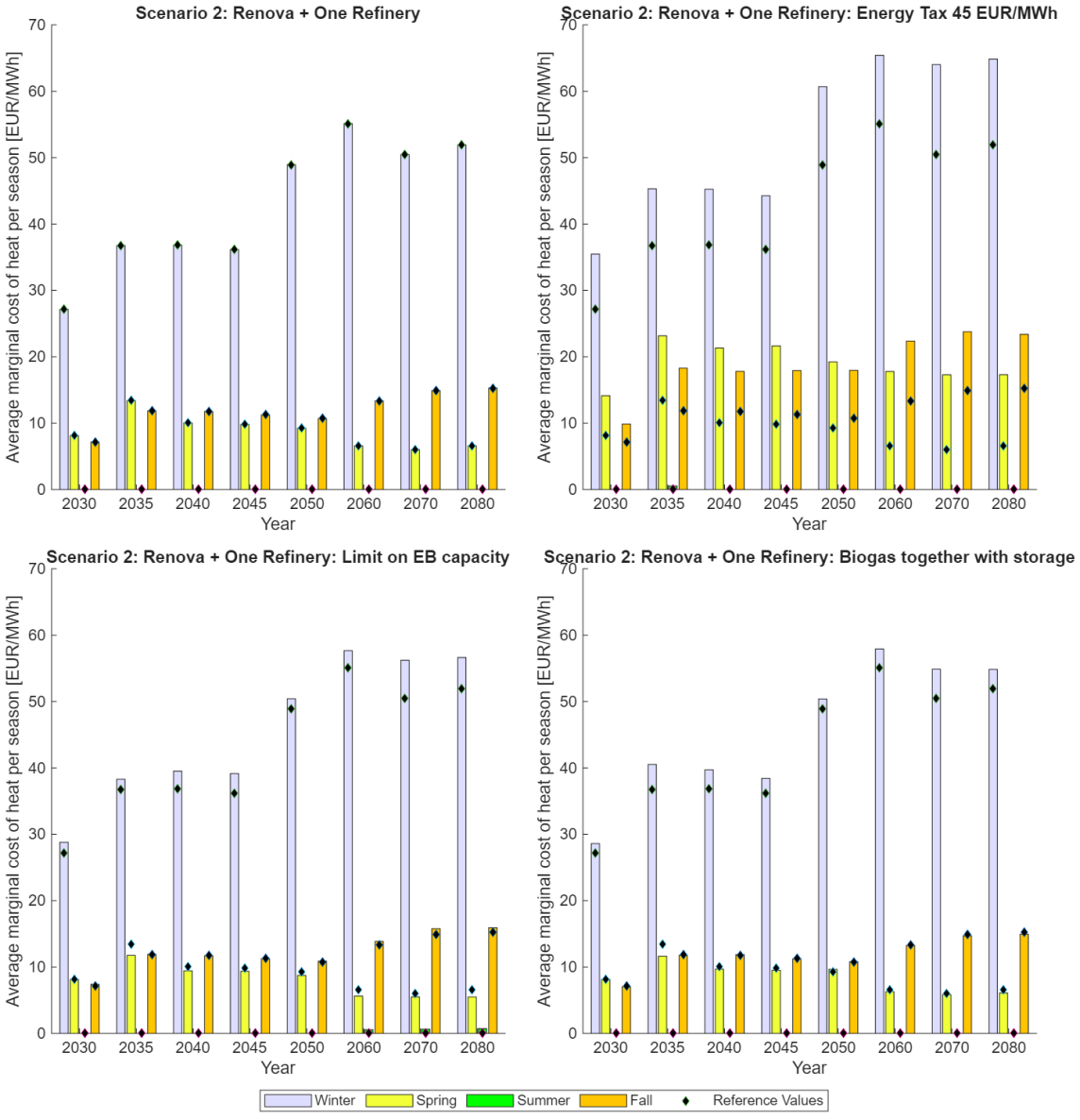

Figure 4.14: Average marginal cost of heat for scenarios where generation units are taxed in different ways. Average cost is divided into seasons of the year.

The biggest difference in terms of average marginal cost of heat occurs when an energy tax of 45 EUR/MWh is applied to the objective function. The reason for this is

that the cost of driving the P2H technologies increases, but not to that extent that it becomes economically viable to invest in significant amounts of new CHP plants due to their high investment costs. Similar trends can be seen for *Scenario 2: Limit EB* and *Scenario 2: Biogas together with storage*, where the cost of producing heat increases during the winter. In the latter case, the reason for this is that when the heating demand increases during the winter, HOB_{WG} will still be the most attractive option even with a slightly higher cost. This is due to the HPs reducing their operation during these hours. The costs remain at a similar level as for the reference case during the remaining seasons when the HOB_{WG} are not utilized. In *Scenario 2: Limit EB*, the increased cost during the winter period can be allocated to a 20% increase in FLH from HOB_{WG} that are used even when the biogas price exceeds the electricity price. This is because the installed capacities of EBs are reduced and HOB_{WG} becomes the next technology in the merit order. During the summer it can also be seen that the average marginal cost of heat is close to zero which is due to the abundance of waste heat from the waste incineration.

The technologies that are influenced the most of the current Swedish tax levels are the EBs as these do not become cost-effective when there are taxes on P2H technologies. HPs are not as influenced by the tax as these have the benefits of producing more useful heat per electricity input due to their higher efficiency. This can be seen by the heat dispatch in figure A.8 in appendix A.7.

4.4.4 Impact of DHn Transmission Constraints

By comparing the difference in installed HP capacities with the current DHn transmission limits between different parts of the city active, limited by the transmission equations in section 3.3, to a case where these constraints are removed gives an indication of the savings that can be achieved if the system were to be cost-minimized, relating to *RQ1*. This can then be compared with the costs of expanding the transmission network to see whether or not an expansion would be feasible in relation to the savings associated with it. Worth to note is that the remaining equations limiting the HPs are still present.

The differences in installed HP thermal capacities between the cases, with- and without DHn transmission constraints, are shown by the bars in figure 4.15 where positive values indicate higher investments without the DHn transmission constraints and vice versa.

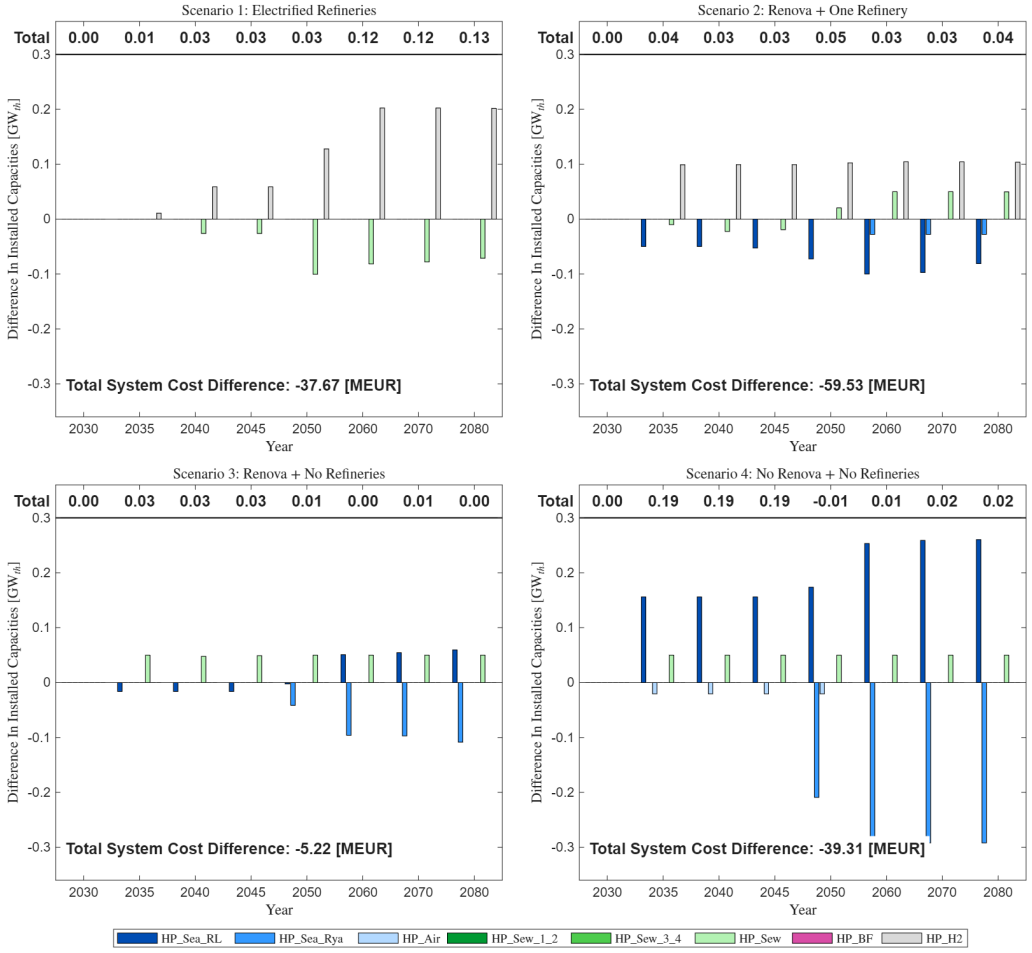

Figure 4.15: Difference in installed HP thermal capacities and total system costs between scenarios with no DHn transmission limits and the reference scenarios.

Without the current DHn transmission limits between different parts of the city it can be seen that new investments in HP_{H2} and HP_{Sew} are preferred when applicable due to their higher relative efficiencies such that they replace other types of HPs,

mainly HP_{Sea}. This is seen by the relative differences in installed HP capacities for *Scenario 2* in figure 4.15. In terms of monetary values, the total system cost decreases for all scenarios, where the largest difference occurs in *Scenario 2*. This is mainly due to the increased capacity in HP_{H2} which replaces investments in HP_{Sew} and simultaneously reduces the investments in peak-load capacities. The reason for this is that these, compared to HP_{Sea}, can be used more flexibly even under higher electricity prices since they require less electricity per heat output due to their increased heat source temperature and COP. Similar reasoning goes for HP_{Sew}. So, as the refineries electrifies the amount of medium-grade waste heat is reduced, but at the same time the amount of heat coming from the electrolyzers is increased.

4.5 Optimal Sizing of TES

The optimal sizing of TES is related to *RQ5*. Depending on the different scenarios and thereby the different future system compositions, the optimal sizing changes. All scenarios storage capacities were plotted alongside each other. This is shown in figure A.9 in appendix A.8. In every scenario, some type of storage investment is beneficial for the system. From the four main scenarios, it is concluded that less waste heat correlates with more TTES. This is more clearly shown in figure 4.16 where the total installed capacities for different storage types for *Scenario 1-4* are visible.

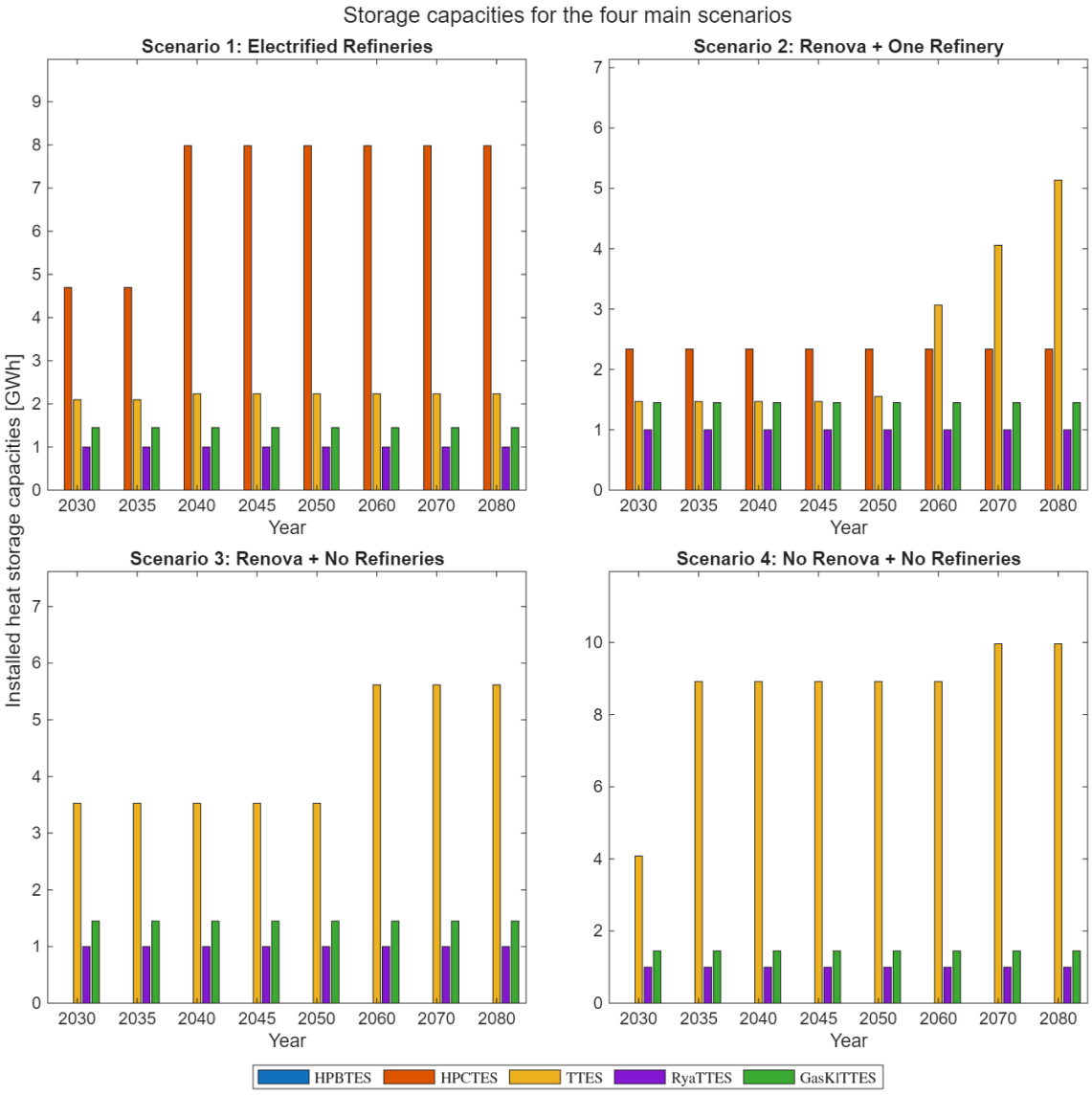

Figure 4.16: Storage capacities from the 4 main scenarios.

The general outcome of all scenarios shows that TTES is the main choice of storage, where the relative differences between the scenarios originate from differences in installed HP capacities. TTES complements the HPs with flexibility when fluctua-

tions in electricity prices occurs such that they can be charged when the electricity prices are low and later be discharged when the electricity prices are increased and the P2H technologies dispatch is reduced. This indicates a need for shifting load in the short-term as the TTES have a higher charge/discharge rate compared to the other storages included in the study. In figure A.10 in appendix A.9, this can be seen for *Scenario 2*, hour 1000-3000 where load and electricity prices fluctuate. The scenarios with more HPs therefore have more installed capacities of TTES as well. The scenarios with most TTES are *Scenario 4* and *Scenario 2: Greenfield*, with approximately 10 GWh installed capacity in both cases. None of the studied scenarios benefit from BTES.

For some scenarios, some kind of investment in CTES is beneficial. *Scenario 2: Limit EB* stands out, as the installed capacity is close to the maximum of 35 GWh allowed for the CTES. Seen in figure 4.17, the EBs are replaced by other technologies to supply the peak demand when a maximum installed capacity is present. This is visualized by the relative differences between the scenarios during hour 8000 - 8400 where it can be seen that when EBs are not constrained for *Scenario 2*, they cover most of the peak demand during these hours. When a maximum installed capacity is implemented in *Scenario 2: Limit EB*, the production from EBs is reduced, indicated by the absence of red in the peak demand. The technologies replacing EBs are mainly CCGT-BP and TES during the years where the CCGT-BP is still active. Later years, mainly TES discharge stands for the peak demand.

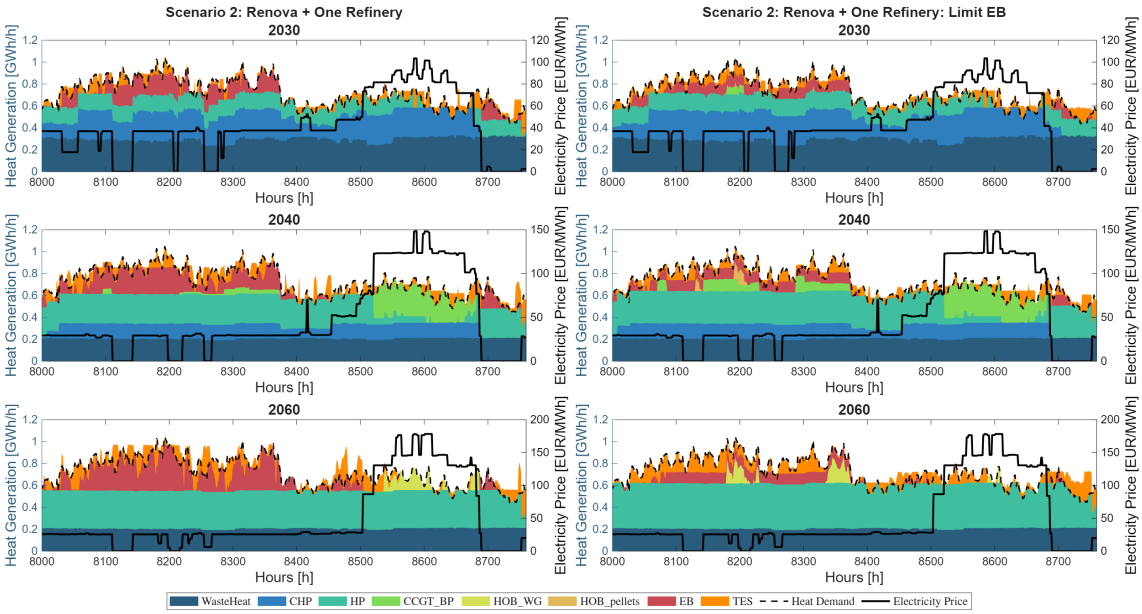

Figure 4.17: Heat dispatch for years 2030, 2040 and 2060, with limited allowed installed capacities of EBs during hours 8000-8760, compared to heat demand and electricity price.

For *Scenario 2: Limit EB*, the CTES acts as a seasonal storage, aligning with the theory, to supply heat instead of the EBs. This is further seen in figure 4.18, when

inspecting the SOC of all storages over specific years. TES covers more and more peak-load over the years, the model thus invests in more CTES, reaching almost 30 GWh in year 2060.

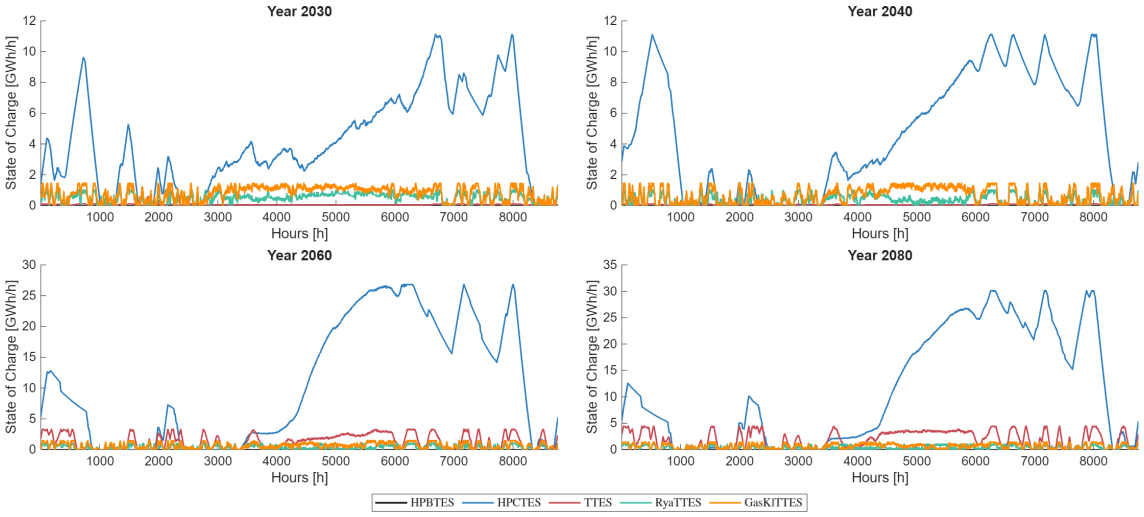

Figure 4.18: Yearly State of Charge for all invested storages over years 2030, 2040, 2060 and 2080.

5
Discussion

One of the research questions was to identify the impact that the electrification of the refineries have on the role of HPs in the DH system. As the refineries are electrified, the available medium-grade waste heat is assumed to be reduced, but the waste heat coming from electrolyzers is increased. This makes it cost-efficient to primarily invest in HPs recovering heat from the electrolyzers, both since electricity to electrolyzers is prioritized and that these HPs have a higher relative efficiency compared to the other ones in this study. This is indicated by the gray bars in figure 4.2. There also seems to be a trend of replacing the decreasing waste heat from the refineries with a larger proportion of HPs, EBs and HOB_{WG} for *Scenario 2-4*. This shows that an energy mix consisting of these technologies is the most cost-optimal given the assumptions made. However, with the high H2 demand active the total installed thermal capacities of HPs are reduced and new CHP plants are introduced.

The assumptions regarding the future availability of waste heat originating from the refineries can be questioned. The available waste heat in this study was assumed to decrease in proportion to the expected decrease in production volume from Preem. This means that the temperature levels of the heat, originating from different processes in the future production of bio- or electrofuels, are assumed to be at the same level as today. If, on the other hand, the temperature levels would be decreased, or the heat would be needed internally in other processes it is expected that the available waste heat would be reduced even more. This would most likely cause reductions in investments in HPs and EBs and increased investments in CHP plants and HOB_{WG} in *Scenario 1* as the electricity grid would become increasingly constrained and more electricity would have to be produced locally. For *Scenario 2*, local grid congestion is not as big of a problem and this scenario is thus likely to not be as sensitive to a reduction in waste heat. There are also uncertainties regarding availability of waste heat from different sources in general which should be seen as a limitation in this study.

Important existing units include the waste heat production from Renova and the refineries. The four main scenarios are based on the levels in these sources of heat, due to their large impact on the DH-system. The DH-system has been shown to be quite unique in Gothenburg, not only due to the large amounts of waste heat, but also due to the abundance of unique production units being concentrated in the North-West part of Gothenburg. These geographical boundaries led to most of the geographical- and technical constraints. The existing infrastructure limits the model to not be able to invest in HPs such as HP_{Sea}, and HP_{H2}, and retain

the installed capacity in HP_{Sew} due to DHn transmission constraints, which limit HP-investments for a long time. This means that the existing units today limits the optimal system configuration for a very long time. This is with the assumption that the transmission capacity cannot increase. This was assumed partly because the costs to increase capacity is hard to estimate, as the costs are very dependent on a geographical resolution.

The current DHn transmission limits between different parts of the city were shown to impact HP implementation, but could not be fully represented due to the modeling limitation of one singular node. If the model would be divided into multiple nodes, the effect of existing units would probably be even greater than in the results shown in this study. As the model has a lot of production in North-West Gothenburg (mainly from HPs), realistically this wouldn't be feasible, as production has to be spread out to meet the demand locally. With more nodes, the total installed capacity would probably increase as well, because the heat demand would have to be covered to some extent by every singular node, with its production units and eventually trade between nodes, with relevant assumptions. This opens up the possibility that the same amount of HPs might not be feasible as the heat sources are concentrated to one area. Studying the impacts of DH transmission limits between different nodes of the city, as well as local bottlenecks in the electricity grid, are proposed for future studies.

When comparing the savings that can be achieved if the current DHn transmission limits are removed it was shown that there is potential in investing in larger capacities of HPs compared to what is possible with the current network layout. However, it should be noted that the costs of expanding the network need to be lower than the savings to be economically feasible. Whether or not this is the case needs further investigation as the costs of expanding the network is different depending on where it is necessary.

Seen in figure 4.7, the total installed capacity in the Brownfield system is approximately 1.78 GW_{th} for year 2030 (without waste heat from the refineries and Renova), which is much greater than the maximum heat demand during the year of approximately 1 GW_{th}. What can be concluded from this, is that the existing capacity of HOBs is not used at all during year 2030 in the Brownfield model. Even new investments in EBs are done as soon as year 2030 to cover for peak demand. When looking at the dispatch in figure 4.5, it is seen that the existing capacities of CHP plants and the CCGT-BP are mainly used in the short term. It was also shown that new investments were smaller in the Brownfield model compared to the Greenfield model, exaggerating the importance of utilizing the existing units in the short term. This might be of even higher importance when it comes to the electrification of the city in the near future since the existing CHP plants help cover up local electricity deficit, thus supporting the energy system until new investments in the offshore wind farm have been approved.

In section 2.6.1 it is described that the DHn of Gothenburg is roughly a 2nd or 3rd

generation DHn, based on the high temperatures in the system. As the existing DHn is mostly dependent on medium-grade waste heat and bio-based incineration, the high temperatures are easy to acquire. Since the DHn is already adapted to such high temperatures, and the production patterns of already existing units, it would be of relevance to see if it is cost-effective to prolong the lifetime of existing units. The most relevant ones being the CHP plants and the CCGT-BP, as these are used more or less across all scenarios. This type of analysis was not conducted, and is recommended to be analyzed in further projects in this area.

When analyzing the operational conditions of HPs and EBs it can be seen that both of the technologies react to external price signals such that they increase production when the electricity price is low and decrease production when it is high. Differences between the two are mainly related to their role in the energy system. Due to the higher CAPEX of HPs compared to EBs, HPs are used as mid-load plants as a larger number of FLH are required to make them competitive. EBs are on the other hand used as peak-load plants to cover up heat-loads of short duration but with high amplitude as their investment costs are lower. This behavior is also related to the variable running costs originating from the electricity price. As HPs have the benefits of producing more useful heat per electricity input compared to EBs these will be preferred to run over a larger variety of electricity prices.

One interesting find, when comparing HPs and EBs, was that EBs showed a higher sensitivity to local congestion in the electricity grid. With no offshore wind, access to cheap electricity became more limited as import from the regional grid was maximized more often, as seen in figure 4.12. Due to this, the installed capacities of EBs were reduced significantly when compared to *Scenario 2*. HPs did however not decrease as much. There could be several possible explanations for this. Firstly, as EBs have a rather similar CAPEX compared to HOB_{WG} they share similar dispatch patterns. Thus, the reduction in EB capacity is offset by a higher production from HOB_{WG} when the heat demand is increased. Secondly, since the CAPEX of CHP plants is much larger than the CAPEX of HPs it would not be cost-efficient to invest in a too high thermal capacity of CHP plants. As a result, HPs are invested in to make use of the hours where the electricity price is low resulting in electricity being prioritized to run the HPs instead of the EBs. All in all EBs thereby seem to be used more opportunistically compared to HPs when there is a surplus production of low-cost electricity.

When analyzing the results and especially the P2H technologies it is evident that the electricity price profile has an important impact on the results. The regional electricity prices originate from generation units with a low marginal cost of electricity and varying production making it hard for local units to outcompete. However, this development is expected to increase, suggesting that the variation in electricity prices will be amplified as more intermittent sources are deployed [2], [3], motivating the usage of the electricity price profiles. These findings are also in line with the results from previous studies including Rosén et al. [13] and Garciá et al. [14] confirming that the electricity prices are an important factor for the future of P2H

technologies, even when applying a more realistic dynamic of different types of HPs.

The implications that the volatility of the electricity prices have in this study are firstly that the flexibility of the P2H technologies together with TES is incentivized to capture the variability of the prices. Secondly, it de-incentivizes new investments in CHP plants as the cost of producing heat is increased when the electricity prices decrease. Furthermore, the electricity prices are based on the weather year 2019, which is the year that also has been used for the heat demand profile, electricity demand profile, weather patterns and so on. As these are related to the ambient temperature it would be of interest to study a variety of weather years to avoid sub-optimizing the investments and dispatch of different units. This is suggested as future work.

A topic closely related to *Scenario 2: No Offshore Wind*, is how the model creates an electricity market that is unrealistic when compared to the real life spot market. When once again discussing the difference between regional- and local electricity prices, figure 4.12 shows a case when imports are constrained many hours during the year. This scenario both constrains the EBs, but also incentivizes CHP plants to be invested in, where the total installed capacity in CHP is greater than HPs from year 2060, seen in figure 4.11. It is important to highlight the method the model uses to solve its heat and electricity balances. As mentioned before, the model is bound to always meet the demand for electricity and heat. When it cannot, it will increase production from somewhere, and in this case, make unrealistic solutions when comparing with the electricity market used in real electricity systems. If there is a trend of higher local marginal costs of electricity due to congestion in the electricity grid, it opens up the discussion if the market structure has to be reformed.

The difference in local- and regional electricity prices could indicate two things. *(1)* Congestion in the electricity grid could be an issue in Gothenburg if the DH is to be electrified. This aligns with previous analysis from Göteborgs Stad [38], which states that the power capacity could be a problem for the city. This means that the installation of the offshore wind park could be of large importance for the energy system of Gothenburg. *(2)* It also means that a local, flexible, energy market (described in section 2.5) could be of use if electricity imports cannot expand to the sufficient amount. If this type of solution is considered, it is of importance in future works to investigate a more nuanced flexibility market structure and to investigate if this type of flexibility measure is the most cost efficient for the city of Gothenburg.

In terms of taxes and tariffs, the largest impact is the energy tax related to converting electricity to heat. With the tax, the cost-optimality of EBs is reduced and the marginal cost of heating is increased for all seasons except during the summer due to the abundance of waste heat. In comparison to EBs, the HPs are not as sensitive to the extra cost added from the energy tax since a lower amount of electricity is needed per unit of heat. For the tariffs related to installed capacities, these were shown to have a smaller impact indicating that future policy frameworks should mainly be focused on reducing the taxes on P2H to enhance sector coupling and

enable the flexible utilization of P2H technologies.

These findings are similar to the findings of Bertilsson et al. [12], with the main difference that the energy tax had a lower impact on the future cost optimality of P2H technologies in this work, even with an increased tax level of 45 EUR/MWh compared to 30 EUR/MWh used in the previous work. This discrepancy could be attributed to the increased level of details of the different kinds of HPs and their relative efficiencies that have been used in this work, compared to only assuming a constant COP-value. This underlines the importance of a higher level of detail when performing energy systems modeling.

There is an ongoing discussion that the taxes related to using electricity to produce heat would make P2H technologies operate less flexibly. What was seen in this study was that the flexibility of HPs was reduced slightly where they operated during a more narrow span of electricity prices resulting in an overall reduced number of FLH for the HPs with lower efficiencies. However, the flexibility of EBs to absorb surplus electricity and support the system during peak loads was substantially reduced, indicating that the taxes impact the system's flexibility.

It is cost optimal for the model to invest in some kind of storage beyond the existing facilities for all scenarios investigated. Earlier stated by Göteborg Energi, is that an additional TTES or the HPCTES is not profitable in their current system composition. This statement can be compared to *Scenario 1* year 2030, where it is cost optimal to invest in approximately 2 GWh TTES, but no realistic amount of HPCTES. No BTES is cost efficient for the system, indicating most likely that slow discharge rates cannot utilize the varying value of heat during the winter. How much storage that is invested in, in the model, is difficult to compare to real life storage dynamics. The storages in the model can currently store energy unspecified from where in the DHn, but can realistically to some extent only store the locally produced energy from neighboring production units. As the model treats each storage type as a fleet, the installed capacity could either be one large storage, or several smaller ones. There would have to be profitability to invest in each individual storage, either a large potential in one place, or several areas with spread out potentials. Due to these uncertainties, smaller values in installed capacities of storages in the model would not necessarily mean that storages could be applicable in the real DHn. However, if the storage capacities are of larger magnitude, there is a large potential to store energy for the system composition, meaning there is a larger chance that a storage would be applicable in the real DHn. For several scenarios, this is the case (see figure A.9). The large investments in TTES indicate a demand for shifting load where the HPs complement the TTES and vice versa due to variations in electricity prices (see figure A.10). The storages could then be coupled in close proximity to the HPs, which could give value to the system. It is also worth to note that only one configuration of CTES was evaluated, and perhaps other configurations has better cost efficiency for the system.

For this particular modeling-year, the electricity prices were low when the heat de-

mand was high during the 2nd heat demand peak, but with a higher penetration of wind this is not unlikely to happen in the future either. Seen generally for different scenarios is that EBs are used to cover this particular peak demand. In a modeling-year where high electricity prices and high heat demand align, the EBs would not be the preferred technology to cover the demand. If another modeling year would be used, the large penetration of EBs might not have been shown. However, as one peak has high electricity prices and one peak has low prices, the model catches the dispatch for both cases. How often high- and low electricity prices align with the peak demand is important to account for, as different technologies will be cost optimal depending on which occur most frequently.

Although the comparison between the cost of producing heat via DH and the cost of producing heat through an individual HP was rather simplified it is still relevant to discuss the causes to the differences. First, large-scale HPs coupled to the DHn can utilize waste heat sources with higher temperatures, meaning that although they have to lift the temperature to higher levels they receive a higher COP on average due to their higher availability of waste heat sources. Second, due to the abundance of medium-grade waste heat, a large portion of the heat can be generated with a very low cost, which is not the case for an individual HP. Third, there is a higher flexibility of utilizing different production units such that P2H technologies can ramp down their production when the electricity prices are increased and HOB_{WG} can be used instead. These behaviors were shown in the results and align with the theory presented in section 2.2.

However, there are also certain things that have to be kept in mind when interpreting the results. As the calculations purely were made on the cost of producing heat, it means that the costs of DH infrastructure are not included. The share of these costs to the total can be of significant amount, so for a more fair comparison the recommendation is that they should be included as well. If one would have looked at the total system cost of connecting one extra customer to the DHn compared to that customer installing an individual HP the results could be different. The reason for this is that producing that extra unit of heat would in the DH case be set by the marginal cost of heating and if all cheap units already are operating at full capacity, this cost would be set by a technology with a high variable cost. In that case it could be cheaper for a customer to install an individual HP. However, similar reasoning goes for the individual HPs since if more and more people would start installing their own HPs there would be an increase in electricity demand which would require building new infrastructure or running expensive units to provide that electricity. This would be extra problematic during colder periods since individual HPs are more tightly linked to the consumer demand compared to what the large-scale HPs in the DH system are. Future studies should hence explore this difference in more detail to enable a nuanced comparison between the DHn and individual solutions.

6
Conclusion

The study aimed to answer and analyze what future role large-scale HPs have in the energy system of Gothenburg. This was done by modifying a linear optimization model for the energy system of Gothenburg. What was concluded specifically from the modeling-part of the study, was that a lot of assumptions were necessary, due to the limitations the model had in terms of granularity with only one node. Future work in this field is recommended to have a model with geographical resolution, not only to asses the future role of large-scale HPs, but also to be able to assess large-scale HPs with individual HPs.

The amount of medium-grade waste heat available in the DHn is fundamental for the city of Gothenburg, resulting in the main scenarios being based on this. The electrification of the refineries is crucial for the climate transition, but comes with complications for both the electricity- and DH systems with higher electricity demand and lower waste heat. In *Scenario 1* where there is waste heat available from the refineries and Renova together with an increased electricity demand from H2 production, HPs have the lowest penetration due to congestion issues in the electricity grid and a large proportion of waste heat still available. This led to a system composition with CHP plants and HPs, with little change across all years. As waste heat availability decreases across the scenarios, more HPs penetrate to produce a larger and larger share of the DH demand. Across scenarios, HPs with higher COP are prioritized. As the refineries disappear, a larger share of electricity is unlocked due to decreased H2 production.

Existing units and the DHn composition proved to affect the availability of HP production. As many HPs were only available for installation in North-West Gothenburg, the DHn transmission limits and existing units in that area affected when, and to what extent, HPs could be installed in Gothenburg. It opened up the discussion if the total installed HP capacity is reasonable as the majority or sometimes all heating production occurs in that area. This once again motivates why more nodes are important in the model, as this could investigate the feasibility of large-scale HP placement in the city. The total installed thermal capacities across all scenarios are much less than that of the existing capacity, which demonstrates an optimal system solution with no room for uncertainty in load. A comparison between the Greenfield and Brownfield model proved that the two systems converged in year 2060, but that smaller investments were necessary in the Brownfield model up until that year. Thus underlining the importance of utilizing existing units until their technical lifetime has run out.

Electricity availability and electricity prices were important for the operation of large-scale HPs. The HPs acted as mid-load in the system where the production volume became sensitive to external price signals. EBs also proved to be sensitive, where they mostly acted as peak-load during the 2nd peak demand, due to low electricity prices during this period. However, without the offshore windfarm, EBs only became viable up until 2050. HPs and EBs were replaced by CHP plants and HOBs in year 2060 due to congestion in the electricity grid without offshore wind. Therefore, the future penetration of HPs was highly dependent on cheap available electricity.

Taxes and tariffs on the P2H technologies proved to increase the marginal cost of heat. Taxes on generation proved to have a larger impact on the marginal cost of heat compared to tariffs on installed capacity. Although taxes increased the marginal cost of heat, the model did not impede HP investments toward CHP generation, underlining the difference in costs between the two technologies. The technology most affected by taxes was EBs, where HOB_{WG} covered peak-load instead.

Flexibility in terms of TES was shown to be cost-effective across all scenarios. HPs and TTES were shown to complement each other with varying electricity prices, indicating a need to shift load in the short-term. A result of less waste heat across the main scenarios, led to more HP- and TTES investments. Only one of the scenarios, with a maximum allowed EB capacity, indicated a need for seasonal storage, as extra peaking generation was needed during the 2nd peak in heat demand. It was important to highlight that this particular outcome worked for a scenario with low electricity prices and high heat demand aligning with each other for the 2nd peak heat demand.

Declaration of AI-use

We acknowledge using MATLAB (R2025b) Copilot for assistance in solving errors in coding, as well as plotting.

We used prompts for plotting through examples of built-in functions that Copilot gave us. One plot was also made almost from scratch from Copilot when another example-plot of our making was presented as a prompt. All plots were reviewed before implementation. A full record of prompts and outputs is available upon request.

We acknowledge using ChatGPT-5 to assist in making of plots and preliminary source handling.

Prompts were given in iterations to generate some of the plots shown in the report and to help handle error messages for own written code. Generated code was then manually designed to adjust smaller tweaks and errors. General questions about MATLAB built-functions were also asked as part of learning. Sources were inserted to make biblatex references, in order to document when and what types the sources were used. In the end of the study, a new biblatex was conducted manually in accordance with Chalmers Library, meaning the sources in the text are not by AI. A full record of prompts and outputs is available upon request.

Bibliography

[1] Swedish Environmental Protection Agency (Naturvårdsverket). "Sweden's Climate Act and Climate Policy Framework." 2026, [Online]. Available: https://www.naturvardsverket.se/en/international/swedish-environmental-work/swedens-climate-act-and-climate-policy-framework/ (accessed on: 2026-05-11).

[2] IEA. "Energy system of Sweden." 2024, [Online]. Available: https://www.iea.org/countries/sweden (accessed on: 2026-01-28).

[3] P. Holmberg and T. P. Tangerås, "The Swedish electricity market – today and in the future," *SVERIGES RIKSBANK ECONOMIC REVIEW 2023*, no. 1, 2022. [Online]. Available: https://www.riksbank.se/globalassets/media/rapporter/pov/artiklar/engelska/2023/230512/2023_1-the-swedish-electricity-market--today-and-in-the-future.pdf (accessed on: 2026-01-29).

[4] R. Calvo García, J. M. Marín Arcos, S. Kumar, S. N. Gunasekara, and J. Thakur, "Techno-economic analysis of flexible sector coupling between electrical and thermal sectors," *Energy Conversion and Management: X*, vol. 27, p. 101 145, Jul. 2025. DOI: https://doi.org/10.1016/j.ecmx.2025.101145.

[5] O. Abdur Rehman, V. Palomba, A. Frazzica, and L. F. Cabeza, "Enabling Technologies for Sector Coupling: A Review on the Role of Heat Pumps and Thermal Energy Storage," *Energies*, vol. 14, no. 24, Dec. 2021. DOI: 10.3390/en14248195.

[6] H. Jouhara et al., "Waste heat recovery technologies and applications," *Thermal Science and Engineering Progress*, vol. 6, pp. 268–289, Jun. 2018. DOI: 10.1016/j.tsep.2018.04.017.

[7] D. Bogdanov, R. Satymov, and C. Breyer, "Impact of temperature dependent coefficient of performance of heat pumps on heating systems in national and regional energy systems modelling," *Applied Energy*, vol. 371, p. 123 647, Oct. 2024. DOI: 10.1016/j.apenergy.2024.123647.

[8] M. G. Nielsen, J. M. Morales, M. Zugno, T. E. Pedersen, and H. Madsen, "Economic valuation of heat pumps and electric boilers in the danish energy system," *Applied Energy*, vol. 167, pp. 189–200, Apr. 2016. DOI: 10.1016/j.apenergy.2015.08.115.

[9] European Commission. "Gothenburg's Journey to Fossil-Free District Heating and Cooling," [Online]. Available: https://eu-mayors.ec.europa.eu/en/Gothenburg-Journey-to-Fossil-Free-District-Heating-and-Cooling (accessed on: 2026-01-29).

[10] A. Muscat, E. de Olde, I. de Boer, and R. Ripoll-Bosch, "The battle for biomass: A systematic review of food-feed-fuel competition," *Global Food Security*, vol. 25, p. 100 330, Jun. 2020. DOI: 10.1016/j.gfs.2019.100330.

[11] D. M. Sneum, M. G. González, and J. Gea-Bermúdez, "Increased heat-electricity sector coupling by constraining biomass use?" *Energy*, vol. 222, p. 119 986, May 2021. DOI: 10.1016/j.energy.2021.119986.

[12] J. Bertilsson, L. Göransson, and F. Johnsson, "Impact of Energy-Related Properties of Cities on Optimal Urban Energy System Design," *Energies*, vol. 17, no. 15, p. 3813, Aug. 2024. DOI: 10.3390/en17153813.

[13] S. Rosén, P. Sobha, and C. Wallmark, "Waste heat availability from hydrogen-based industries in district heating systems – A Swedish case study," *Energy Reports*, vol. 14, pp. 432–444, Dec. 2025. DOI: 10.1016/j.egyr.2025.06.028.

[14] R. Calvo García, J. M. Marín Arcos, S. Kumar, S. N. Gunasekara, and J. Thakur, "Techno-economic analysis of flexible sector coupling between electrical and thermal sectors," *Energy Conversion and Management: X*, vol. 27, p. 101 145, Jul. 2025. DOI: 10.1016/j.ecmx.2025.101145.

[15] D. P. Loucks, "Linear optimization modeling," in *Public Systems Modeling: Methods for Identifying and Evaluating Alternative Plans and Policies*. Cham: Springer International Publishing, 2022, pp. 89–109.

[16] L. Göransson et al., "Tre elsystem som kan möta omställningen av industri- och transportsektorerna," Department of Space, Earth and Environment, Chalmers University of Technology, Gothenburg, Sweden, 2025. [Online]. Available: https://research.chalmers.se/publication/546563/file/546563_Fulltext.pdf (accessed on: 2026-02-03).

[17] L. Göransson, "The impact of wind power variability on the least-cost dispatch of units in the electricity generation system," Ph.D. dissertation, Department of Energy and Environment, Chalmers University of Technology, Gothenburg, Sweden, 2014. [Online]. Available: https://publications.lib.chalmers.se/records/fulltext/196126/196126.pdf.

[18] H. Gadd and S. Werner, "Daily heat load variations in Swedish district heating systems," *Applied Energy*, vol. 106, pp. 47–55, Jun. 2013. DOI: 10.1016/j.apenergy.2013.01.030.

[19] O. Opadokun, Y. X. Tao, and J. Lamb, "A review of waste heat sources for district heating," *Energy Reports*, vol. 14, pp. 1051–1070, Dec. 2025. DOI: 10.1016/j.egyr.2025.07.015.

[20] M. Abugabbara et al., "How to develop fifth-generation district heating and cooling in sweden? Application review and best practices proposed by middle agents," *Energy Reports*, vol. 9, pp. 4971–4983, Dec. 2023. DOI: 10.1016/j.egyr.2023.04.048.

[21] H. Averfalk, P. Ingvarsson, U. Persson, M. Gong, and S. Werner, "Large heat pumps in Swedish district heating systems," *Renewable and Sustainable Energy Reviews*, vol. 79, pp. 1275–1284, Nov. 2017. DOI: 10.1016/j.rser.2017.05.135.

[22] S. Frederiksen and S. Werner, *District Heating and Cooling*. Lund, Sweden: Studentlitteratur, 2014.

[23] "Chapter 10 Pinch point analysis," in *Integrated Design and Simulation of Chemical Processes*, ser. Computer Aided Chemical Engineering, A. C. Dimian, Ed., vol. 13, Elsevier, 2003, pp. 393–434. DOI: 10.1016/S1570-7946(03)80034-2.

[24] H. Jouhara et al., "High-temperature heat pumps: Fundamentals, modelling approaches and applications," *Energy*, vol. 303, p. 131 882, Sep. 2024. DOI: 10.1016/j.energy.2024.131882.

[25] H. Pieper, T. Ommen, J. K. Jensen, B. Elmegaard, and W. B. Markussen, "Comparison of COP estimation methods for large-scale heat pumps used in energy planning," *Energy*, vol. 205, p. 117 994, Aug. 2020. DOI: 10.1016/j.energy.2020.117994.

[26] J. K. Jensen, T. Ommen, L. Reinholdt, W. B. Markussen, and B. Elmegaard, "Heat pump COP, part 2: Generalized COP estimation of heat pump processes," in *Proceedings of the 13th IIR-Gustav Lorentzen Conference on Natural Refrigerants*, Valencia, Spain, 2018, pp. 1136–1145. [Online]. Available: https://backend.orbit.dtu.dk/ws/portalfiles/portal/151965635/MAIN_Final.pdf (accessed on: 2026-03-15).

[27] D. Bogdanov et al., "Radical transformation pathway towards sustainable electricity via evolutionary steps," *Nature Communications*, vol. 10, p. 1077, Mar. 2019. DOI: 10.1038/s41467-019-08855-1.

[28] O. Ruhnau, L. Hirth, and A. Praktiknjo, "Time series of heat demand and heat pump efficiency for energy system modeling," *Scientific Data*, vol. 6, p. 189, Oct. 2019. DOI: 10.1038/s41597-019-0199-y.

[29] D. Müller, C. Bott, M. Hagström, and P. Bayer, "Cavern thermal energy storage: State of play and prospects," *Applied Energy*, vol. 404, p. 127 141, Feb. 2026. DOI: 10.1016/j.apenergy.2025.127141.

[30] M. Erlström, C. Mellqvist, G. Schwarz, M. Gustafsson, and P. Dahlqvist, "Geologisk information för geoenergianläggningar – en översikt," Sveriges geologiska undersökning (SGU), Uppsala, Sweden, SGU-rapport 2016:16, 2016. [Online]. Available: https://www.sgu.se/globalassets/samhallsplanering/energi/geologisk-information-for-geoenergianlaggningar.pdf (accessed on: 2026-02-24).

[31] H. Sadeghi, R. Jalali, and R. M. Singh, "A review of borehole thermal energy storage and its integration into district heating systems," *Renewable and Sustainable Energy Reviews*, vol. 192, p. 114 236, Mar. 2024. DOI: 10.1016/j.rser.2023.114236.

[32] W. Hua, X. Lv, X. Zhang, Z. Ji, and J. Zhu, "Research progress of seasonal thermal energy storage technology based on supercooled phase change materials," *Journal of Energy Storage*, vol. 67, p. 107 378, Sep. 2023. DOI: 10.1016/j.est.2023.107378.

[33] J. Rodin, private communication, Feb. 2026.

[34] S. Homaei, S. Roussanaly, and A. Tomasgard, "Analysis of short-run and long-run marginal costs of electricity generation in the power market," *Energy Economics*, vol. 155, p. 109 169, Mar. 2026. DOI: 10.1016/j.eneco.2026.109169.

[35] G. Antonopoulus, G. Fulli, M. Masera, and S. Vitiello, "Nodal pricing in the European internal electricity market," Publications Office of the European Union, Luxembourg, JRC119977, 2020. [Online]. Available: https://op.europa.eu/en/publication-detail/-/publication/50ac5c62-8055-11ea-b94a-01aa75ed71a1/language-en (accessed on: 2026-04-20).

[36] S. Chondrogiannis, J. Vasiljevska, A. Marinopoulos, I. Papaioannou, and G. Flego, "Local electricity flexibility markets in Europe," Luxembourg, JRC130070, 2022. [Online]. Available: https://op.europa.eu/en/publication-detail/-/publication/61463d72-4850-11ed-92ed-01aa75ed71a1/language-en (accessed on: 2026-04-20).

[37] E. Moberg, "The value of flexibility in a future electric power distribution system," M.S. thesis, Industrial Engineering and Management, Uppsala, Sweden, 2021. [Online]. Available: https://www.diva-portal.org/smash/record.jsf?pid=diva2:1574462.

[38] Göteborgs Stad, *Göteborgs Stads energiplan 2022–2030*, Online; PDF, 2023. [Online]. Available: https://www4.goteborg.se/prod/Stadsledningskontoret/LIS/Verksamhetshandbok/Forfattn.nsf//30944AE15043B0DDC1258845003CE158/$File/C12574360024D6C7WEBVCPA387.pdf?OpenElement (accessed on: 2026-03-03).

[39] Göteborg Energi, "ÅRS- OCH HÅLLBARHETSREDOVISNING 2019," Gothenburg, Sweden, Tech. Rep., 2019. [Online]. Available: https://www.goteborgenergi.se/Files/Webb20/Kategoriserad%20information/Informationsmaterial/%C3%85rsredovisningar/G%C3%B6teborg%20Energi%20%C3%85rs-%20och%20h%C3%A5llbarhetsredovisning%202019.pdf?TS=637193583890764103 (accessed on: 2026-02-16).

[40] L. Holmquist, private communication, Feb. 2026.

[41] M. Lehtveer, private communication, Feb. 2026.

[42] Renova AB. "Ett viktigt steg mot minskad klimatbelastning från avfall!" Renova AB, [Online]. Available: https://www.mynewsdesk.com/se/renova/pressreleases/ett-viktigt-steg-mot-minskad-klimatbelastning-fraan-avfall-3318348 (accessed on: 2026-02-27).

[43] K. Jacobson and F. Törnqvist, "Implementation of Dry Hydrated Potassium Carbonate Carbon Capture: A case study of Renova's Waste-to-Energy plant in Sävenäs," M.S. thesis, Department of Space, Earth and Environment, Division of Energy Technology, Gothenburg, Sweden, 2024. [Online]. Available: https://odr.chalmers.se/server/api/core/bitstreams/f4b50aa6-c2b6-42a0-8e2c-7fde5f84d629/content.

[44] C. Hammar, "Heat integration between CO_2 Capture and Liquefaction and a CHP Plant: Impact on Electricity and District Heating Delivery at Renova's CHP Plant in sävenäs," M.S. thesis, Department of Space, Earth and Environment, Division of Energy Technology, Gothenburg, Sweden, 2022. [Online]. Available: https://odr.chalmers.se/server/api/core/bitstreams/2e58e1da-48c9-4510-ac6f-21a469bcde84/content.

[45] Danish Energy Agency, *Technology Data for Energy Storage*. [Online]. Available: https://ens.dk/en/analyses-and-statistics/technology-data-energy-storage (accessed on: 2026-02-16).

[46] L. Hjalmarsson, private communication, Feb. 2026.

[47] V. Henisch, L. Göransson, M. Odenberger, and F. Johnsson, "Interconnection of the electricity and heating sectors to support the energy transition in cities," *International Journal of Sustainable Energy Planning and Management*, vol. 24, 2019. DOI: 10.5278/ijsepm.3328.

[48] V. Heinisch, L. Göransson, R. Erlandsson, H. Hodel, F. Johnsson, and M. Odenberger, "Smart electric vehicle charging strategies for sectoral coupling in a city energy system," *Applied Energy*, vol. 288, p. 116 640, 2021. DOI: 10.1016/j.apenergy.2021.116640.

[49] S. Rosén, L. Göransson, M. Taljegard, and M. Lehtveer, "Timely delivery of electricity for industrial hydrogen demands: Path dependencies in the transition of urban energy systems," *International Journal of Hydrogen Energy*, vol. 218, p. 153 975, 2026. DOI: 10.1016/j.ijhydene.2026.153975.

[50] S. Rosén, L. Göransson, M. Taljegård, and M. Lehtveer, "Modeling of a "Hydrogen Valley" to investigate the impact of a regional pipeline for hydrogen supply," *Frontiers in Energy Research*, vol. 12 - 2024, 2024. DOI: 10.3389/fenrg.2024.1420224.

[51] Danish Energy Agency, "Technology data catalogue for electricity and district heating," Danish Energy Agency, Copenhagen, Denmark, 2025, Updated version published May 2025, original first published August 2016; version 0016. [Online]. Available: https://ens.dk/media/6571/download (accessed on: 2026-02-20).

[52] SMHI. "Ladda ner observationer från havet," [Online]. Available: https://www.smhi.se/data/hitta-data-for-en-plats/ladda-ner-observationer-fran-havet/seatemperature/33089 (accessed on: 2026-02-12).

[53] J. Elken, I. Maljutenko, P. Lagemaa, R. Uiboupin, and U. Raudsepp, "Oceanographic preconditions for planning seawater heat pumps in the Baltic Sea – an example from the Tallinn Bay, Gulf of Finland," *State of the Planet*, vol. 4-osr8, p. 9, 2024. DOI: 10.5194/sp-4-osr8-9-2024.

[54] Copernicus. "Powering cities with seawater heat pumps," [Online]. Available: https://marine.copernicus.eu/services/use-cases/powering-cities-seawater-heat-pumps (accessed on: 2026-02-15).

[55] SMHI. "Ladda ner väderobservationer," [Online]. Available: https://www.smhi.se/data/hitta-data-for-en-plats/ladda-ner-vaderobservationer/airtemperatureInstant (accessed on: 2026-02-08).

[56] B. Bach, "Integration of Heat Pumps in Greater Copenhagen," M.S. thesis, Division of Strategy and Innovation, Copenhagen, Denmark, Mar. 2014. [Online]. Available: https://www.researchgate.net/publication/314094868_Integration_of_Heat_Pumps_in_Greater_Copenhagen?channel=doi&linkId=58b53644a6fdcc6f03ffb101&showFulltext=true.

[57] Göteborg Energi. "Bästa platsen för värmepumpar är i fjärrvärmen," [Online]. Available: https://www.goteborgenergi.se/i-var-stad/artikelbank/basta-platsen-for-varmepumpar-ar-i-fjarrvarmen (accessed on: 2026-02-23).

[58] F. Lindblom, private communication, Feb. 2026.

[59] D. Tommasini, N. Marx, Y. Wimmer, S. Reuter, and H. Kauko, "Electrolysis waste heat utilization for district heating — a Norwegian case study," *Smart Energy*, vol. 20, p. 100 207, 2025. DOI: 10.1016/j.segy.2025.100207.

[60] Göteborg Energi. "Framtidens batterifabrik kyls med – avloppsvatten," [Online]. Available: https://www.goteborgenergi.se/i-var-stad/artikelbank/framtidens-batterifabrik-kyls-med-avloppsvatten (accessed on: 2026-02-25).

[61] NOVO. "Volvo Cars announces an operational pause in NOVO Energy as search for battery technology partner continues," [Online]. Available: https://www.novoenergy.se/volvo-cars-announces-an-operational-pause-in-novo-energy (accessed on: 2026-02-25).

[62] A.-S. Borglund, "Avloppsvatten ska kyla batterifabriken i Göteborg," Oct. 3, 2024. [Online]. Available: https://www.energi.se/artiklar/2024/oktober/avloppsvatten-ska-kyla-batterifabriken-i-goteborg/ (accessed on: 2026-02-25).

[63] Eolus Vind AB. "Västvind vindkraftspark," [Online]. Available: https://www.eolus.com/projects/vastvind-vindkraftpark/ (accessed on: 2026-03-23).

[64] L. Wiginton, H. Nguyen, and J. Pearce, "Quantifying rooftop solar photovoltaic potential for regional renewable energy policy," *Computers, Environment and Urban Systems*, vol. 34, no. 4, pp. 345–357, 2010. DOI: 10.1016/j.compenvurbsys.2010.01.001.

[65] I. Zagrodzki, M. Bryk, P. J. Ziółkowski, T. Kowalczyk, P. J. C. Santana, and J. Badur, "Modelling and Performance Assessment of a Ground-Coupled Ammonia Heat Pump System: The EMPEC Ustka Case Study," *Sustainability*, vol. 18, no. 4, 2026. DOI: 10.3390/su18041719.

[66] V. Månborg, private communication, Feb. 2026.

[67] J. J. Aguilera et al., "Operational challenges in large-scale ammonia heat pump systems," Aug. 2021, pp. 1842–1853. DOI: 10.52202/062738-0163.

[68] P. Aalto, "Utilization of seawater heat pumps in buildings – system energy study of heating cooling performance," English, M.S. thesis, LAPPEENRANTA-LAHTI UNIVERSITY OF TECHNOLOGY LUT, 2021. [Online]. Available: https://lutpub.lut.fi/handle/10024/162794.

[69] A. Volkova, H. Pieper, T. Ommen, W. Brix Markussen, and B. Elmegaard, "Modelling framework for integration of large-scale heat pumps in district heating using low-temperature heat sources," *International Journal of Sustainable Energy Planning and Management*, vol. 20, May 2019. DOI: 10.5278/ijsepm.2019.20.6.

[70] B. Elmegaard, B. Zühlsdorf, L. Reinholdt, and M. Bantle, Eds., *Book of presentations of the International Workshop on High Temperature Heat Pumps*. Copenhagen, Denmark: Technical University of Denmark, 2017.

[71] M. Edvall, L. Eriksson, S. Harvey, J. Kjärstad, and J. Larfeldt, "Vätgas på Västkusten," RISE, Gothenburg, Sweden, 2022:31, 2022. [Online]. Available: https://ri.diva-portal.org/smash/record.jsf?pid=diva2%3A1640678&dswid=1381 (accessed on: 2026-03-11).

[72] Preem AB, "Annual and Sustainability Report 2024," Preem AB, Stockholm, Sweden, 2025. [Online]. Available: https://www.varopreem.com/media/ldrdvh5e/preem-annual-sustainablity-report-2024.pdf (accessed on: 2026-03-22).

[73] Konsumenternas Energimarknadsbyrå. "Energiskatt - skattesatser och kostnader," [Online]. Available: https://www.energimarknadsbyran.se/el/dina-elavtal-och-kostnader/fakturering-och-betalning/elrakningen/energiskatt/ (accessed on: 2026-05-05).

[74] Göteborg Energi. "Priser och avtal," [Online]. Available: https://www.goteborgenergi.se/foretag/vara-nat/gasnat/priser-och-avtal (accessed on: 2026-03-23).

[75] Vattenfall AB. "Prishistorik över rörligt elpris," [Online]. Available: https://www.vattenfall.se/elavtal/elpriser/rorligt-elpris/prishistorik/ (accessed on: 2026-05-08).

[76] St1 Nordic Oy, "GAME CHANGER 2024," St1 Nordic Oy, Helsingfors, Finland, 2024. [Online]. Available: https://media.ffycdn.net/eu/st1/kyTJEvDYN9xf8PnTjSwQ.pdf (accessed on: 2026-03-22).

[77] A. Lätt et al., "Avfallets roll i framtidens energisystem," Energiforsk AB, Uppsala, Sweden, 2019:589, 2019. [Online]. Available: https://energiforsk.se/media/26467/avfallets-roll-i-framtidens-energisystem-energiforskrapport-2019-589.pdf (accessed on: 2026-03-31).

[78] U. Sagebrand, C. Nordström, and B. Widarsson, "Uppföljning värmelager i bergrum," Energiforsk, Uppsala, Sweden, 2024:1054, 2024. [Online]. Available: https://energiforsk.se/rapporter/uppfoljning-varmelager-i-bergrum/ (accessed on: 2026-02-18).

A

Model Description & Technical Data

A.1 Electricity prices and Wind Profile

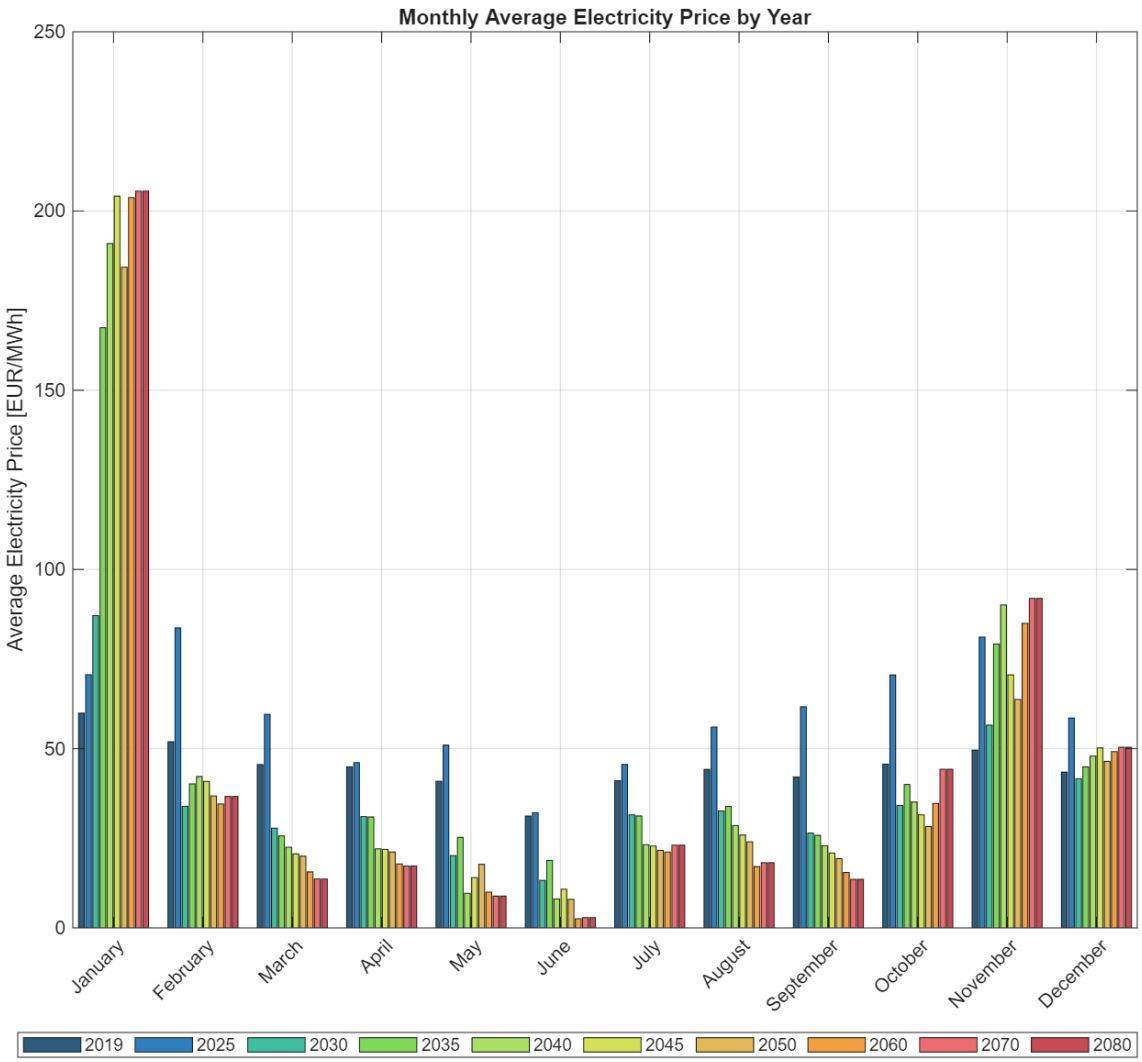

Figure A.1: Comparison of electricity prices for 2019, 2025 and modeled years. Prices for 2019 and 2025 comes from Nord Pool spot market [75].

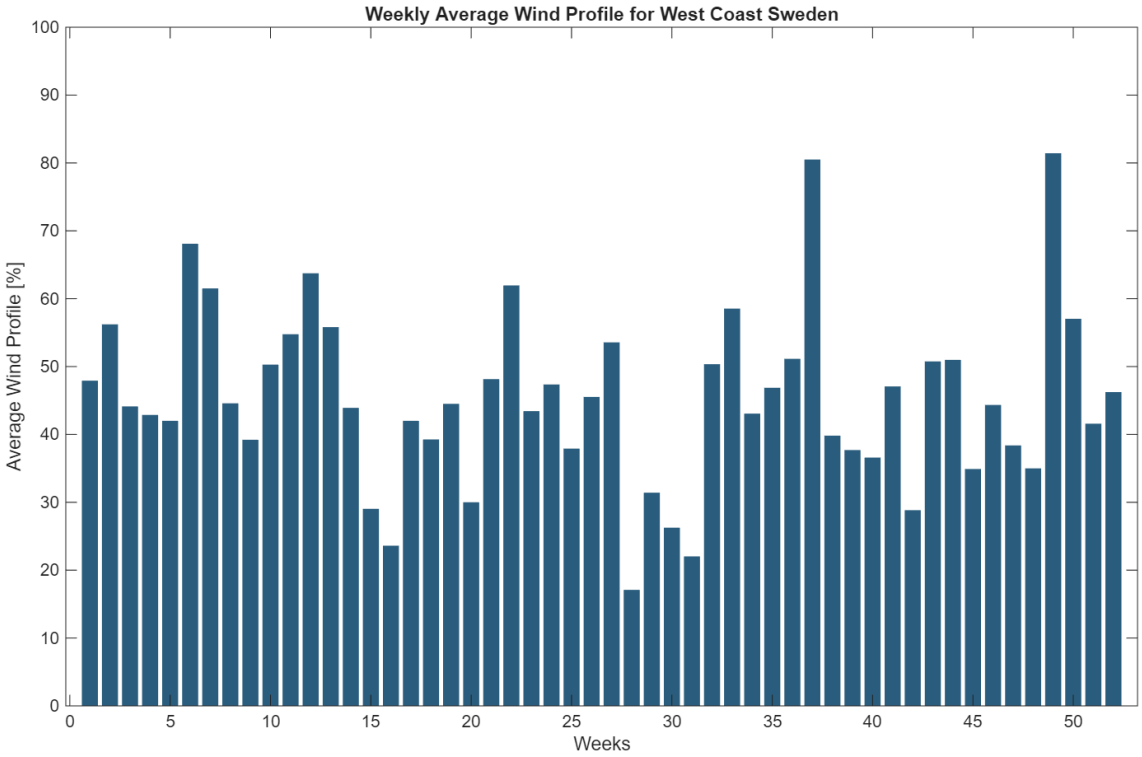

Figure A.2: Average wind profile for the West Coast of Sweden, year 2019, determining the percentage of installed capacity of wind power that can be used.

A.2 Technology costs

Table A.1: DEA costs for the different technologies that have been used in this study.

	CAPEX (EUR/kW)								O&M fix	O&M var
Technology	**2030**	**2035**	**2040**	**2045**	**2050**	**2060**	**2070**	**2080**	(EUR/kW)	(EUR/MWh)
WOFF	1800	1740	1680	1660	1640	1640	1640	1640	39	3.89
PVOpt	380	350	320	305	290	290	290	290	9.5	1.1
PVRoof	840	770	699	667.5	636	636	636	636	10.7	1.1
Peak_{WG}	600	587.5	575	562.5	550	550	550	550	19.8	0.4
CCGT_{WG}	882	874	866	858	850	850	850	850	29.56	0.8
$\text{CCGT}_{BP,WG}$	1276	1249	1222	1195	1168	1168	1168	1168	29.56	0.7
CHP_{W}	3560	3510	3460	3410	3360	3360	3360	3360	102	2.1
HOB_{W}	450	445	440	435	430	430	430	430	36.1	3.76
HOB_{WG}	60	55	50	50	50	50	50	50	1	1.17
$\text{HOB}_{Pellets}$	720	702.5	685	667.5	650	650	650	650	33.28	2.79
HP_{Sea}	420	420	420	420	420	420	420	420	4.25	1.8
HP_{Sew}	420	420	420	420	420	420	420	420	4.25	1.8
HP_{Air}	851	851	851	851	851	851	851	851	2.13	1.8
HP_{H2}	641	641	641	641	641	641	641	641	2.13	1.8
HP_{BF}	641	641	641	641	641	641	641	641	2.13	1.8
EB	60	60	60	60	60	60	60	60	1	1
PEM	600	525	450	387.5	325	325	325	325	12	0
HPCTES	1.1	1.1	1.1	1.1	1.1	1.1	1.1	1.1	0	0
HPBTES	0.5	0.5	0.5	0.5	0.5	0.5	0.5	1.1	0	0
TTES	3	3	3	3	3	3	3	3	0.009	0
H2_{tank}	48	38.5	29	25.5	22	22	22	22	0.53	0

Table A.2: Fuel costs used in the study

Fuel	Fuel cost [EUR/MWh]
Biomass	40
Biogas	77.14
Natural gas	34.27
Pellets	62
Bio-oil	136
Fossil oil	66.8

A.3 Detailed scenario descriptions

A.3.1 Electrified Refineries (Scenario 1)

Scenario 1 represents a future where both of the refineries in Gothenburg transition to producing bio- and electrofuels for the transport sector through the use of H2 and that Renova implements CCS. Preem has announced plans to produce 5 million m^3 of bio- and electrofuels annually by the year 2035, accounting to approximately one third of today's production volume of both fossil- and renewable fuels [72]. ST1 has invested in a biorefinery which is producing aviation fuel, renewable diesel and other bio-based products up to 200 000 tons per year [76]. As it is very hard to analyze the exact effects of the refineries transition, it is assumed that the waste heat availability from the refineries decreases in relation to the decreased production volume to one third of the current level. This assumption was also made by Rosén [50]. For Renova, it is assumed to be at the same level as today. If Renova continues operation in Gothenburg, the plant has to invest in CCS to become climate neutral. As previously mentioned, CCS won't affect the waste heat profile. It is also assumed that the waste heat profile won't be affected by future scenarios in sorting of plastic from municipal solid waste (MSW). When sorting plastic from MSW, the caloric heating value of the waste decreases [77]. This would lead to a decrease in waste heat. However, there is also incentives to increase imports of MSW from other countries, meaning Renova could have the possibility to expand the incineration volume, thus the heat profile is assumed to not change due to uncertainty in future outcomes.

A.3.2 One Refinery with Renova (Scenario 2)

Scenario 2 depicts a future state where electrification of the refinery process is the same as in the first scenario, however with the outcome of one refinery leaving Gothenburg. As the H2 demand is allocated only to the refineries, and with the demand split equal between the two, the H2 demand is assumed to half. The waste heat from the refineries are thus cut in half. The remaining refinery is assumed to have the one third of current level operation, meaning the waste heat profile in total is reduced more than the first scenario. This opens up more potential investments in Rya. Renova is assumed to stay and adopt CCS in this scenario as well with same level of operation.

A.3.3 Decommissioned Refineries (Scenario 3)

Scenario 3 assumes both refineries leaving Gothenburg as a consequence of not finding feasibility in the transition to producing renewable fuels. As the H2 demand is allocated only to the refineries, the total H2 demand is zero meaning that the model cannot invest in HPs utilizing excess waste heat from electrolyzers. In this scenario neither of the refineries profits from transitioning into new operation in Gothenburg, deciding to either reduce operation or move the operation elsewhere. The model is thus limited to investing in less effective HPs which will give an indication of how

sensitive the model is to COP-values.

A.3.4 No Refineries without Renova (Scenario 4)

Scenario 4 is made to asses a "worst-case scenario for the DH system". As Gothenburg has built the DH system with respect to a lot of waste heat, an interesting case would be to remove the waste heat completely from the system. This would mean no refineries and that Renova has to shut down. Renova shutting down is a consequence of future ban on combustion of MSW. The shut down could also be a consequence of a combination with CCS not being possible for operation and that Gothenburg won't allow combustion of fossil CO2.

As DC is currently dependent on the waste heat from Renova and refineries, it is assumed that DC from the absorption chillers are shut down as well in this scenario. This affects the total heat demand profile during the summer, with approximately a reduction of 65 GWh of heat. As previously mentioned, the temperature of supply and return temperature increases during summer to supply enough temperature for the DC absorption chillers (see figure 2.2, and figure 2.3). As the chillers are shut down, the supply and return temperatures won't increase with increasing ambient temperature. This thus affects the availability profile and the COP profile for all HPs in this scenario. The temperature profiles are assumed constant with ambient temperature from the lowest value.

A.4 Calculations for Biogas Storage – Sensitivity Analysis

The storage size is calculated with the assumption of constant charge of the storage, where the charge is dependent on total demand over each year. To calculate storage size, the discharge profile (the demand) is added together with the charge profile. With the assumption of zero losses, a SOC profile can be done. The SOC for a theoretical biogas storage is seen in figure A.3 for Scenario 2.

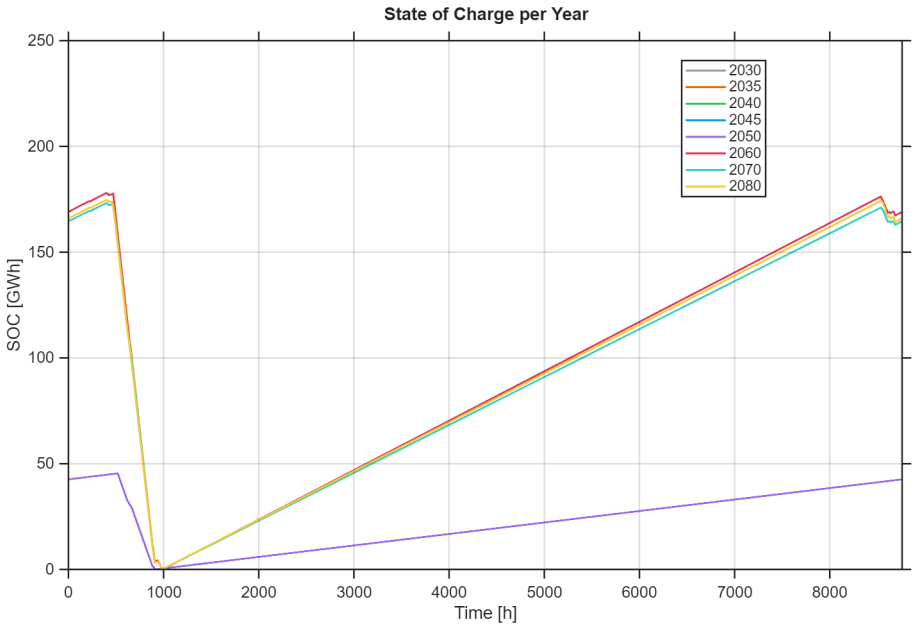

Figure A.3: State of Charge for Biogas Storage for all studied years (Scenario 2).

In this case, the ratio between installed capacity in HOB_{WG} and storage size is not linear from year to year, meaning it becomes difficult to allocate costs to either the fuel or the investments. However, there is more incentives to allocate the cost to the actual usage of biogas due to the already installed capacity of HOB_{WG}. If the cost is allocated to the investment cost, only new HOBs would gain capacity of a imaginary storage in the model. If the cost is allocated to the usage of biogas, then the investment would cover automatically both to the new installed capacity and the already existing ones. This would guarantee that the actual costs of a biogas storage would penalize both new- and old capacity of the HOB_{WG}. In order to allocate the storage cost to the fuel, the following equations are done.

$$\text{Cycles} = \frac{\sum_{t \in \tau} g_{y,HOB_{WG},t}}{i_{y,WG_{St}}} \quad \forall\ y \in Y \tag{A.1}$$

$$\text{Fuel}_{cost} = \frac{C^{inv}_{y,WG_{st}} \cdot \frac{1}{(1+r)^{y-Y_{start}}}}{\text{Cycles}} \quad \forall\ y \in Y \tag{A.2}$$

Resulting in the following table:

Table A.3: Biogas storage investment cost allocated to fuel consumption

Year	2030	2035	2040	2045	2050	2060	2070	2080
Annualized Investment EUR/MWh$_{st}$/yr	16.97							
Cycles [yr^{-1}]	-	-	-	-	1.0470	1.150	1.1460	1.1570
Additional fuel cost EUR/MWh	-	-	-	-	16.21	14.75	14.81	14.67

The chosen value is for year 2070, as this is the highest number of the most applicable years due to the low investment during 2050.

A.5 Heat Dispatch for Scenario 1, 3 and 4

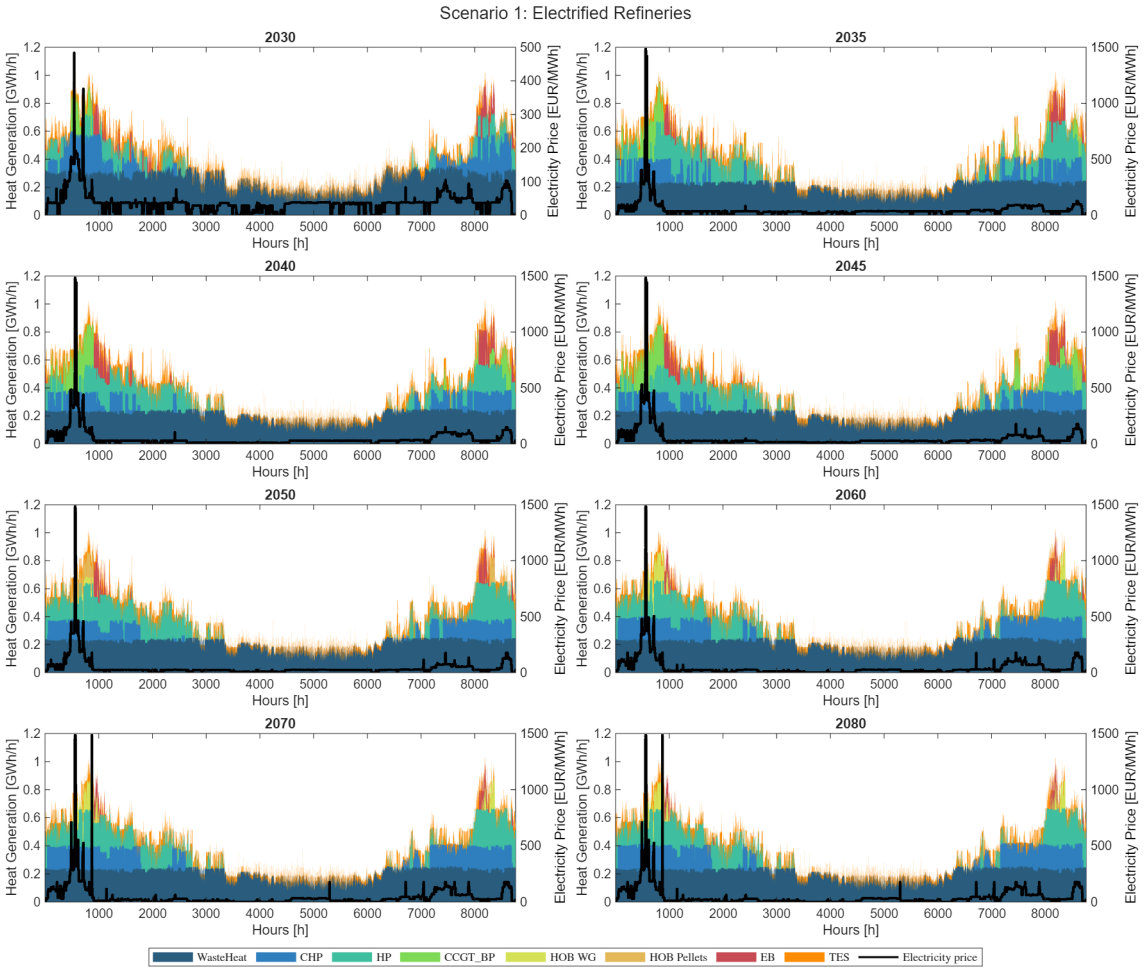

Figure A.4: Heat dispatch of Scenario 1 for all studied years compared to the electricity price.

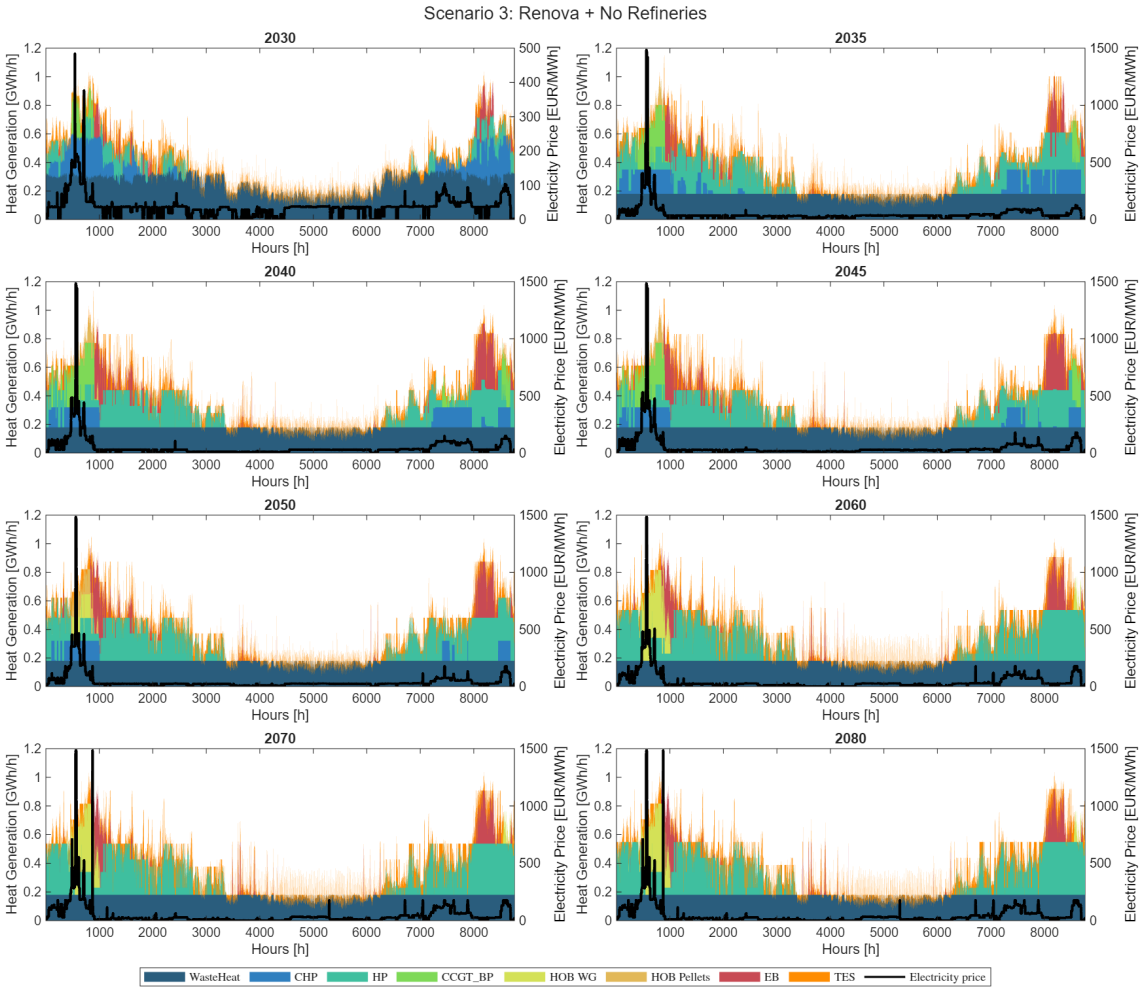

Figure A.5: Heat dispatch of Scenario 3 for all studied years compared to the electricity price

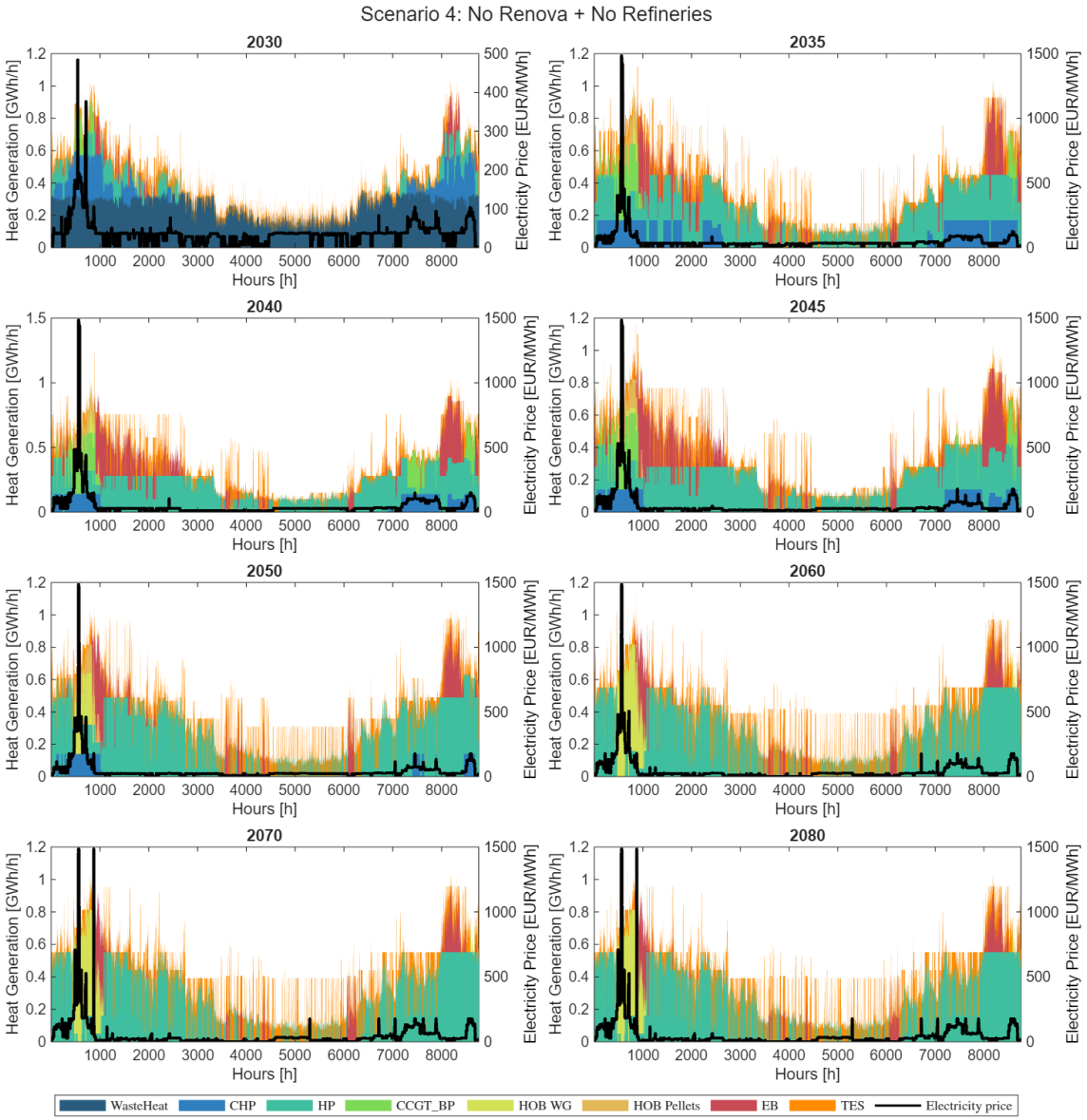

Figure A.6: Heat dispatch of Scenario 4 for all studied years compared to the electricity price

A.6 Heat Pump- and Electric Boiler Production Comparison

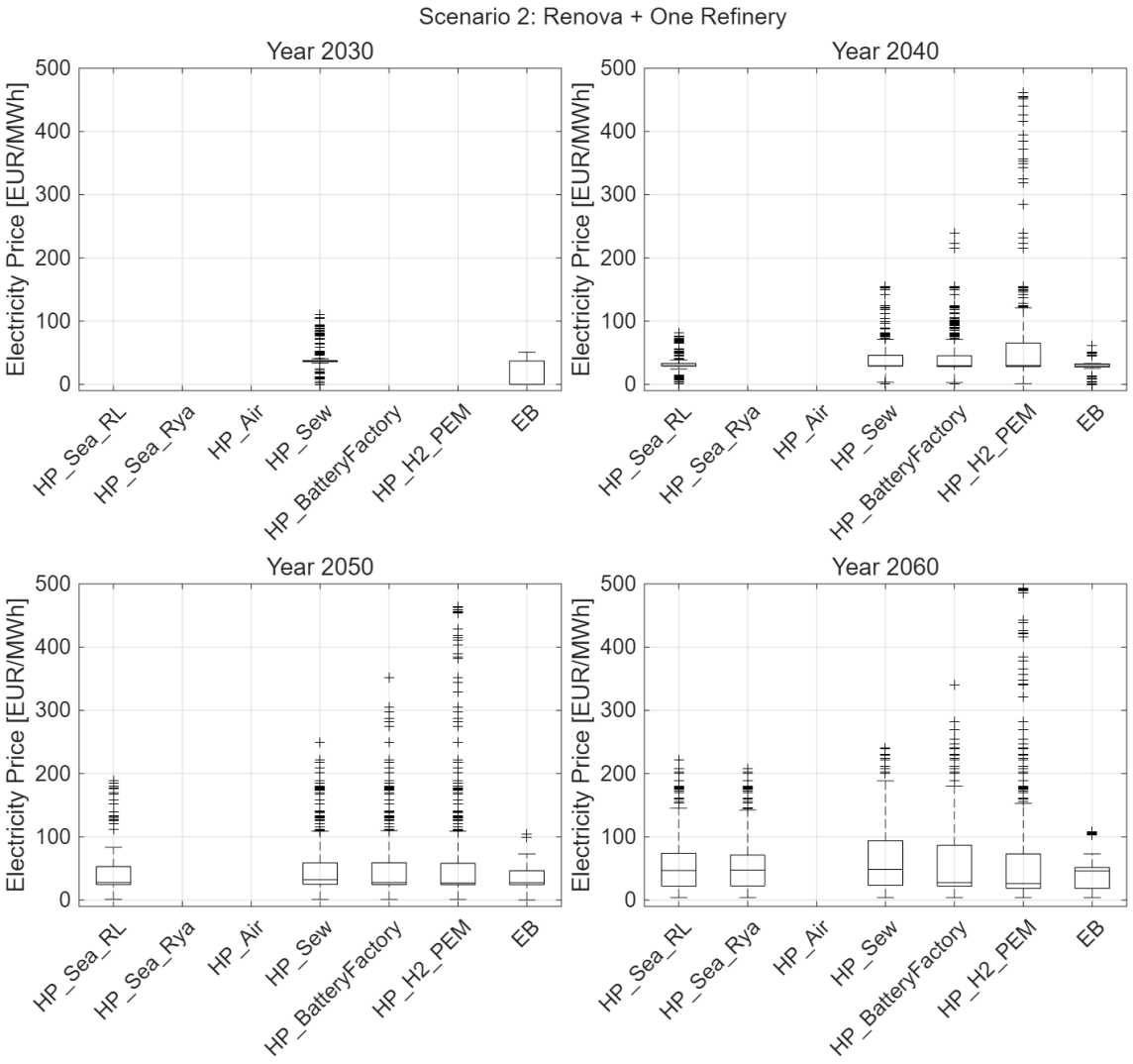

Figure A.7: Box plot showing which electricity prices different HPs and EBs produce. Shows median, upper- and lower quartile, lowest and highest values, plus outliers (Scenario 2).

A.7 Heat dispatch for scenario 2 with energy tax

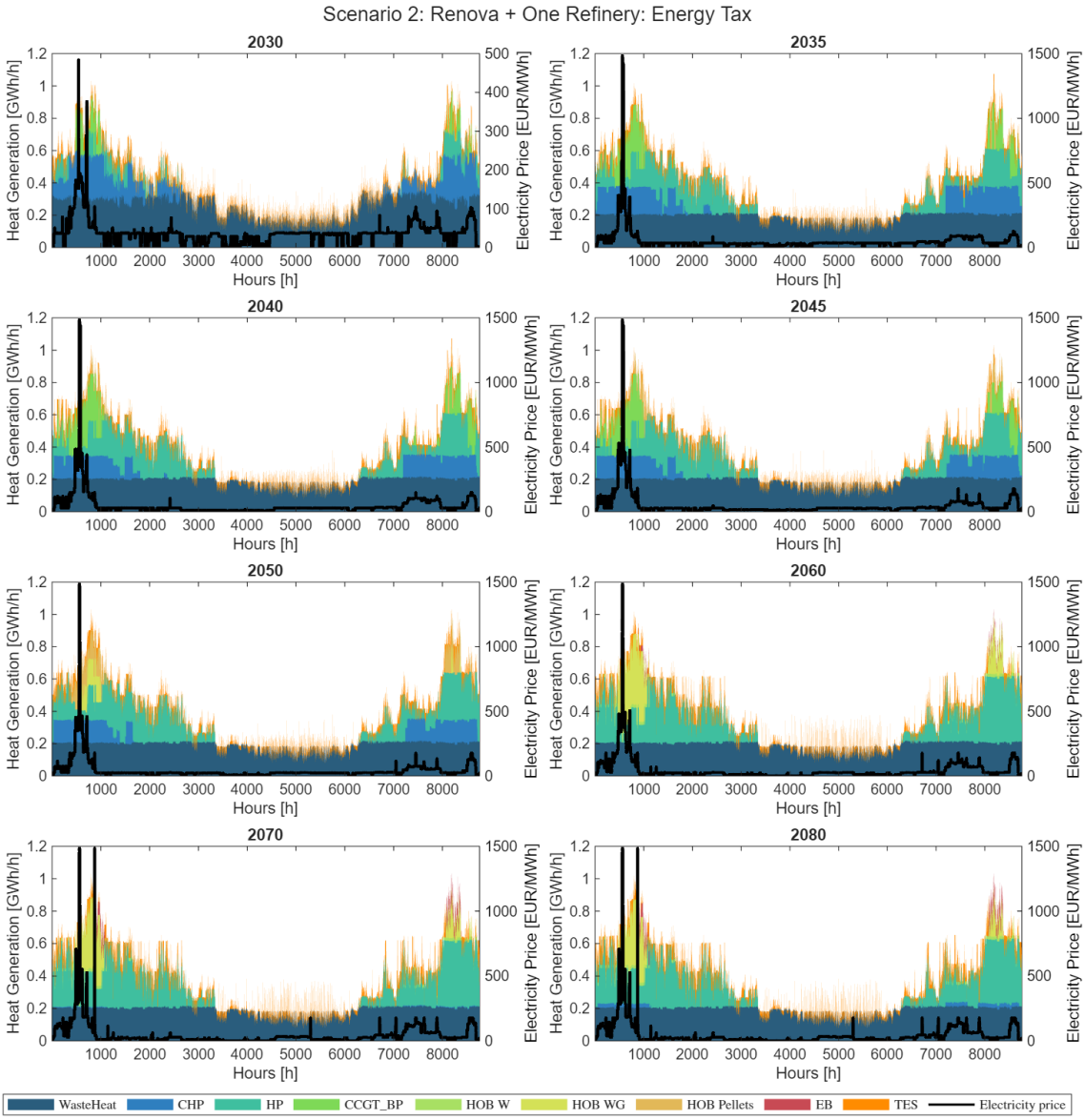

Figure A.8: Heat dispatch of scenario 2: Energy tax for all studied years compared to the electricity price

A.8 Storage Capacities for each Scenario and Sensitivity Analysis

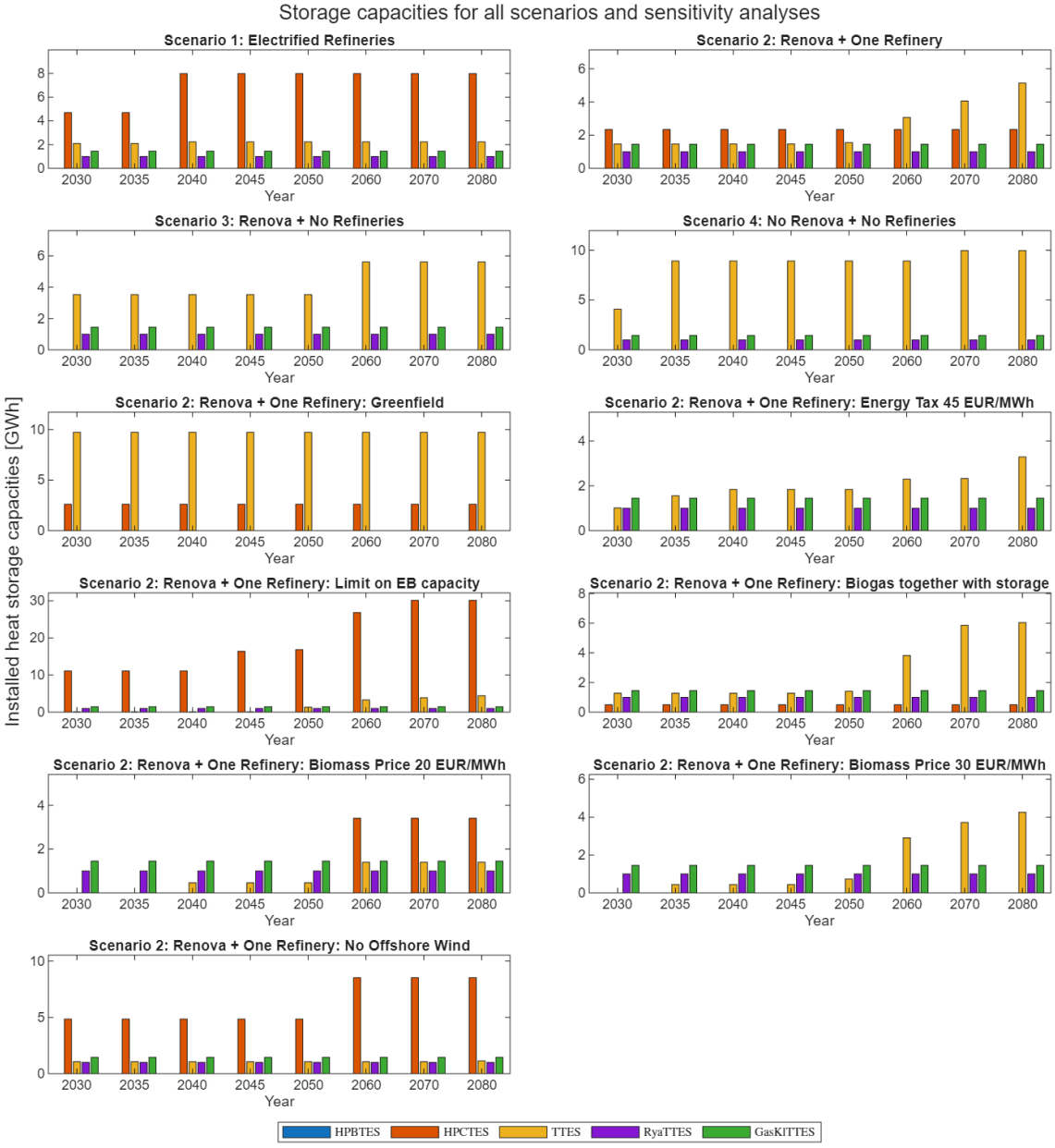

Figure A.9: Storage capacities for all scenarios and sensitivity analyses. The y-axis shows the installed capacities in GWh.

A.9 Heat Pump and Storage Complement (Scenario 2)

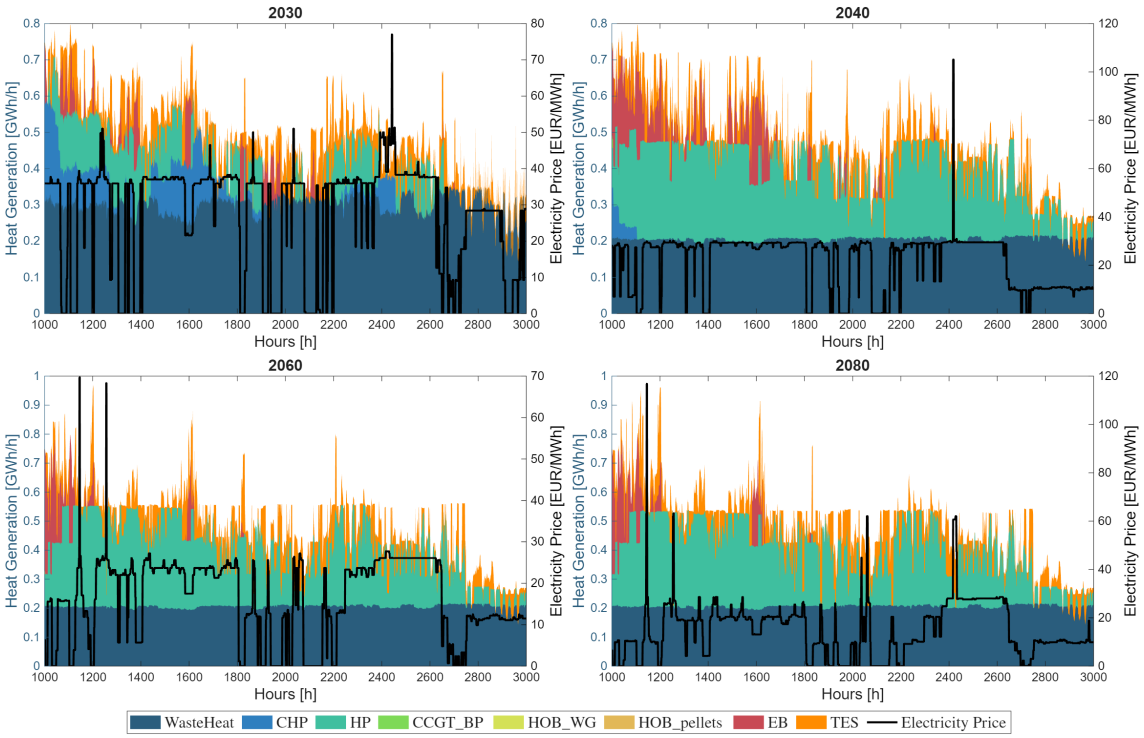

Figure A.10: Heat dispatch for HPs and TTES complementing each other during hours 1000-3000 and years 2030, 2040, 2060 and 2080 with varying electricity price (Scenario 2).

A.10 Storage Modeling and Definition of Boundary for SOC

More options of CTES were evaluated in the study, but was decided to not be included as storage technologies were not in the focus. The only option included in the study has in reality two operating conditions, depending on the difference in storage temperature and DH supply temperature. A heat exchanger would be used when storage temperature is higher than DHn supply temperature. A HP would only have be used while storage temperature is lower. Instead, it was assumed for the modeling that a HP would always upgrade the heat from the storage to the DHn, because the hot side of the storage had to be lowered to 70 °C, to not overestimate the performance of the storage. This was also done for Mälarenergi and their storage [78]. Lowering the cold side down to 30 °C lead to a lower COP for the HP, but was indicated reasonable in order to have a conservative performance of the storage.

The SOC-equation was defined as before the HP to be able to work with every storage. Seen in figure A.11 the boundary is defined before the HP. Storages without a HP will have the SOC-equation directly coupled to the DHn. Previously mentioned, the HPs are accounted for in the heat equation (3.3) with an additional term of COP to account for inserted work from the HP. Equation (3.2), determining the electricity balance in the system also had to be edited to account for electricity insertion when discharging the storages coupled with HPs.

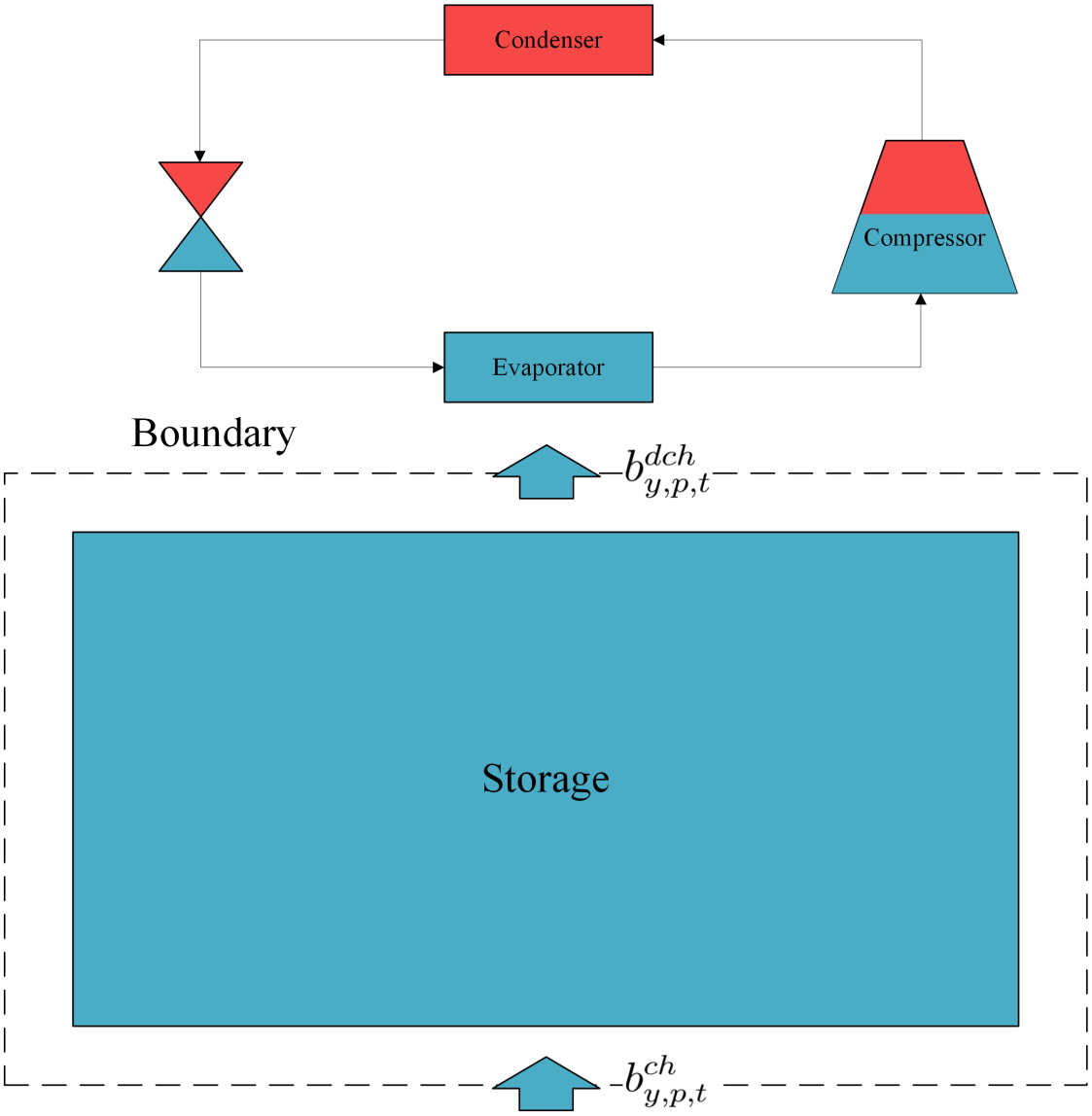

Figure A.11: Boundary definition of charge and discharge from- and to TES. Visualization how a storage is coupled with a HP, used for heat and electricity balances.

DEPARTMENT OF ENVIRONMENTAL AND ENERGY SCIENCES
CHALMERS UNIVERSITY OF TECHNOLOGY
Gothenburg, Sweden
www.chalmers.se

CHALMERS
UNIVERSITY OF TECHNOLOGY